THE UNIVERSITY OF MICHIGAN

INDUSTRY PROGRAM OF THE COLLEGE OF ENGINEERING

THE CONDENSATION OF SUPERHEATED FREON-114 AND STEAM VAPORS OUTSIDE A HORIZONTAL TUBE

Garen Balekjian

This dissertation was submitted in partial fulfillment of the requirements for the degree of Doctor of Philosophy in the University of Michigan.

September, 1956

IP-181

We wish to express our appreciation to the author for permission to distribute this thesis under the Industry Program of the College of Engineering.

THE PROBLEM

The mechanism of heat removal from a superheated vapor as it approaches a surface below the dew point of the vapor is not entirely understood. Experimental studies reported in the literature on the condensation of superheated vapors outside horizontal tubes are meager. A theoretical approach to the condensation of superheated vapors is needed to predict the behavior of superheated vapors at extreme conditions of low pressures and high superheats. Determination of the conditions under which the condensing surface is no longer wetted with a film of condensate is of special importance for the proper design of superheated vapor condensers. The condensation of superheated vapors is studied on the outside of a horizontal tube. Experimental heat fluxes are presented in a form useful in engineering design. The general theory for the interphase transfer of mass and energy is applied to the analyzed results to correlate experimental condensing loads and calculated interfacial vapor film coefficients. The behavior of superheated vapors is interpreted satisfactorily by interphase transfer theory.

ACKNOWLEDGMENTS

The author wishes to express his sincere appreciation to a number of individuals for their assistance during the course of this study and in particular to the following:

Professor Donald L. Katz for his continuous interest, encouragement, suggestions, and advice.

Professors Julius T. Banchero, Stuart W. Churchill, Joseph J. Martin, and Gordon J. Van Wylen for their interest and suggestions during various phases of this work.

Secretaries of the Chemical and Metallurgical Engineering Department for their help in material purchasing.

Messrs. Cleatis Bolen and George Foster of the Chemical and Metallurgical Engineering Department for their valuable help during construction of the experimental apparatus.

Continental Oil Company for their generous financial support which made possible the experimental work completed during 1955.

SUMMARY

A review of the literature on the condensation of superheated vapors indicated meager information for superheated vapors condensing on the outside of a horizontal tube and a general lack of understanding of the behavior of superheated vapors under widely different conditions.

The condensation of superheated Freon-114 and steam was investigated on the outside of a plain 0.750-inch-diameter horizontal copper tube housed in a 6-inch-diameter shell. Experimental data with measured wall temperatures were obtained for superheated Freon-114 condensing at pressures of 43.7 and 77.0 lb per sq in. absolute and for superheated steam condensing at 9.16, 23.35, 23.87, and 44.09 lb per sq in. absolute.

It was observed that superheat in the vapor caused a lowering of the tube surface temperature. Studies indicated that this was related to a lowering of the condensate surface temperature as well. A general lowering of the heat flux as much as 23.4 per cent below that of the saturated vapor was obtained with increasing superheat. This lowering of the heat flux was explained and correlated with the condensing load. The overall performance obtained with the condensation of superheated vapors under various conditions of pressures, superheats, and tube surface temperatures was explained by the relative importance of interphase, and intraphase processes of mass and energy transfer.

The general theory of interphase mass and energy transfer was applied to explain the condensation of superheated vapors by a mechanism of mass and heat transfer through the vapor-liquid interface. The behavior of superheated vapors under widely different conditions was predicted by in-

terphase transfer theory. The theoretical equation was modified and used to correlate satisfactorily the experimental condensing load and the calculated temperature and pressure conditions at the interface with the degree of superheat. The applicability of the correlating equation to predict condensing loads and interfacial film conditions for fluids other than Freon-114 and steam was discussed.

The calculated condensate surface temperatures were used to determine the temperature drop through the interfacial film. Interfacial film coefficients were calculated and correlated with the temperature drop through the interfacial film and the temperature and pressure conditions at the vapor-liquid interface. The variation of the interfacial film coefficient and heat flux in the region close to the "dry point" was obtained by extrapolation of the calculated interfacial film coefficients. The prediction of the "dry point" for a given application was presented and illustrated in a method correlating the interfacial film coefficient with the free convection and radiation film coefficients at the "dry point."

Condensate film coefficients calculated by the conventional method used for the design of superheated vapor condensers were evaluated by comparison with the experimental results. The limitations of this procedure were pointed out. The equation correlating the results from the filmwise condensation of superheated Freon-114 and steam was used in the outline and illustration of a basic procedure for the design of condensers involving the filmwise condensation of superheated vapors outside horizontal tubes. The applicability of this method for peculiar conditions of low pressures, high superheats, and high condensate surface temperatures was discussed.

TABLE OF CONTENTS

LIST OF TABLES

LIST OF ILLUSTRATIONS

LIST OF ILLUSTRATIONS (concluded)

INTRODUCTION

The condensation of superheated vapors is an important process encountered frequently in industry. Compounds prepared by gas or vapor-phase reactions yield the product in the form of a superheated vapor which is subsequently condensed into the liquid or solid state. The manufacture of titanium tetrachloride is a typical example. Superheated refrigerant vapors are condensed in refrigeration units. Superheated steam used extensively in power plants may sometimes be condensed in the superheated state.

A superheated vapor in contact with a surface at temperatures below the dew point of the vapor will form a film of liquid condensate on the surface. The heat extracted from the vapor passes through the liquid film much as in the condensation of saturated vapors. The differences in the condensation of superheated vapors from the process for saturated vapors lies in the removal of the superheat from the vapor at a short distance from the surface of the liquid film and the effect which this process has on the temperature of the liquid at the vapor-liquid interface.

The proper design of a superheated vapor condenser requires a knowledge of the effect of superheat on important variables such as the condensing load, condensate surface temperature, and the corresponding temperature drop at the vapor-liquid interface. A generalized correlation of these variables for all fluids is necessary as a fundamental method for the design of a superheated vapor condenser. This requires also the

formulation of a theory whereby the behavior of superheated vapors may be predicted for a wide range of pressures and superheats in order to anticipate the peculiar condenser condition when the tube surface is no longer wetted with a liquid film or the "dry point."

At present a theoretical approach to the condensation of superheated vapors is available for the special case of vapors condensing inside a vertical tube.[37] Experimental study of this theory is reported in the literature at one superheat for steam.[23] Experimental work on the more common case of condensation on the outside of horizontal tubes is limited to generalized statements concerning the overall heat flux for superheated steam[23,33] and heat flux and condensing coefficient studies for Freon-12.[26] The design of superheated vapor condensers is based on the condensate film coefficient calculated from Nusselt's equation 1 discussed in the next section. The latent heat for a saturated vapor is replaced by the heat removed in desuperheating and condensing the superheated vapors. Although this procedure is found useful in many engineering applications its validity for conditions of low pressure or high superheats is very questionable. In some applications where the superheat is of the order of 1000°F the necessary condensing capacity is obtained by increasing the condenser area determined by the conventional design method.

A systematic study of the important variables is made in this work for the condensation of superheated Freon-114 and superheated steam on the outside of a horizontal tube. Two fluids with widely different physical properties enable a more thorough approach to the desired generalized correlation. The studies include the condensation of superheated Freon-114 at two pressures of 43.7 and 77.0 lb per sq in. absolute, with a maximum superheat of 180°F and superheated steam at 9.16, 23.35, 23.87,

and 44.09 lb per sq in. absolute with a maximum superheat of 184°F. The effect of superheat on the overall heat flux and condensing load is presented. The results are further analyzed to obtain the calculated condensate surface temperature, the temperature drop across the condensate film, the temperature drop across the vapor-liquid interface, and the corresponding condensate film and interfacial coefficients. The general theory of interphase mass and energy transfer is applied to the condensation of superheated vapors and used for the interpretation of results. The condensation coefficient (f) derived from the kinetic theory of gases is used to correlate the experimental condensing load and the calculated interfacial temperature and pressure conditions with the degree of superheat. The results are also correlated as a function of the interfacial heat transfer coefficient, the interfacial temperature and pressure conditions, and the temperature drop through the interfacial film.

A comparison is made between the heat transfer film coefficient calculated according to the conventional design procedure and the experimental film coefficient evaluated on the same basis. A more fundamental procedure for the design of superheated vapor condensers is outlined and illustrated for superheated Freon-114 in Appendix E.

LITERATURE AND INTRODUCTORY THEORY

The condensation of superheated vapors is a special case of the process of condensation and the general operation of interphase mass and energy transfer. For a thorough understanding of this special problem a brief survey of the literature and the theory concerning condensation of saturated and superheated vapors is presented in this section. In addition, the theory which has been developed for interphase mass and energy transfer is discussed.

SATURATED VAPORS

Nusselt's classical work[37] presents theoretical equations for the condensation of vapors on different surfaces. The derivation of these equations and a detailed discussion of experimental data on this subject is available in several references.[23,24,33,35] The following is the equation derived by Nusselt for the prediction of the condensate film coefficient for saturated vapors condensing on the outside of a horizontal tube:[14]

$$h_c = 0.725 \sqrt[4]{\frac{k_f^3 \rho_f^2 g (-\Delta H)}{\mu_f D_o \Delta t_c}} \qquad (1)$$

where

h_c = condensate film coefficient, Btu per (hr)(°F)(sq ft outside)

$(-\Delta H)$ = total heat removed, latent heat for saturated vapors, Btu per lb

{Subscript

f = condensate properties at the mean film temperature, T_f, °F

k = thermal conductivity, Btu per (hr)(°F)(ft)

ρ = density, lb per cu ft

μ = viscosity, lb per (ft)(hr)

g = gravitational acceleration, 4.17×10^8 ft per hr per hr

D_o = outside tube diameter, ft

Δt_c = temperature difference through condensate film, $(T_{sv} - t_o)$, °F

T_{sv} = saturation temperature, °F

t_o = outside tube surface temperature, °F.

Based on the assumption of a linear temperature gradient through the film and a linear variation of the fluidity $(1/\mu)$ with temperature the following equation is derived by Drew[33] for the mean condensate film temperature:

$$T_f = T_{sv} - 3/4\ \Delta t_c \qquad (2)$$

where T_f = mean condensate film temperature, °F.

The following equation shows better agreement with experimental data and is recommended for the evaluation of the mean film temperature:

$$T_f = T_{sv} - 1/2\ \Delta t_c \ . \qquad (3)$$

The simplifying assumptions used by Nusselt in deriving equation 1 consist of the following:[35]

1. Linear temperature gradient through the condensate film.
2. Heat transfer only by conduction through the condensate film.
3. Linear variation of condensate film properties with temperature.
4. Clean and smooth surface.
5. Laminar flow of condensate film.
6. No effect due to condensate film curvature.
7. Constant tube wall temperature.

The validity of these assumptions is shown by the fact that experimentally determined condensate film coefficients are generally found to

be about 10 to 20 per cent above those predicted from equation 1.[24] Bromley[13] points out that correct evaluation of the integral

$$\frac{4}{3}\int_0^{\pi} \sin^{1/3}\phi \, d\phi$$

in Nusselt's derivation gives a value of 0.728 for the coefficient in equation 1. Equation 1 becomes complicated when the temperature profile through the film is not assumed to be linear and the effect of cross flow within the film is considered. The following correction factor to equation 1 is recommended by Rohsenow[43] as an improvement over an earlier contribution by Bromley:[12]

$$\sqrt[4]{1 + 0.60\,\frac{C_p\,\Delta t_c}{(-\Delta H)}} \qquad (4)$$

where C_p = specific heat of condensate, Btu per (lb)(°F). This correction factor is recommended as a satisfactory approximation to the more complex equation for the range of

$$0 < \frac{C_p\,\Delta t_c}{-\Delta H} < 1.0 \quad .$$

The effect of condensate film turbulence on the condensate film coefficient is observed by Kirkbride.[28] Other factors such as vapor velocity and its effect on turbulence of the condensate film and literature related to them are reviewed in reference 44.

SUPERHEATED VAPORS

The condensation of superheated vapors is discussed in the original work of Nusselt.[37] In a manner similar to the derivation of equation 1, the differential equation representing the overall heat balance is integrated for the height of a vertical condensing surface to give the following equation:[24]

$$H = \frac{\rho_f^2 g(-\Delta H)}{\mu_f k_f}\left(\frac{Y_H^4}{4} + \frac{RY_H^5}{5} + \frac{R^2Y_H^6}{6} + \ldots\right) \qquad (5)$$

where

H = height of the vertical surface, ft

Y_H = thickness of the condensate film at lower end of surface, ft

$R = \frac{h_v(T_g - T_{sv})}{k_f(T_{sv} - t_o)}$, ft^{-1}

h_v = convection coefficient from the superheated vapor to the condensate surface, Btu per (hr)(°F)(sq ft outside)

T_g = superheated vapor temperature, °F.

The condensate film thickness Y_H determined from equation 5 by trial and error is substituted in equation 6[24] to calculate the condensing rate on the vertical surface of height H:

$$m = \frac{\rho_f^2 g\, Y_H^3}{3\,\mu_f} \qquad (6)$$

where m = condensing load, lb per (hr)(ft of surface width).

Stender[47] and Merkel[34] use an approximation for equation 5 to predict the effect of superheat on the heat flux of vapors condensing on a vertical surface.[35] The ratio of the heat flux for a superheated vapor to that of the saturated vapor is related graphically to the function

$$\frac{h_v(T_g - T_{sv})}{h_c(T_{sv} - t_o)} .$$

This relationship predicts an increase of up to 37 per cent in the heat flux due to superheat.

A discussion of Nusselt's equation for the condensation of superheated vapors inside a vertical tube considering the effect of vapors at constant velocity and an improved equation allowing for the variation of

vapor velocity along the condensing length is given by Jakob.[23,24] Studies with steam at one atmosphere pressure and 405°F superheat indicate a small increase in the heat flux due to superheat at low heat fluxes. This effect is reversed at higher heat fluxes.

A survey of the literature on condensation of superheated steam is presented by McAdams.[33] Generally with steam at one atmosphere pressure, a small increase of heat flux is reported due to superheat. Further discussions on this effect are included in references 15, 16, 19, and 29. Patents are available for devices which may be used to desuperheat steam.[10,36]

Experimental data reported in the literature on the condensation of superheated vapors on the outside of a horizontal tube are meager. Katz et al.[26] report the results of their studies for superheated Freon-12 condensing on the outside of plain and finned tubes. No effect of superheat as compared to saturated vapors is observed for the range of pressures 103 to 172 lb per sq in. absolute and the maximum superheat of 122.5°F.

Nusselt's derivation of equation 1 applied to superheated vapors gives a similar equation where the factor $(-\Delta H)$ represents the total heat removed in condensing the superheated vapors rather than the latent heat of condensation. This equation predicts a small increase in heat flux due to superheat. It is assumed that the vapor at the condensate surface is in equilibrium with the liquid and is at its saturation temperature. This implies there is no resistance to mass and energy transfer at the vapor-liquid interface. Conventional design of superheated vapor condensers is based on the condensate film coefficient predicted by this method. Equation 1 is useful in many engineering applications where vapors with 100°F to 200°F superheat are condensed at normal pressures of

one to five atmospheres. The validity of this method is doubtful for applications where peculiar conditions of high superheat, high wall temperatures, and low pressures prevail.

THE MECHANISM OF MASS AND ENERGY TRANSFER

The mechanism which controls the condensation of molecules moving toward a cold surface involves the effect of superheat on the condensate surface temperature. The importance of the liquid surface temperature at the vapor-liquid interface has been recognized for some time. In 1928 Jakob[23] has suggested that a condensate-surface temperature lower than the saturation temperature may prevail during the condensation of superheated steam in order to account for the lower heat flux obtained in evaporators using superheated steam as compared to the performance of saturated steam. A theoretical attempt to prove this hypothesis is made by Bosnjakovic.[23] Starting with the kinetic theory of gases and using several simplifying assumptions he derives an equation relating the condensing load for superheated steam with the lowering of the condensate surface temperature below that at saturation. A discussion of this study is given in the section presenting the interpretation and correlation of experimental results. The calculations of Bosnjakovic indicate that the condensation of steam at one atmosphere pressure and a superheat of 405°F requires a condensate surface temperature 12.6°F below the saturation temperature of 212°F. Subcooling of the condensate surface desuperheats partially the adjacent vapor molecules and gives a density of vapor molecules at the liquid surface comparable to that with saturated steam. Bosnjakovic considers the subcooling as necessary to condense high-velocity superheated steam molecules as they penetrate into the liquid surface. This discussion does not differentiate between intraphase film temperature

difference in the vapor and interphase film temperature difference at the vapor-liquid interface.

The condensation of superheated vapors belongs to those operations which involve the transfer of momentum, mass, and energy across a phase boundary. The mechanism of such processes has not been analyzed adequately because of the equilibrium conditions usually assumed. In contrast with studies concerning the diffusional transfer processes, for an interphase transfer operation the velocity of one phase relative to that of the other is assumed to be zero, the temperature of the two phases at the interface is assumed to be the same, and in the case of a multi-component system the composition of the two phases is assumed to be that at thermodynamic equilibrium.

The kinetic theory of gases has useful applications in studying interphase transfer processes because it describes the behavior and the bulk properties of a group of molecules at a given temperature and pressure. The following equation is referred to frequently in the literature concerning interphase mass transfer:

$$m_s = f(P_s^* - P_g)\sqrt{\frac{g_c M}{2\pi RT_s}} \qquad (7)$$

where

m_s = net mass of molecules transferred, lb (mass) per (hr)(sq ft interfacial area)

M = molecular weight of fluid, lb (mass) per lb mole

R = gas constant, 1544 (ft)(lb force) per (lb mole)(°R)

T_s = temperature of liquid or solid surface, °R

P_g = pressure of gas phase at vapor-liquid interface, lb (force) per sq ft absolute

P_s^* = equilibrium pressure corresponding to T_s, lb (force) per sq ft absolute

g_c = conversion factor, 4.17×10^8 (lb mass)(ft) per (lb force) (sq hr).

The condensation coefficient f is defined as the following ratio:

$$f = \frac{\text{Number of molecules condensed}}{\text{Total number of molecules striking the surface}} \cdot \quad (8)$$

Equation 7 is derived by combining the number of collisions predicted by the kinetic theory of gases with the molecular density in the gas phase calculated for an ideal gas.[18] This simple derivation involves the following assumptions:

1. Ideal gas behavior.
2. Molecular velocity distribution identical to that of a uniform gas described by Maxwell's probability distribution function.[18]
3. Equilibrium at the phase boundary.

Assumptions (1) and (2) are valid for many applications. The behavior of molecules of a non-uniform gas involving intraphase transfer of energy is expected to show deviations from these assumptions. The molecular behavior of a condensing vapor is uniform within the vapor phase and non-uniform only through the short distance represented by the thickness of the interfacial film across which heat transfer and cooling of molecules occur. In most instances where the use of equation 7 is encountered in the literature the third assumption of the equilibrium of the two phases is overlooked. Equation 7 is applied frequently to correlate experimental data on condensation and evaporation and to estimate the temperature difference across the vapor-liquid interface, whereas its derivation implies that the vapor and liquid are at the same temperature

at the phase boundary. This confusion is partly due to the fact that most interphase transfer studies involve also intraphase transfer. This is shown for the condensation of superheated steam inside vertical tubes by measurement of the temperature gradient in a direction normal to the condensing surface. Roecke and Jakob[23] report independently a zone about one millimeter thick in which extensive cooling of superheated steam occurs. This distance is many times thicker than the interfacial film which is of the order of magnitude of one mean free path of the condensing molecules. A theoretical equation for the temperature gradient in the vapor phase of a superheated vapor is derived by Cornell.[17]

Except for the theoretical work of Bosnjakovic[23] the application of theoretical equations based on the kinetic theory of gases is limited to studies of interphase mass transfer in which no superheated vapor phase exists. A thorough survey of this literature is presented in the recent work of Schrage.[45] Early studies in this field are aimed at the determination of the value of the condensation coefficient (f) for various substances. During evaporation the coefficient (f) represents the relative number of molecules which leave the liquid phase and move away from the surface, and (1-f) represents the relative number of molecules which move away from the liquid surface by reflection after striking the surface. For a substance at steady-state conditions of temperature and pressure the evaporation and condensation coefficients are equal. For the special case of evaporation or condensation at zero pressure in the vapor phase equation 7 assumes the simpler form:[2]

$$m_e = f P_s^* \sqrt{\frac{g_c M}{2\pi R T_s}} \qquad (9)$$

where

m_e = maximum rate of evaporation or condensation of a substance

= mass evaporating into a perfect vacuum

= (mass of saturated vapor which strikes unit area of the surface per unit time) times (fraction f of incident molecules which are able to remain on the surface.

Early attempts to determine the condensation coefficient for various solids and liquids are reviewed in reference 45. In an early paper Alty[1] reports a value of about 0.01 for water at low pressures. In another paper[5] Alty and Nicoll describe the method used to determine this value. Experimental data obtained for the rate of evaporation of water at various pressures are extrapolated to zero pressure. Equation 9 is then solved for the unknown (f). Alty[2] recognizes the uncertainty of the final value of f determined by extrapolation and uses a more reliable method in which the temperature of the drop surface is calculated from the measured drop geometry. The value of f calculated from equation 7 is 0.036 for water and unity for carbon tetrachloride. Alty[3] also reports experimental values of f for benzene (1.0), alcohol (small), iodine (1.0), naphthalene (1.0), synthetic camphor (0.172), and benzoic acid (0.29). These values of the condensation coefficient are related to the electrical structure of the compound and it is concluded that the condensation coefficient of polar compounds is relatively small, whereas that of non-polar compounds is very close to unity.

Prüger[39] has determined the condensation coefficient of water and carbon tetrachloride at atmospheric pressure. The values of f of 0.04 and unity for water and carbon tetrachloride, respectively, agree with those reported by Alty and co-workers. A recent study[21] on the rate of condensation of water vapor under vacuum presents a correlation based on equation 9.

Using the value of 0.036 determined by Alty for the condensation coefficient (f) of water, and assuming the slope of the vapor-pressure curve of water to be a constant for reasonably small increments, Silver[46] combines the Clapeyron equation with equation 7 to obtain the following relationship:

$$m_s = 778\, f \sqrt{\frac{g_c M}{2\pi\, RT_s}}\ \frac{(-\Delta H)\,\rho_L}{T}\,(T_s - T_{sv}) \qquad (10)$$

where

ρ_L = density of liquid, lb per cu ft

T = average temperature between T_s and T_{sv}, °R.

Defining an interfacial vapor film coefficient of heat transfer (h_i) as

$$h_i = \frac{m_s\,(-\Delta H)}{(T_s - T_{sv})} \qquad (11)$$

and combining it with equation 10 the following equation is derived for the interfacial film coefficient:[46]

$$h_i = 778\, f \sqrt{\frac{g_c M}{2\pi\, RT_s}}\ \frac{(-\Delta H)^2\,\rho_L}{T} \qquad (12)$$

where

h_i = interfacial vapor film coefficient, Btu per (hr)(°F)(sq ft outside)

f = 0.036.

Silver recommends the use of equation 12 to calculate the interfacial vapor film coefficient and the interfacial film resistance for saturated steam condensing at low pressures. The fraction of the total temperature drop across the liquid film and across the interfacial vapor film is determined by the fraction of the total resistance to heat transfer due to the respective films:

$$\frac{1}{h_o} = \frac{1}{h_i} + \frac{1}{h_c} \qquad (13)$$

where

h_o = overall outside film coefficient, Btu per (hr)(°F(sq ft outside).

Equation 12 is used by Cornell[17] in a method recommended for the evaluation of the condensate surface temperature (T_s), the interfacial film coefficient (h_i), and the temperature drop across the interfacial vapor film for the condensation of superheated steam. It is assumed that the vapor at the interface is at the saturation temperature, and the temperature drop through the interfacial film is of the same order as that for a saturated vapor. It will be shown in a subsequent section that the use of equation 12 derived from equation 7 is not valid because the interfacial temperature drop is assumed to be zero.

This discussion indicates that in all these investigations the experimental results are interpreted in terms of a transfer mechanism across the vapor-liquid interface. However, the equations used to calculate these results assume thermodynamic equilibrium across the interface and are not valid for the non-equilibrium cases to which they are applied. The proper mathematical relations describing the interphase transfer of mass and energy are derived by Schrage[45] and are presented in the next section.

THEORY OF INTERPHASE MASS AND ENERGY TRANSFER

The process of interphase mass and energy transfer may be described by the statistical behavior of the molecules at the vapor-liquid interphase. The rate of evaporation and condensation of molecules may be determined if the velocity distribution of the molecules is known as a

function of the absolute temperature. Usually the mean velocity of the molecules in the liquid or solid surface is assumed to be zero. In most practical applications this assumption is justified because of the large difference in the density of the vapor and liquid or solid phases. Therefore the absolute rate of evaporation (m_e) defined by equation 9 is assumed to depend on the thermodynamic properties of the surface, for instance, the pressure P_s^* and temperature T_s. During studies of the condensation coefficient (f) of water vapor Alty and co-workers[4] observed that although only a fraction of the vapor molecules striking the liquid surface condense, all molecules attain the liquid surface temperature after colliding with the surface.

The molecular density within a given volume of velocity space is defined by the following equation:

$$dn = sdC \tag{14}$$

where

dn = the number density of molecules with velocity C in the velocity space dC

s = velocity distribution function.

The extent of the rigorous mathematical approach used to analyze interphase transfer operations depends on the selection of the particular velocity distribution function(s) in equation 14. A function of the velocity distribution obtained from statistical mechanics is used by Lennard-Jones and Devonshire[31] to describe exactly the behavior of simple molecules held by Van der Waal's forces. This study is useful for the prediction of the behavior of simple gases (hydrogen, helium) striking a surface.

For a uniform gas at steady-state conditions the form of the velocity

distribution function(s) predicted by statistical mechanics is the Maxwell velocity distribution defined as:[45]

$$s = n \frac{B^3}{\pi^{3/2}} e^{-B^2[(U-\bar{U})^2 + (V-\bar{V})^2 + (W-\bar{W})^2]} \qquad (15)$$

where

n = number density of molecules

U,V,W = molecular velocities in the x, y, and z directions, respectively of the Cartesian coordinates drawn at the liquid surface (U and x are positive in a perpendicular direction away from the liquid surface)

$\bar{U},\bar{V},\bar{W}$ = mean absolute velocity of the molecules in the x, y, and z directions, respectively

$$B = \sqrt{\frac{g_c M}{2RT}} \quad .$$

During evaporation or condensation the behavior of gas molecules deviates from that of a uniform gas because of the disturbing effect of the liquid surface. Additional deviations from uniform gas behavior may be due to the fact that at the vapor-liquid interface there is intraphase heat transfer among the gas molecules. In general these deviations from the Maxwell velocity distribution will be small and will be indicated by the agreement between theory and experimental results.

Thermodynamic equilibrium at the vapor-liquid interface implies that $\bar{U} = \bar{V} = \bar{W} = 0$ and the vapor and liquid temperatures are equal at the interface ($T_g = T_s$). Substituting for the velocity distribution function(s) from equation 15 in equation 14 and integrating over all velocity space, Schrage[45] derives equation 9 for the absolute rate of evaporation at equilibrium. This is equal to the absolute rate of condensation and

there is no net interphase mass or energy transfer.

The Absolute Rate of Condensation under non-equilibrium conditions can be predicted from the Maxwell velocity distribution if uniform gas behavior is assumed very close to the vapor-liquid interface. In this case the mass rate of flow of molecules moving toward the interface is negative ($U < 0$). Using U_g instead of $\overline{U}$ as the term corresponding to the rate of mass transfer in equation 15, and with $\overline{V} = \overline{W} = 0$ corresponding to the mass transfer conditions, Schrage[45] derives the following equation for the absolute rate of condensation under non-equilibrium conditions:

$$m_c = - \frac{\rho_g}{2B_g \pi^{1/2}} \Gamma \qquad (16)$$

where subscript g refers to vapor properties at the vapor-liquid interface.

m_c = absolute rate of condensation, lb per (hr)(sq ft interfacial area)

Γ = a correction factor involving the error integral $\Phi (B_g U_g)$ and defined as

$$\Gamma = e^{-B_g^2 U_g^2} - B_g U_g \pi^{1/2} [1 - \Phi (B_g U_g)] . \qquad (17)$$

Substituting for the gas density and B_g and comparing equation 16 with equation 9, the absolute rate of condensation is expressed by the following equation:

$$m_c = - \left(\frac{P_g}{P_s^*}\right) \left(\frac{T_s}{T_g}\right)^{1/2} \Gamma m_e \quad . \qquad (18)$$

When the two phases are at equilibrium the absolute rate of condensation and evaporation are equal since in equation 18 at $U_g = 0$, $\Gamma = 1.0$,

and

$$\left(\frac{P_g}{P_s^*}\right) = \left(\frac{T_s}{T_g}\right) = 1.0 \quad .$$

The Rate of Mass Transfer for a pure substance at the vapor-liquid interface is obtained[45] by adding equations 9 and 18:

$$m_s = f\sqrt{\frac{g_c M}{2\pi RT_s}}\left[P_s^* - P_g\left(\frac{T_s}{T_g}\right)^{1/2}\Gamma\right] \qquad (19)$$

where

m_s = condensing load, lb per (hr)(sq ft interfacial area)

T_g = vapor temperature at the vapor-liquid interface, °R.

The following assumptions are implied in the derivation of equation 19:

1. Vapor behaves ideally.
2. Vapor molecules behave similar to those of a uniform gas.
3. No intraphase mass and energy transfer in the vapor.
4. Condensation coefficient (f) is constant and independent of the molecular vector velocity. It is a function of the state of the surface and the kind of molecules involved.[45]
5. Behavior of molecules described by the Maxwell velocity distribution.
6. Non-equilibrium conditions at the vapor-liquid interface.

When the two phases are at equilibrium and both (T_s/T_g) and Γ are unity equation 19 becomes similar to equation 7 presented earlier and discussed frequently in the literature. Use of equation 19 requires the evaluation of the correction factor Γ. Equation 17 presents Γ as a function of B_gU_g or ϕ_g ($B_gU_g = \phi_g$). The quantity ϕ_g is expressed by the following equation:[45]

$$\phi_g = \frac{1}{2\pi^{1/2}} \frac{m_s}{m_e} \left(\frac{P_s^*}{P_g}\right) \left(\frac{T_g}{T_s}\right)^{1/2} . \qquad (20)$$

Calculated values of (Γ -1) are presented graphically as a function of $|\phi_g|$ for the range $1 \geq |\phi_g| \geq 10^{-3}$.[45]

The use of equation 19 to predict the deviation from equilibrium for actual cases is made difficult by the functional interdependence of m_s, m_e, f, Γ, and ϕ. Schrage applies equation 19 to predict the deviation from equilibrium (ρ_g/ρ_s*) during evaporation and condensation at different values of the ratio (m_s/m_e). Although equilibrium conditions are not assumed at the interface, a value of unity is used for (T_s/T_g) and f in order to simplify the evaluation and use of Γ in equation 19.

A relationship equivalent to equation 19 with the assumption of Γ equal to unity is presented by Bosnjakovic in connection with discussion of the condensation of superheated steam.[23,45] This theoretical attempt seems to be the only one reported in the literature on superheated vapors and does not distinguish between the interphase film and intraphase film temperature differences. There is no evidence of the application of the theory of interphase mass and energy transfer presented by Schrage for the interpretation of experimental results with superheated vapors condensing on the outside of a horizontal tube. Application of this theory and the resulting equation 19 is made in the next section to correlate the experimental condensing load and superheat with the calculated interfacial temperature and pressure conditions for superheated Freon-114 and steam. The calculated results are also correlated as a function of the interfacial vapor film coefficient, the interfacial film temperature difference, and the interfacial temperature and pressure conditions. A method is outlined for the design of superheated vapor condensers using

these correlations. The use of equation 19 is simplified by expressing (Γ -1) as a simple function of $|\phi_g|$ and combining the resulting equation with equations 19 and 20 to eliminate Γ from equation 19. The relative importance and effects of interphase film and intraphase film temperature differences are also discussed in the next section.

EXPERIMENTAL APPARATUS AND MATERIALS

The experimental apparatus consists of a closed system for generating vapor, superheating it, condensing the superheated vapor and returning condensate to the vapor generator. Figure 1 shows the entire experimental unit and Figure 2 is the flow diagram describing the various units. Details of the apparatus are given in Appendix A and Figures 3 and 4.

The essential feature of the apparatus is the horizontal condenser tube, 3/4-inch outside diameter and 3 feet long housed in a 6-inch shell. Table I gives the condenser shell and experimental tube characteristics. Four thermocouples are installed in the tube wall to measure the temperature. Water at a controlled temperature is circulated through the tube to extract the heat from the condensing vapor. The heat transfer rate is determined by the temperature rise of the water measured with mercury-in-glass thermometers and by the flow rate of water indicated by a calibrated rotameter. Thermocouples in the vapor space of the condenser indicate the temperature of the vapor. A pressure gage or manometer gives the pressure in the condenser. The degree of superheat in the vapor is automatically controlled by an electric superheater.

Water and Freon-114 are selected for this study as two fluids with widely different properties. Freon-114 is chosen as the organic fluid because generally it gives stable film condensation, it has a suitable vapor pressure, and its cost is not prohibitive. The condensation of superheated Freon-114 vapor is encountered in industrial refrigeration units.

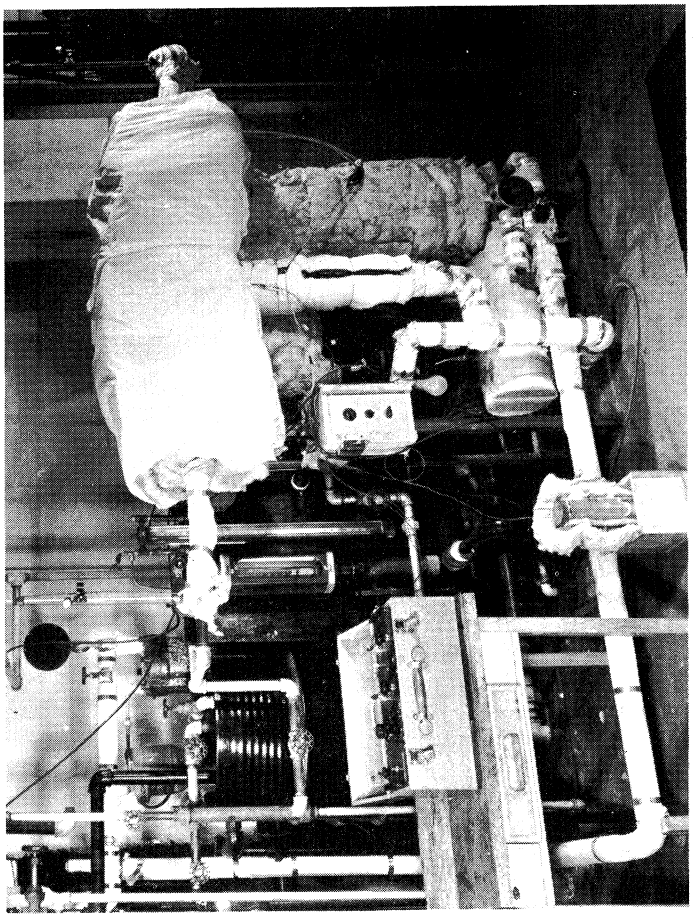

FIGURE 1— EXPERIMENTAL APPARATUS

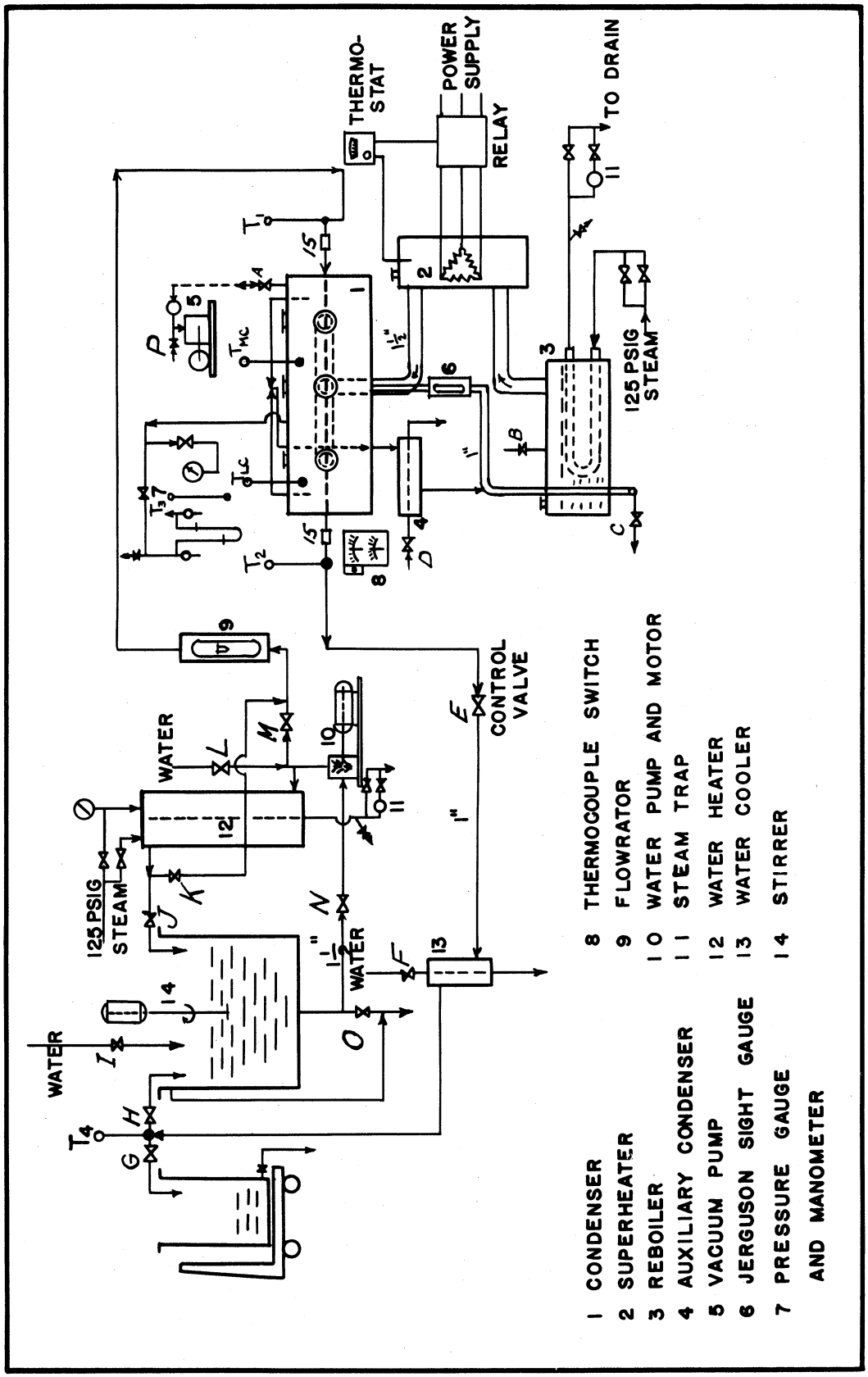

FIGURE 2—FLOW DIAGRAM OF EQUIPMENT

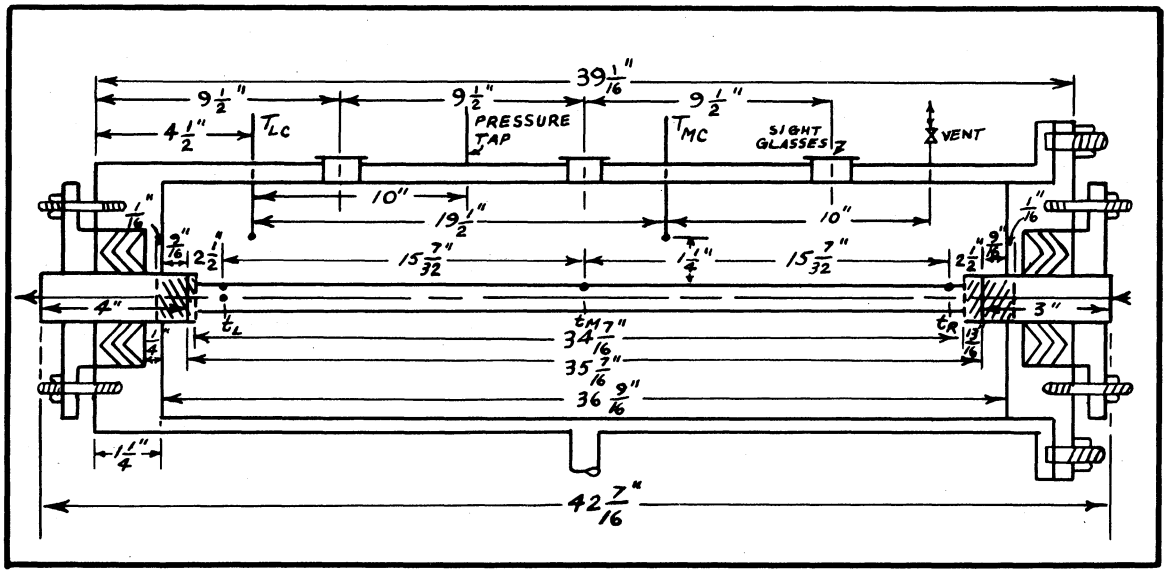

FIGURE 3— DETAILS OF CONDENSER SHELL AND TUBE

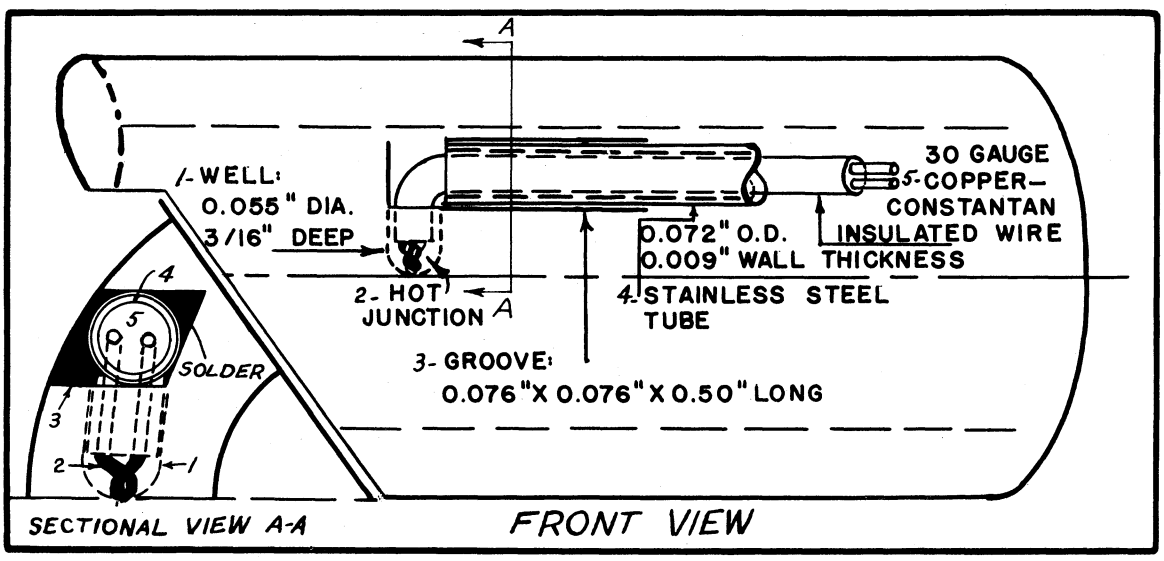

FIGURE 4— DETAILS OF WALL THERMOCOUPLE INSTALLATION

TABLE I

CONDENSER SHELL AND EXPERIMENTAL TUBE CHARACTERISTICS

Condenser Shell		Experimental Tube	
Material - Galvanized Plain Carbon Steel Pipe		Material - Plain Copper Tube	
Outside diameter, inches	6.648	Outside diameter, inch	0.750
Inside diameter, inches	6.066	Inside diameter, inch	0.531
Wall thickness, inch	0.291	Wall thickness, inch	0.1095
Header spacing, inches	36.5625	Exposed length of tube in condenser, inches	34.4375
Overall length, inches	39.0625	Outside area, A_o, sq ft/ft	0.1962
Right-end removable header		Inside area, A_i, sq ft/ft	0.1390
Outside diameter, inches	8.5	Area ratio, A_o/A_i	1.41
Inside diameter, inches	6.0	Total outside heat-transfer area, sq ft	0.565
Bolt circle diameter, inches	7.5	Inside cross-sectional area, sq ft	0.001533
Eight 0.5-inch bolts		Logarithmic mean diameter, inch	0.636
Gasket: Garlock No. 7022, 0.125 inch thick		Metal resistance at 212°F, $k_m = 218 \frac{\text{Btu}}{\text{hr-°F-ft}}$, $\frac{\text{hr-°F-sq ft outside}}{\text{Btu}}$	0.000049
End packings		For Runs 56 to 72:	
Chevron type 530		Exposed length of tube in condenser, inches	35.4375
Outside diameter, inches	2.0	Exposed length of brass collar at each end in condenser, inch	0.5625
Inside diameter, inches	1.5	Outside diameter of brass collar, inches	1.50
Depth, inch	1.0	Outside heat-transfer area of collars, sq ft	0.0552
Sight windows		Outside heat-transfer area of tube, sq ft	0.582
Number of windows	6	Total outside heat-transfer area, sq ft	0.6372
Diameter, inches	2.0	Total inside heat-transfer area, sq ft	0.424
Glass thickness, inch	0.50	Area ratio, A_o/A_i	1.504
Inner gasket: Teflon, 0.125 inch thick			
Outer gasket: Crainite, 0.0625 inch thick			

A study of superheated steam is particularly interesting because of its frequent use and the possibility of condensing superheated steam in industrial power plants. At the time steam was selected, it was expected that it could be made to condense filmwise. However, for most of the data on steam, the condensation was a mixture of dropwise and film condensation.

EXPERIMENTAL PROCEDURE AND DATA

The cleaning and assembling of the condenser shell and tube is important, particularly with steam since dropwise condensation occurs under certain conditions. The charging of the apparatus with water or Freon-114 is described as the second step in the procedure. The measurements made on condensing superheated Freon-114 and superheated steam are presented along with tabulations of the data.

CLEANING AND ASSEMBLY OF CONDENSER SHELL AND TUBE

The experimental tube is cleaned thoroughly by first treating with hydrochloric acid, then rinsing with water, and finally rubbing the outside with an acetone-wet pad to remove grease. The condition of the outside surface is important with regard to the type of condensation which is obtained. Low-surface tension fluids in general form a smooth film upon condensation. Stable film condensation is obtained during the condensation of superheated Freon-114. This is illustrated in Figure 5. The actual tube surface can be seen beneath the clear condensate film.

The clean experimental tube does not offer a stable surface for the film condensation of superheated steam. Apparently, small specks of grease or dirt are sufficient to cause the formation of active centers of dropwise condensation. The nature of the surface and its effect on the type of condensation has been studied extensively.[33] An interesting description of the two types of condensation is given by Jakob.[23] Fatica and Katz[20] present a fundamental study and a method of predicting dropwise condensation of steam. A more recent study by Hampson[22] gives also

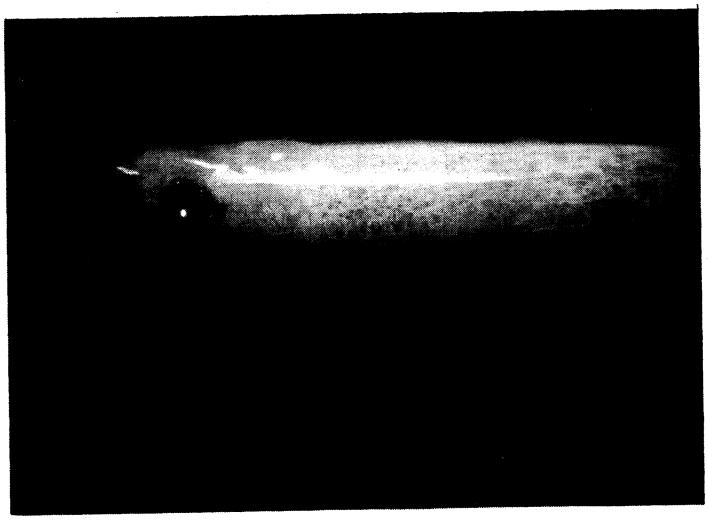

FIGURE 5– FILM CONDENSATION OF SUPERHEATED FREON–114

FIGURE 6– DROPWISE CONDENSATION OF SUPERHEATED STEAM

many references in this field.

Several attempts made during this investigation to obtain stable film condensation with superheated steam include various degrees of polishing of the surface, and the use of very small amounts of organic polar compounds (e.g., alcohols) as wetting agents. No appreciable variation in the transition period from initial film to eventual mixed condensation of steam is observed by such technics. Figure 6 illustrates dropwise condensation of superheated steam.

The clean tube is placed in the condenser in such a manner that the brass collars protrude at the two ends as shown in Figure 3. The tube is secured tightly with Chevron packing and the packing glands. Tube assembly is completed by connecting the tube to the water line with the rubber hose connections (No. 15 in Figure 2) and joining the four thermocouples to the main thermocouple circuit through Cinch-Jones connectors.

CHARGING AND OPERATING THE EQUIPMENT

The experimental apparatus is evacuated prior to charging. A Duo-Seal vacuum pump is used for about one hour to reduce the pressure in the apparatus to about 0.1 inch Hg absolute, as shown in Figure 2. At the end of this period valve A is shut off and the vacuum pump is stopped and separated from the condenser vent. The system is charged with Freon-114 by placing the cylinder in a horizontal position and connecting it to vent A. Valves J, K, and N are shut off and cold water is run through the condenser tube by turning on valve L. Valve A is opened and the system charged by condensing Freon-114. The reboiler level is sufficiently high when about 50 lb of Freon-114 are introduced.

To charge the system with distilled water, vent A is shut off after

evacuating the apparatus, and a 3-gallon bottle of distilled water connected to the reboiler vent b. The reboiler level is sufficiently high when about 2.75 gallons of water are introduced. No cold water is run through the condenser tube during this period.

The auxiliary equipment is arranged to provide hot water at a constant temperature and flow rate. Valves G, K, L, M, and O are shut off and the reservoir is filled with water up to a level 10 inches from the top. Valve N is turned on, the stirrer and the centrifugal pump are started, and the water is circulated through the water heater and raised to the desired temperature level. Valve M is then turned on completely and the desired water flow rate is maintained with control valve E. The selected condenser pressure is obtained by controlling the steam flow rate into the reboiler.

To superheat the vapor the thermostat is set at the desired temperature and the power switched on.

The average tube-side water temperature is maintained constant by a combination of the following methods: by controlling the steam pressure of the water heater, by varying the amount of cooling in the water cooler, and by draining some hot water from the reservoir through valve O and introducing some cold water through valve I.

The system is purged from non-condensables by bleeding vapor through vent A and the manometer vent. The system is free of all non-condensables when no variation is obtained for the tube-side temperature rise under steady operating conditions. During the condensation of steam under vacuum the vacuum pump is used to apply a continuous suction through vent A. This avoids the accumulation of non-condensables due to leakage.

The experimental data consist of the following measurements: condenser

temperatures, condenser tube-wall temperatures, tube-side water flow rate, inlet and outlet water temperatures, room temperature, and barometric pressure.

EXPERIMENTAL DATA

Experimental data are presented for Freon-114 at two pressures, steam at four pressures, and for "dry point" studies for steam under vacuum. The procedure consisted of condensing saturated vapor followed by various degrees of superheat up to 180°F for Freon-114 and 184°F for steam. A sample of the original data is shown in Table IX of Appendix C along with the calculation of results.

Condensation of Freon-114 is studied at two pressures of 77.0 and 43.7 lb per sq in. absolute and different vapor superheats ranging from 0°F to 179.67°F. These experimental data and the calculated results are given in Table II as run numbers 1 through 26.

The condensation of superheated steam involves several studies. Four sets of data are taken comparable to those of Freon-114 at constant pressures of 9.16, 23.87, 23.35, and 44.09 lb per sq in. absolute with maximum superheats varying from 109.12°F to 184.25°F. These runs are presented in Table III. The wall temperature is measured for run numbers 40 through 55. Run numbers 56 through 72 are made without measurement of the experimental wall temperatures and are taken on the original tube without the four thermocouples and with characteristic given at the end of Table I. These runs are interesting because they constitute the only data obtained in this study with relatively stable film condensation of steam. Wall temperatures for runs 56 through 72 are calculated from the experimentally determined equation for the prediction of the tube-side heat transfer coefficient, as shown in Appendix B.

TABLE II

EXPERIMENTAL DATA AND CALCULATED RESULTS FOR SUPERHEATED FREON-114
(Film Condensation)

1	2	3	4	5	6	7	8	9	10	11	12	13	14	15	16	17	18	19	20	21	22	23	24	25	26	27	28
Run No.	Condenser Pressure, P_s, psia	Condenser Temp., T_s, °F	Saturation Temp., °F T_{sv}, °F	Superheat, ΔT_s, °F	Water Flow Rate W_t, lb/hr	Avg. Water Temp., t_w, °F	Water Temp. Rise Δt_t, °F	Total Heat Transferred Q, Btu/hr	Heat-Transfer Rate Q/A, Btu/hr-sq ft	Overall Temp. Difference, ΔT_{ov}, °F	Overall Coefficient U_o, Btu/hr-°F-sq ft out	Outside Tube Surface Temp. t_o, °F	Outside Film Temp. Difference Δt_o, °F	Outside Film Coefficient h_o, Btu/hr-°F-sq ft out	−Enthalpy Change, −ΔH, Btu/lb	Condensing Load, W_s, lb/hr	Condensing Rate, M_s, lb/hr-sq ft	Condensate Film Temp. Difference, Δt_c, °F	Condensate Film Coefficient, h_c, Btu/hr-°F-sq ft out	Interphase Film Temp. Difference Δt_i, °F	Interphase Film Coefficient, h_i, Btu/hr-°F-sq ft out	Condensate Surface Temp. T_s, °F	Film Resistances, r_s, hr-°F-sq ft out/Btu: Outside, r_o	Condensate, r_c	Interphase, r_i	$h_c' = \frac{Q/A}{(T_{sv} - t_o)}$, Btu/hr-°F-sq ft out	$h_c' = 0.725 \sqrt[4]{\frac{k^3 \rho^2 g (-\Delta H)}{\mu d (T_{sv} - t_o)}}$, Btu/hr-°F-sq ft out
1	77.22	135.38	135.38	0	2510	48.92	2.843	7150	12,650	84.46	149.9	58.89	74.49	170.0	49.29	145.1	256.0	74.49	170.0	--	--	135.38	0.00589	0.00589	---	170.0	
2	76.73	138.94	138.94	0	2480	48.72	2.88	7150	12,650	84.22	150.1	58.66	74.28	170.4	49.01	145.8	256.0	74.28	170.4	--	--	152.94	0.00586	0.00586	---	170.3	175.8
3	---	135.44	--	0.28	2480	48.72	2.88	7150	12,650	84.72	149.2	58.80	74.64	169.5	49.41	145.0	256.5	70.90	178.8	3.74	5580	129.70	0.00590	0.00560	0.00050	170.2	175.8
4	---	135.07	--	1.91	2480	48.92	2.843	7060	12,500	86.15	145.0	60.35	74.72	167.2	49.78	141.8	251.0	69.90	179.0	4.82	2590	130.25	0.00598	0.00554	0.00044	171.8	176.0
5	---	136.89	--	3.73	2455	49.12	2.805	6894	12,200	87.77	139.0	58.57	78.32	156.0	50.05	137.8	243.9	66.90	182.7	11.42	1068	125.47	0.00641	0.00549	0.00092	163.3	176.3
6	---	140.80	--	7.04	2455	49.20	2.824	6940	12,280	91.00	135.0	60.39	79.81	154.0	50.62	137.0	242.5	67.50	181.8	12.51	997	127.89	0.00650	0.00550	0.00100	168.7	177.0
7	---	139.08	--	25.86	2455	49.38	2.843	6990	12,360	109.64	112.8	59.21	99.81	123.8	53.81	130 0	230.1	66.60	185.4	33.21	374	125.81	0.00809	0.00540	0.00269	167.1	179.8
8	---	169.57	--	32.21	2455	49.32	2.862	7035	12,430	116.05	107.1	58.89	186.48	116.8	54.88	126.2	229.9	66.50	187.0	39.98	312	125.39	0.00857	0.00535	0.00322	167.4	180.8
9	---	170.88	--	[illegible]	2455	49.32	2.824	6940	12,280	121.56	101.0	58.75	118.13	109.4	55.88	124.2	219.8	64.30	189.3	47.33	259.5	123.55	0.00914	0.00529	0.00385	165.0	181.2
10	---	189.35	--	56.19	2455	49.46	2.88	7060	12,500	139.89	89.4	58.39	130.96	95.5	59.26	119.2	211.0	65.00	190.4	65.96	189.5	123.39	0.01048	0.00520	0.00528	167.1	183.7
11	---	197.02	--	63.86	2455	49.46	2.88	7060	12,500	147.56	84.7	58.07	138.95	90.0	60.65	116.2	205.7	64.60	193.5	74.35	168.2	122.67	0.01111	0.00516	0.00595	166.3	185.2
12	---	208.17	--	75.01	2455	49.48	2.918	7150	12,660	158.69	79.8	54.25	153.92	82.2	62.58	114.0	201.8	64.30	196.8	89.62	141.1	118.55	0.01218	0.00509	0.00709	160.4	186.7
13	---	206.72	--	93.56	2455	49.48	2.938	7207	12,750	177.24	71.9	57.11	169.61	75.2	66.00	109.2	193.3	64.40	198.8	105.21	121.0	121.51	0.01350	0.00504	0.00846	167.8	189.0
14	---	246.13	--	112.99	2455	49.50	3.003	7380	13,060	196.65	66.5	56.54	189.61	68.9	69.58	106.0	187.6	65.40	199.6	124.21	105.0	121.94	0.01452	0.00501	0.00951	170.2	191.2
15	---	263.43	--	130.27	2455	49.50	3.06	7510	13,300	213.93	62.1	54.18	209.25	63.6	72.78	103.2	182.7	65.50	203.4	143.75	92.5	119.68	0.01572	0.00493	0.01079	168.3	193.7
Avg. Value	76.98		135.16		2484	49.25																					
16	43.74	96.42	96.42	0	2570	48.73	2.16	5555	9,820	47.69	206.0	57.35	39.09	251	53.39	104.2	184.2	39.09 (Assumed constant - Runs 16-20)	251.0	0	---	96.42	0.00398	0.00398	0	251	217
17	---	106.25	--	9.83	2570	48.73	2.197	5680	10,000	57.47	174.0	56.88	49.37	202.5	55.06	102.6	181.6	39.09	256.0	10.28	974	95.97	0.00494	0.00391	0.00103	253	218.6
18	---	122.90	--	26.48	2570	48.78	2.214	5694	10,070	74.12	135.8	57.15	65.75	153.0	57.79	98.5	174.2	39.09	257.4	26.66	377	96.24	0.00654	0.00389	0.00265	256	221
19	---	138.51	--	42.09	2570	48.78	2.214	5694	10,070	89.73	112.1	56.47	82.04	122.7	60.40	94.3	166.8	39.09	257.4	42.95	234	95.56	0.00816	0.00389	0.00427	252	224
20	---	157.77	--	61.35	2570	48.75	2.214	5694	10,070	109.04	92.3	55.42	102.35	98.5	65.76	89.5	158.0	39.09	257.4	63.26	159	94.51	0.01018	0.00389	0.00629	245.6	227
21	---	202.67	--	106.25	2570	48.60	2.086	5360	9,500	154.07	61.6	53.55	149.12	63.7	71.56	75.0	152.8	41.00	251.5	108.12	87.9	94.55	0.0157	0.00333	0.001137	222	233.6
22	---	205.56	--	109.14	2570	48.60	2.07	5320	9,430	156.96	60.0	50.67	154.89	60.9	72.11	73.9	150.7	40.20	254.5	114.69	82.2	90.87	0.01643	0.00326	0.01217	206	234
23	---	211.09	--	114.67	2570	48.56	2.086	5360	9,500	162.53	58.5	53.52	157.77	60.2	73.06	73.4	150.0	40.55	253.8	117.22	81.0	93.87	0.0166	0.00329	0.01231	220	234.3
24	---	230.59	--	134.17	2570	48.64	1.98	5090	9,000	181.95	49.5	51.67	178.92	50.3	76.61	66.4	117.4	37.00	242.4	141.92	63.5	88.67	0.0199	0.00412	0.01578	201	237.6
25	---	257.61	--	161.19	2570	48.60	1.98	5090	9,000	209.01	43.0	50.77	206.84	43.5	81.53	62.4	110.5	36.20	242.0	170.64	52.7	86.97	0.0230	0.00404	0.01896	197	241
26	---	276.09	--	179.67	2570	48.48	1.942	4990	8,850	227.61	38.9	49.44	226.65	39.0	84.96	58.65	104.0	34.70	254.4	191.95	46.0	84.14	0.02565	0.00393	0.02172	182.5	244
Avg. Value	43.74		96.42		2570	48.66																					

TABLE III

EXPERIMENTAL DATA AND CALCULATED RESULTS FOR SUPERHEATED STEAM

1	2	3	4	5	6	7	8	9	10	11	12	13	14	15	16	17	18	19	20	21	22	23
Run No.	Condenser Pressure P_g, psia	Condenser Temp., T_g, °F	Saturation Temp., T_{sv}, °F	Superheat ΔT_s, °F	Water Flow Rate W_t, lb/hr	Avg. Water Temp., t_w, °F	Water Temp. Rise Δt_t, °F	Total Heat Transferred Q, Btu/hr	Heat Transfer Rate Q/A, Btu/hr-sq ft	Overall Temp. Difference, ΔT_{OA}, °F	Overall Coefficient U_o, Btu / hr-°F-sq ft out	Outside Tube Surface Temp. t_o, °F	Outside Film Temp. Difference Δt_o, °F	Outside Film Coefficient h_o, Btu / hr-°F-sq ft out	− Enthalpy Change, $-\Delta H$, Btu / lb	Condensing Load, W_g, lb/hr	Condensing Rate, M_g, lb/hr-sq ft	Condensate Film Temp. Difference, Δt_c, °F	Condensate Film Coefficient, h_c, Btu / hr-°F-sq ft out	Interphase Film Temp. Difference Δt_i, °F	Interphase Film Coefficient, h_i, Btu / hr-°F-sq ft out	Condensate Surface Temp. T_s, °F
Mixed Condensation																						
40	9.149	192.46	189.04	3.42	2666	177.60	3.26	8,700	15,400	14.86	1037	188.76	3.70	4160	986.37	8.82	15.6	0.28	55,000	3.42	4505	189.04
41	9.168	200.69	189.14	11.55	2666	177.20	3.31	8,840	15,620	23.49	665.0	188.70	11.99	1302	990.17	8.93	15.8	0.285	54,900	11.705	1334	188.985
42	9.098	223.33	188.78	34.55	2666	177.60	2.90	7,740	13,700	45.73	229.6	187.02	36.31	377.0	1001.43	7.72	13.68	0.238	57,600	36.07	380	187.26
43	9.218	269.69	189.39	80.30	2666	178.00	2.88	7,690	13,600	91.69	148.2	181.85	87.84	154.8	1023.03	7.50	13.28	0.234	58,100	87.61	155.2	182.08
44	9.168	288.43	189.14	99.29	2666	177.20	2.824	7,550	13.340	111.23	119.8	183.96	104.47	127.8	1032.25	7.51	12.92	0.228	58,600	104.24	128	184.19
45	9.168	298.26	189.14	109.12	2666	177.60	2.52	6,720	11,900	120.66	98.6	178.97	119.29	99.6	1037.05	6.49	11.49	0.195	61,000	119.10	99.9	179.16
Avg. Value	9.16		189.10		2666	177.53																
Mixed Condensation																						
46	23.87	237.28	237.28	0	6050	177.40	11.08	67,000	118,500	59.88	1978	209.90	27.38	4330	953.97	70.3	124.2	27.38	4,330	—	--	237.28
47	---	253.96	---	16.68	6050	178.0	10.4	63,000	111,400	75.96	1468	209.55	44.41	2510	962.38	65.5	116.0	25.10	4,440	19.31	5760	234.65
48	---	260.89	---	23.61	6050	178.25	10.30	62,400	110,200	82.64	1334	209.48	51.41	2145	965.89	64.5	114.1	24.80	4,450	26.61	4150	234.28
49	---	268.10	---	30.82	6050	178.40	10.4	62,900	111,200	89.70	1240	209.42	58.68	1892	969.57	64.9	114.8	25.00	4,450	33.68	3300	234.42
50	---	304.70	---	67.42	6050	178.20	9.99	60,500	107,000	126.5	846	207.18	97.52	1098	987.39	61.3	108.4	23.5	4,450	74.02	1447	230.68
51	---	360.00	---	122.72	6050	177.75	9.50	57,500	101,800	182.25	558	199.10	160.90	632	1013.97	56.6	100.2	21.9	4,650	139.0	732	221.00
52	---	370.49	---	133.21	6050	180.72	9.45	57,100	101,200	189.77	534	203.94	166.55	608	1018.97	56.1	99.4	21.7	4,660	144.85	699	225.64
53	---	390.10	---	152.82	6050	176.95	9.50	57,500	101,800	213.15	477	197.10	193.00	526	1028.47	56.0	99.0	21.75	4,680	171.25	594	218.85
54	---	408.00	---	170.72	6050	178.00	9.41	57,000	101,000	230.0	439	202.91	205.09	492	1036.57	55.0	97.3	21.5	4,700	183.59	550	224.41
55	---	421.53	---	184.25	6050	176.82	9.24	55,900	99,000	244.71	404	194.70	226.83	435.5	1043.37	53.5	94.6	20.8	4,750	206.03	480	215.5
Avg. Value	23.87		237.28		6050	178.05																
Film Condensation (t_o calculated from predicted tube-side water film coefficient — Appendix B)																						
56	23.441	236.52	236.52	0	4855	177.40	7.20	35,000	54,900	59.12	928	212.03	24.49	2240	954.26	36.7	57.6	24.49	2,218	--	--	236.52
57	23.299	236.19	236.19	0	4855	177.56	7.13	34,650	54,400	58.83	925	211.66	24.53	2220	954.68	36.32	57.0	24.53	2,215	--	--	236.19
58	23.312	236.22	236.22	0	4855	177.35	7.10	34,430	54,000	58.87	919	211.42	24.80	2180	954.66	36.10	56.6	24.80	2,220	--	--	236.22
59	---	246.38	---	10.07	4855	176.20	6.79	33,000	51,650	68.18	758	210.77	35.61	1450	959.74	34.40	54.0	23.0	2,246	12.61	4100	233.77
60	---	265.96	---	29.65	4855	177.32	6.65	32,350	50,650	88.64	571	209.35	56.61	895	969.52	33.40	52.4	22.4	2,262	34.21	1480	231.75
61	---	283.60	---	47.29	4855	177.56	6.71	32,600	51,100	106.04	482	209.66	73.74	694	978.18	33.35	52.3	22.6	2,263	51.14	1000	232.46
62	---	288.83	---	52.52	4855	177.12	6.65	32,300	50,600	111.71	454	209.15	79.68	635	980.78	32.95	51.6	22.2	2,280	57.48	881	231.35
63	---	335.29	---	98.98	4815	177.22	6.43	31,000	48,500	158.07	307	207.90	127.39	380	1003.10	30.85	48.5	20.90	2,318	106.49	455	228.80
64	---	366.50	---	130.19	4855	177.09	6.18	30,000	47,050	189.41	248.2	206.82	159.68	295	1018.10	29.5	46.3	20.16	2,340	139.52	338	226.98
65	---	395.07	---	158.76	4855	176.76	5.92	28,800	45,100	218.31	206.4	205.32	189.75	238	1031.60	27.9	43.7	18.98	2,380	170.83	264	224.24
66	---	402.77	---	166.46	4855	177.75	6.30	30,600	48,000	225.02	213	208.10	194.67	246.5	1035.50	29.6	46.4	20.50	2,340	174.17	275.5	228.60
Avg. Value	23.351		236.31		4851	177.38																
Film Condensation (t_o calculated from predicted tube-side water film coefficient — Appendix B)																						
67	44.088	273.17	273.17	0	4855	178.79	11.58	56,200	88,200	94.38	935	234.21	38.96	2260	929.54	60.5	94.9	38.96	1,963	--	--	273.17
68	---	302.48	---	29.31	4855	176.96	9.93	48,150	75,600	125.52	602	224.66	77.82	972	944.94	51.0	80.0	36.9	2,044	40.92	1850	261.56
69	---	372.83	---	99.66	4855	177.75	9.50	46,100	72,400	195.08	370.5	223.39	149.44	484	980.14	47.05	73.9	34.5	2,097	114.94	630	257.89
70	---	378.32	---	105.15	4855	177.02	9.635	46,800	73,400	201.30	364.5	223.32	155.00	473	983.04	47.55	74.6	35.2	2,082	119.80	612	258.52
71	---	416.5	---	143.33	4855	177.46	9.51	45,200	71,000	239.04	297	222.29	194.21	365	1001.64	45.15	70.9	33.6	2,115	160.61	441	255.89
72	---	418.91	---	145.74	4855	177.38	9.36	45,500	71,400	241.53	296	222.43	196.48	363	1002.64	45.3	71.1	33.8	2,106	162.68	439	256.23
Avg. Value	44.088		273.17		4855	177.56																

Runs 27 through 39 are made with superheated steam under vacuum to study the wall temperature and heat flux under conditions where a superheated vapor might not condense and wet the surface. These runs are summarized in Table IV.

Runs 73 through 105 are made with saturated steam at 225.76°F to 248.59°F to study the tube-side heat transfer coefficient for water. Runs 73 through 84 are made prior to the installation of wall thermocouples whereas runs 85 through 105 are made with measured wall temperatures. The conditions for all runs are controlled to give Wilson-plot type data.[49] Appendix B presents the calculation and discussion of these results and those on the longitudinal temperature gradient in the tube wall based on runs 101 through 105. Experimental data and calculated results for runs 73 through 105 are given in Tables VI, VII, and VIII in Appendix B.

TABLE IV

EXPERIMENTAL DATA AND CALCULATED RESULTS FOR SUPERHEATED STEAM
(Mixed Condensation - Dry-Point Runs)

1	2	3	4	5	6	7	8	9	10	11	12	13	14	15	16	17	18
Run No.	Condenser Pressure P_g, psia	Condenser Temp., T_g, °F	Saturation Temp., T_{sv}, °F	Superheat ΔT_s, °F	Water Flow Rate W_t, lb/hr	Avg. Water Temp., t_w, °F	Water Temp. Rise Δt_t, °F	Total Heat Transferred Q, Btu/hr	Heat-Transfer Rate Q/A, Btu/hr-sq ft	Overall Temp. Difference, ΔT_{oa}, °F	Overall Coefficient U_o, Btu/hr-°F-sq ft out	Outside Tube Surface Temp. t_o, °F	Outside Film Temp. Difference Δt_o, °F	Outside Film Coefficient h_o, Btu/hr-°F-sq ft out	Temp. Difference ($T_{sv}-t_o$), °F	Condensing Load, W_s, lb/hr	**Condensing Rate,** M_s, lb/hr-sq ft
27	9.0	235.00	188.28	46.72	4215	176.23	1.062	4480	7940	58.77	135.0	179.56	55.44	143.2	8.72	4.45	7.88
28	8.8	231.95	187.22	44.73	4215	176.17	0.936	3950	7000	55.78	125.3	179.17	52.78	132.6	8.05	3.925	6.95
29	8.6	230.16	186.17	43.99	4215	176.19	0.774	3260	5765	53.97	107.0	178.80	51.36	112.3	7.37	3.24	5.74
30	8.0	226.12	182.86	43.26	4215	176.00	0.396	1670	2960	50.12	59.0	177.47	48.65	60.9	5.39	1.656	2.93
31	7.8	222.80	181.69	41.11	4215	175.84	0.288	1214	2150	46.96	45.8	177.25	45.55	47.2	4.44	1.207	2.135
32	7.7	220.33	181.11	39.22	4215	175.73	0.252	1062	1880	44.60	42.1	177.10	43.23	43.5	4.01	1.056	1.867
33	7.6	218.89	180.52	38.37	4215	175.70	0.198	835	1480	43.19	34.3	177.00	41.89	35.3	3.52	0.830	1.470
34	7.5	217.24	179.94	37.30	4215	175.60	0.162	684	1210	41.64	29.0	176.91	40.33	30.0	3.03	0.679	1.202
Avg. Value					4215	175.93											
35	9.35	266.35	190.04	76.31	2666	191.80	←	Very Small	→	74.55	Very Small	191.08	←	Very Small	→	-1.04	Surface Condition: Dry
36	9.27	270.66	189.64	81.02	2666	189.10	---	---	---	81.56	---	188.64 Low	---	---		1.00	Wet
37	9.11	267.77	188.83	78.94	2710	189.20	---	---	---	78.57	---	188.80 Low	---	---		0.03	Getting Dry
38	8.98	266.85	188.18	78.67	2710	189.20	---	---	---	77.65	---	188.88	---	---		-0.70	Dry
39	8.89	269.42	187.70	81.72	2710	188.30	---	---	---	81.12	---	188.60 High	---	---		-0.90	Dry

CALCULATION AND CORRELATION OF RESULTS

This section presents the experimental results obtained from the original data, the discussion of the mechanism and theory of filmwise condensation of superheated vapors, the correlation of experimental and calculated results, and an outline for the design of superheated vapor condensers.

The experimental results are presented in a manner which shows the effect of superheat on the overall heat flux, the condensing load, and the overall outside film coefficient. These results are given in Table II for Freon-114 and Table III for steam. The variation of these results for the case where the degree of superheat of the vapor does not vary appreciably while the saturation temperature of the vapor approaches that of the outside tube surface is discussed and summarized in Table IV.

The concept of the vapor-liquid interfacial film is applied to the condensation of superheated vapors. The calculated condensate surface temperature is used to obtain the temperature difference across the condensate film and the interfacial vapor film. The temperature difference through the interfacial film is used to determine the interfacial film coefficient. The results of these calculations are shown in Tables II and III for Freon-114 and steam, respectively. The assumptions involved in the application of this mechanism is discussed.

The experimental results are correlated on the basis of the interphase mass and energy transfer theory presented and discussed in the literature review. The effect of assuming interfacial equilibrium

$$\frac{T_s}{T_g} = 1.0$$

is discussed and illustrated in the correlation of results. The experimental condensing load is correlated with the degree of superheat and the interfacial temperatures and pressures as a function of the condensation coefficient (f). The calculated interfacial film coefficients are correlated with the temperature drop through the interfacial film and the interfacial temperatures and pressures as a function of the condensation coefficient. Table V presents the results of these calculations.

A comparison is made between the condensate film coefficient obtained by the conventional design method presented previously and the experimental coefficients calculated on the same basis. The recommended correlations are used to outline a method for the design of superheated vapor condensers.

OVERALL PERFORMANCE OF CONDENSER WITH SUPERHEATED VAPORS

The experimental heat transfer rates and condensing loads are presented in this section. The rate of heat transfer in the condenser is determined from the tube-side water flow rate and the temperature rise of the water by the following equation:

$$\frac{Q}{A} = \frac{W_t C_p (T_2 - T_1)}{A} \qquad (21)$$

where

Q = total heat transferred, Btu per hr

W_t = water flow rate, lb per hr

T_2 = outlet water temperature, °F

T_1 = inlet water temperature, °F

C_p = specific heat of water, Btu per (lb)(°F)

A = total outside heat transfer area, sq ft.

TABLE V

CORRELATION OF CALCULATED CONDENSING RATES AND INTERPHASE FILM COEFFICIENTS
(Based on Results in Figure 18)

1	2	3	4	5	6	7	8	9	10	11	12	13	14	15
Run No.	Condensate Surface Temp., T_s, °F	Condensate Surface Pressure, P_s, psia	Square Root of Absolute Temp., $\sqrt{T_s}$, °R	Interphase Pressure Difference (P_g-P_s), psi	Function of Condensation Coefficient $E(f) = \frac{m_s\sqrt{T_s}}{(P_g-P_s)}$	Superheat, ΔT_s, °F	Depression of Condensate Surface Temp., $(T_{sv}-T_s)$, °F	Interphase Film Temp. Difference Δt_i, °F	Interphase Film Coefficient h_i, $\frac{\text{Btu}}{\text{hr-°F-sq ft out}}$	Correlating Function $F(f) = \frac{h_i\sqrt{T_s}}{(-\Delta H)(P_g-P_s)}$	Interphase Temp. Ratio $\left(\frac{T_s\ °R}{T_g\ °R}\right)$	Pressure Difference Group, psi $\left[P_g\left(\frac{T_s}{T_g}\right)^{1/2} - P_s\right]$	Function of Condensation Coefficient $G(f) = \frac{m_s\sqrt{T_s}}{\left[P_g\left(\frac{T_s}{T_g}\right)^{1/2} - P_s\right]}$	Correlating Function $H(f) = \frac{h_i\sqrt{T_s}}{-\Delta H\left[P_g\left(\frac{T_s}{T_g}\right)^{1/2} - P_s\right]}$
Freon-114 Film Condensation at $\Delta T_s = 0$ $T_s = T_{sv} = 28.00°F$ $P_s = P_g = 71.43$ psia														
1	128.00	71.43	24.32	0	---	0	0	0	---	---	---	---	---	---
2	128.00	71.43	24.32	0	---	0	0	0	---	---	---	---	---	---
3	127.58	70.998	24.24	0.432	14,420	5.44	0.42	5.86	2160	2460	0.9901	0.077	81,000	13,820
4	127.46	70.872	24.24	0.558	10,920	7.07	0.54	7.61	1640	1433	0.9872	0.098	62,200	8,160
5	127.31	70.70	24.24	0.71	8,350	8.89	0.69	9.58	1272	870	0.9839	0.150	39,450	4,120
6	127.06	70.462	24.23	0.968	6,090	12.20	0.94	13.14	934	462	0.9782	0.178	33,100	2,510
7	125.63	68.997	24.20	2.433	2,300	31.02	2.37	33.39	370	68.5	0.9460	0.483	11,530	345
8	125.15	68.51	24.19	2.92	1,880	37.37	2.85	40.22	309	46.5	0.9357	0.590	9,300	231
9	124.74	68.096	24.18	3.334	1,592	42.88	3.26	46.14	266	34.6	0.9268	0.664	8,000	173
10	123.36	66.718	24.15	4.712	1,080	61.35	4.64	65.99	189.2	16.32	0.8984	0.982	5,190	78.5
11	122.79	66.152	24.13	5.278	939	69.02	5.21	74.23	168.2	12.68	0.8871	1.128	4,390	59.3
12	121.96	65.33	24.12	6.10	796	80.17	6.04	86.21	146.8	9.26	0.8710	1.330	3,660	42.4
13	120.61	64.029	24.09	7.401	630	98.72	7.39	106.11	120.2	5.92	0.8455	1.651	2,820	26.8
14	119.20	62.682	24.07	8.748	517	118.15	8.80	126.95	102.8	4.06	0.8202	2.008	2,250	17.7
15	117.972	61.523	24.04	9.907	443	135.43	10.03	145.46	91.5	3.06	0.7990	2.327	1,888	13.0
Freon-114 Film Condensation at $\Delta T_s = 0$ $T_s = T_{sv} = 98.00°F$ $P_s = P_g = 44.89$ psia														
16	98.00	44.89	23.62	0	---	0	0	0	---	---	---	---	---	---
17	97.405	44.458	23.61	0.432	9,910	8.25	0.595	8.845	1132	1122	0.9844	0.080	53,600	6,060
18	96.21	43.592	23.58	1.298	3,170	24.90	1.79	26.69	377	118.3	0.9542	0.258	15,900	596
19	95.104	42.805	23.56	2.085	1,880	40.51	2.896	43.406	232	43.4	0.9275	0.425	9,240	213
20	93.756	41.852	23.53	3.038	1,224	59.77	4.244	64.01	157.2	19.1	0.8964	0.648	5,740	89.5
21	90.69	39.755	23.46	5.135	609	104.67	7.31	111.98	84.9	5.44	0.8310	1.165	2,680	23.9
22	90.496	39.625	23.46	5.265	581	107.56	7.504	115.06	82.0	5.06	0.8271	1.205	2,545	22.2
23	90.126	39.375	23.45	5.515	554	113.09	7.874	120.96	78.5	4.56	0.8197	1.265	2,410	19.9
24	88.834	38.520	23.42	6.37	431	132.59	9.166	141.76	63.5	3.05	0.7947	1.500	1,835	12.9
25	87.074	37.38	23.39	7.51	343	159.61	10.926	170.54	52.7	2.01	0.7624	1.815	1,422	8.34
26	85.89	36.62	23.36	8.27	293	178.09	12.11	190.20	46.5	1.542	0.7416	2.04	1,190	6.26
Steam Mixed Condensation at $\Delta T_s = 0$ $T_s = T_{sv} = 189.10°F$ $P_s = P_g = 9.1608$ psia														
40	188.87	9.1158	25.47	0.0450	8,840	3.36	0.23	3.59	4290	2460	0.9945	0.0196	20,300	5,650
41	188.30	9.0045	25.46	0.1653	2,580	11.59	0.80	12.39	1260	207	0.9812	0.0699	5,760	464
42	186.73	8.7042	25.43	0.4566	761	34.23	2.37	36.60	374	20.8	0.9464	0.2076	1,680	45.9
43	183.57	8.1254	25.37	1.0354	325	80.59	5.53	86.12	158	3.77	0.8820	0.4778	704	8.18
44	182.31	7.904	25.34	1.2568	260	99.33	6.79	106.12	125.8	2.45	0.8582	0.5826	561	5.28
45	181.65	7.790	25.33	1.3710	212	109.16	7.45	116.61	102.0	1.815	0.8462	0.6370	456	3.91
Steam Mixed Condensation at $\Delta T_s = 0$ $T_s = T_{sv} = 238.00°F$ $P_s = P_g = 24.080$ psia														
46	238.00	24.080	26.42	0	---	0	0	0	---	---	---	---	---	---
47	236.20	23.303	26.38	0.777	3,930	15.96	1.80	17.76	6280	221	0.9751	0.475	6,440	362
48	235.43	22.978	26.37	1.102	2,720	22.89	2.57	25.46	4320	106.8	0.9646	0.672	4,460	175.4
49	234.63	22.643	26.35	1.437	2,100	30.10	3.37	33.47	3320	62.9	0.9540	0.877	3,445	102.8
50	230.59	21.012	26.28	3.068	930	66.70	7.41	74.11	1442	12.5	0.9031	1.872	1,522	20.5
51	224.62	18.779	26.16	5.301	494	122.00	13.38	135.38	751	3.64	0.8349	3.224	812	6.00
52	223.50	18.382	26.14	5.699	455	132.49	14.50	146.99	690	3.10	0.8230	3.464	749	5.10
53	221.43	17.668	26.11	6.412	403	152.10	16.57	168.67	604	2.38	0.8016	3.892	664	3.94
54	219.56	17.042	26.07	7.038	361	170.00	18.44	188.44	535	1.912	0.7829	4.265	594	3.16
55	218.15	16.582	26.04	7.498	329	183.53	19.85	203.38	486	1.622	0.7693	4.538	545	2.68
Steam Film Condensation at $\Delta T_s = 0$ $T_s = T_{sv} = 234.50°F$ $P_s = P_g = 22.589$ psia														
56	234.50	22.589	26.35	0	---	0	0	0	---	---	---	---	---	---
57	234.50	22.589	26.35	0	---	0	0	0	---	---	---	---	---	---
58	234.50	22.589	26.35	0	---	0	0	0	---	---	---	---	---	---
59	233.71	22.262	26.34	0.327	4,350	11.88	0.79	12.67	4090	343	0.9821	0.124	11,460	905
60	232.42	21.738	26.31	0.851	1,617	31.46	2.08	33.54	1512	48.2	0.9538	0.322	4,280	127.6
61	231.26	21.276	26.29	1.313	1,043	49.10	3.24	52.34	978	20.02	0.9296	0.504	2,730	52.2
62	230.92	21.142	26.28	1.447	940	54.33	3.58	57.91	876	16.26	0.9227	0.556	2,440	42.2
63	227.90	19.980	26.23	2.609	489	100.79	6.60	107.39	451	4.53	0.8650	1.029	1,238	11.5
64	225.89	19.236	26.19	3.353	362	132.00	8.61	140.61	335	2.57	0.8299	1.343	901	6.41
65	224.07	18.582	26.15	4.007	284	160.57	10.43	171.00	264	1.66	0.8000	1.622	704	4.11
66	223.58	18.411	26.15	4.178	289	168.27	10.92	179.19	268	1.618	0.7923	1.696	715	3.99
Steam Film Condensation at $\Delta T_s = 0$ $T_s = T_{sv} = 265.00°F$ $P_s = P_g = 38.539$ psia														
67	265.00	38.539	26.93	0	---	0	0	0	---	---	---	---	---	---
68	262.63	37.040	26.88	1.495	1,440	37.48	2.37	39.85	1898	36.1	0.9477	0.478	4,500	113.2
69	258.22	34.375	26.80	4.164	475	107.83	6.78	114.61	631	4.15	0.8624	1.415	1,400	12.2
70	257.88	34.175	26.79	4.364	457	113.32	7.12	120.44	609	3.80	0.8563	1.488	1,342	11.1
71	255.52	32.824	26.75	5.715	332	151.5	9.48	160.98	441	2.06	0.8163	1.996	950	5.90
72	255.38	32.747	26.75	5.792	328	153.91	9.62	163.53	436	2.00	0.8140	2.023	940	5.74

Detailed sample calculations are given for run 21 in Appendix C.

The condensing load is obtained from the rate of heat transfer and the enthalpy change of the condensing superheated vapor. Because of the temperature drop through the condensate film, the condensate leaving the condenser is normally assumed to be subcooled. Measurement of the condensate temperature in the liquid return line to the reboiler (Figure 2) indicates that the liquid leaving the condenser is essentially at its saturation temperature. This is due to the intimate contact of the condensate with the superheated vapor in the lower half of the condenser. The proper enthalpy change of the vapor is that corresponding to the condensation of the superheated vapor to the saturated liquid. The condensing load is calculated from the following equation:

$$m_s = \frac{Q}{A(-\Delta H)} \quad . \tag{22}$$

The degree of superheat is defined as the difference between the temperature of the superheated vapor and the saturation temperature corresponding to the condenser pressure. The experimental heat fluxes calculated from equation 21 are presented in Figure 7 for Freon-114 and in Figure 8 for steam. The general trend indicated is a gradual decrease in the heat flux due to superheat. The effect of superheat on the heat flux varies for the various pressures. At 140°F superheat the reduction in heat flux compared to the heat flux at saturation varies from 6.4 per cent for superheated Freon-114 condensing at 43.7 lb per sq in. absolute to 23.4 per cent for superheated steam condensing at 9.2 lb per sq in. absolute. An increase in heat flux with superheat is indicated only by the Freon-114 data obtained at 77.0 lb per sq in. absolute. At a superheat of 140°F the heat flux of superheated Freon-114 is 5.8 per cent higher than the corresponding saturated vapor.

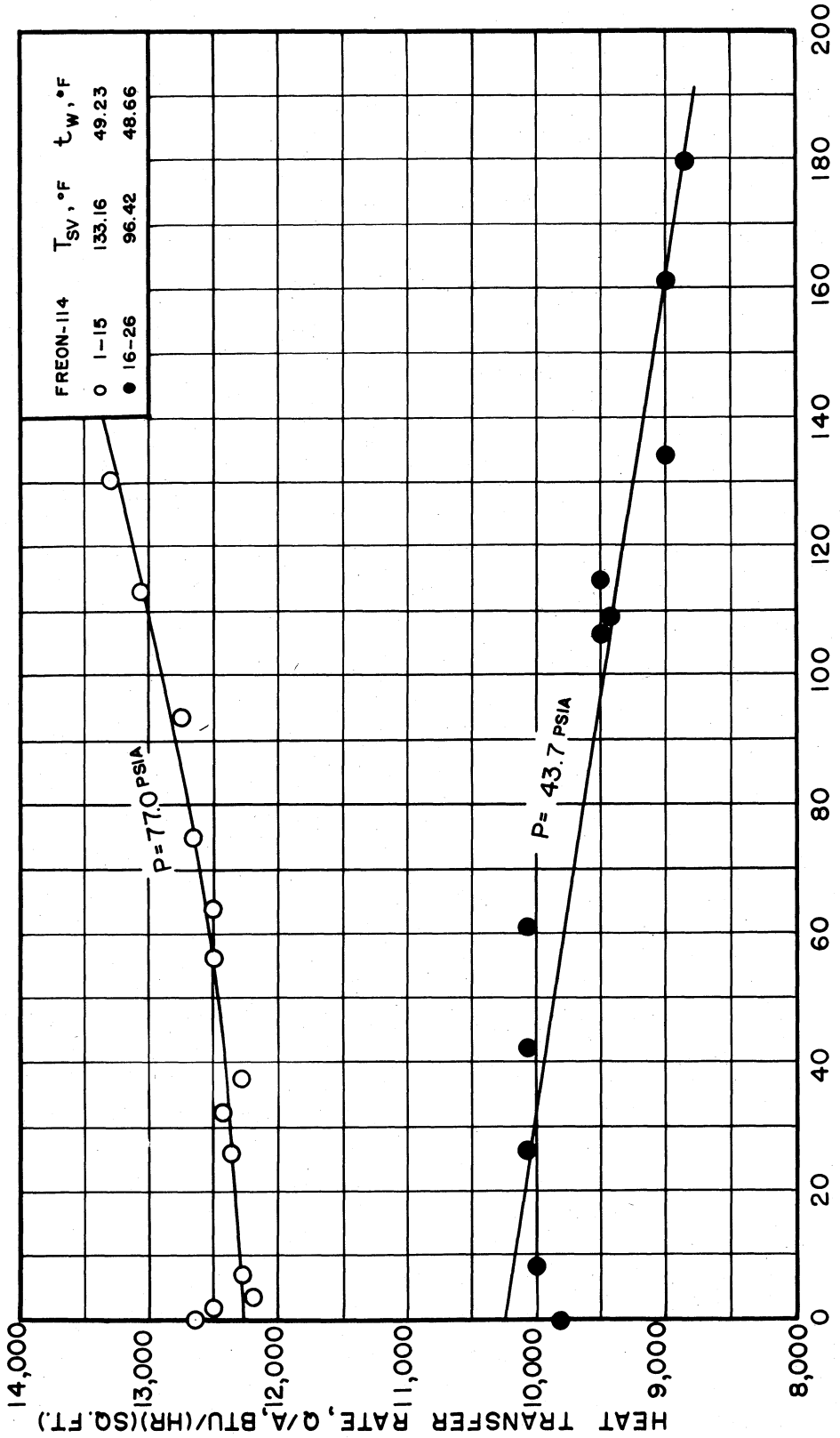

FIGURE 7- EFFECT OF SUPERHEAT ON HEAT FLUX FOR CONDENSATION OF FREON-114

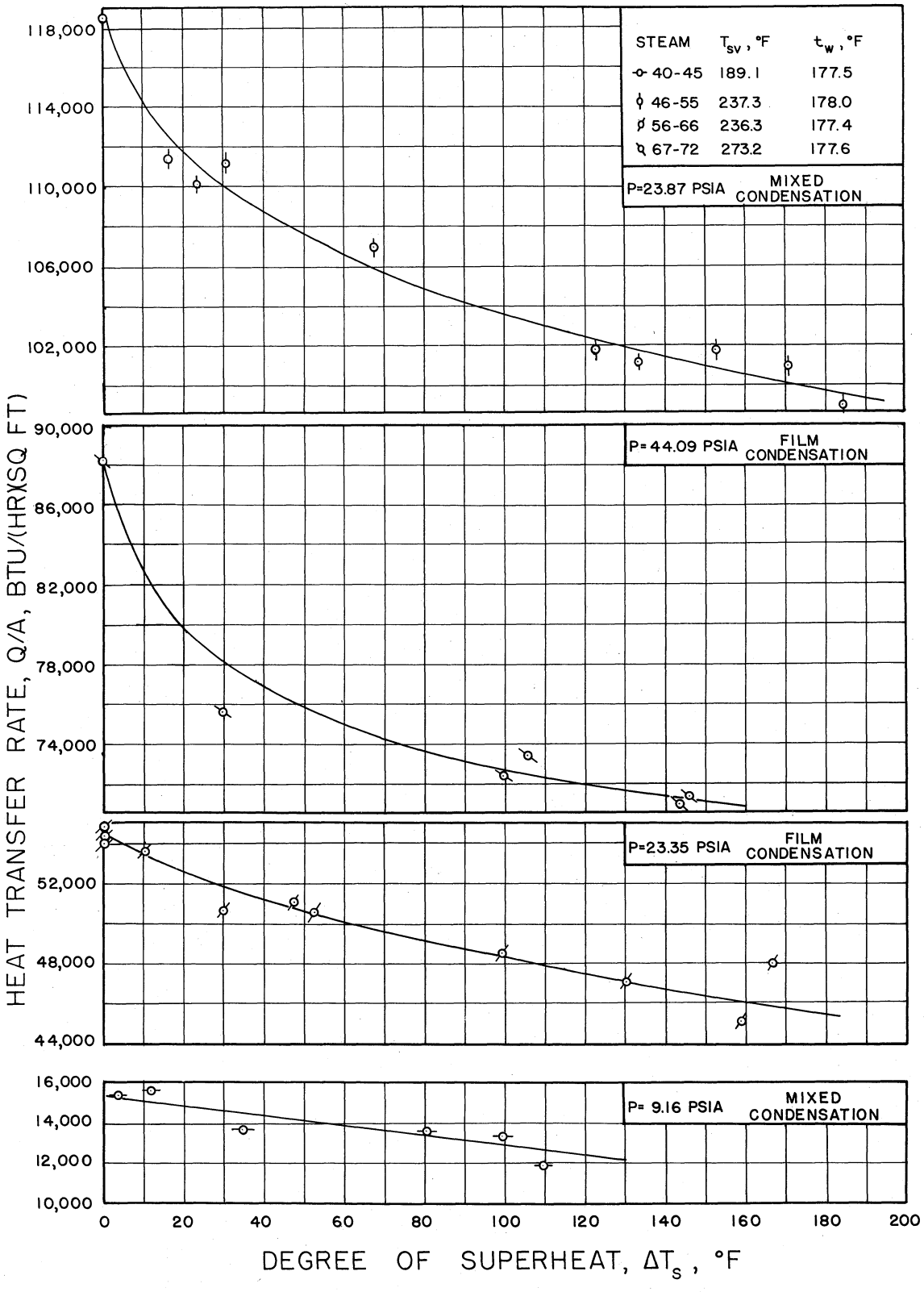

FIGURE 8— EFFECT OF SUPERHEAT ON HEAT FLUX FOR CONDENSATION OF STEAM

It is interesting to observe the trend indicated for the effect of superheat on the condensing load in order to interpret the overall performance of superheated vapors. The condensing loads calculated from equation 22 are presented in Figure 9 on a semilogarithmic plot of the condensing load versus the degree of superheat. In all cases for both Freon-114 and steam the condensing load decreases gradually with the superheat. A comparison of Figures 7 and 8 with Figure 9 indicates that at the lowest condensing loads represented by the steam data at 9.2 lb per sq in. absolute the reduction in heat transfer for a 140°F superheat is a maximum of 23.4 per cent. For intermediate condensing loads this reduction is 14.1 to 19.0 per cent. For the higher condensing loads represented by the Freon-114 data at 43.7 lb per sq in. absolute the reduction in the heat transfer rate is a minimum of 6.4 per cent for the same degree of superheat. At the highest condensing loads with Freon-114 condensing at 77.0 lb per sq in. absolute the trend in the heat transfer rate is reversed and there is an increase of 5.8 per cent in the heat flux.

These results indicate that the trend obtained for the effect of superheat on the heat flux curve depends on the condensing load, Figure 9a. This is due to the fact that an uncertain amount of desuperheating of the vapor occurs in the condenser because of the intimate contact of the subcooled condensate flowing from the tube surface with the vapor zone surrounding it. During this process of desuperheating of the vapor and heating of the condensate some vaporization of the condensate may occur specially at high superheats. This process of heat transfer and that due to intraphase heat transfer will be referred to as the secondary process of heat transfer to differentiate it from heat transfer occurring at the

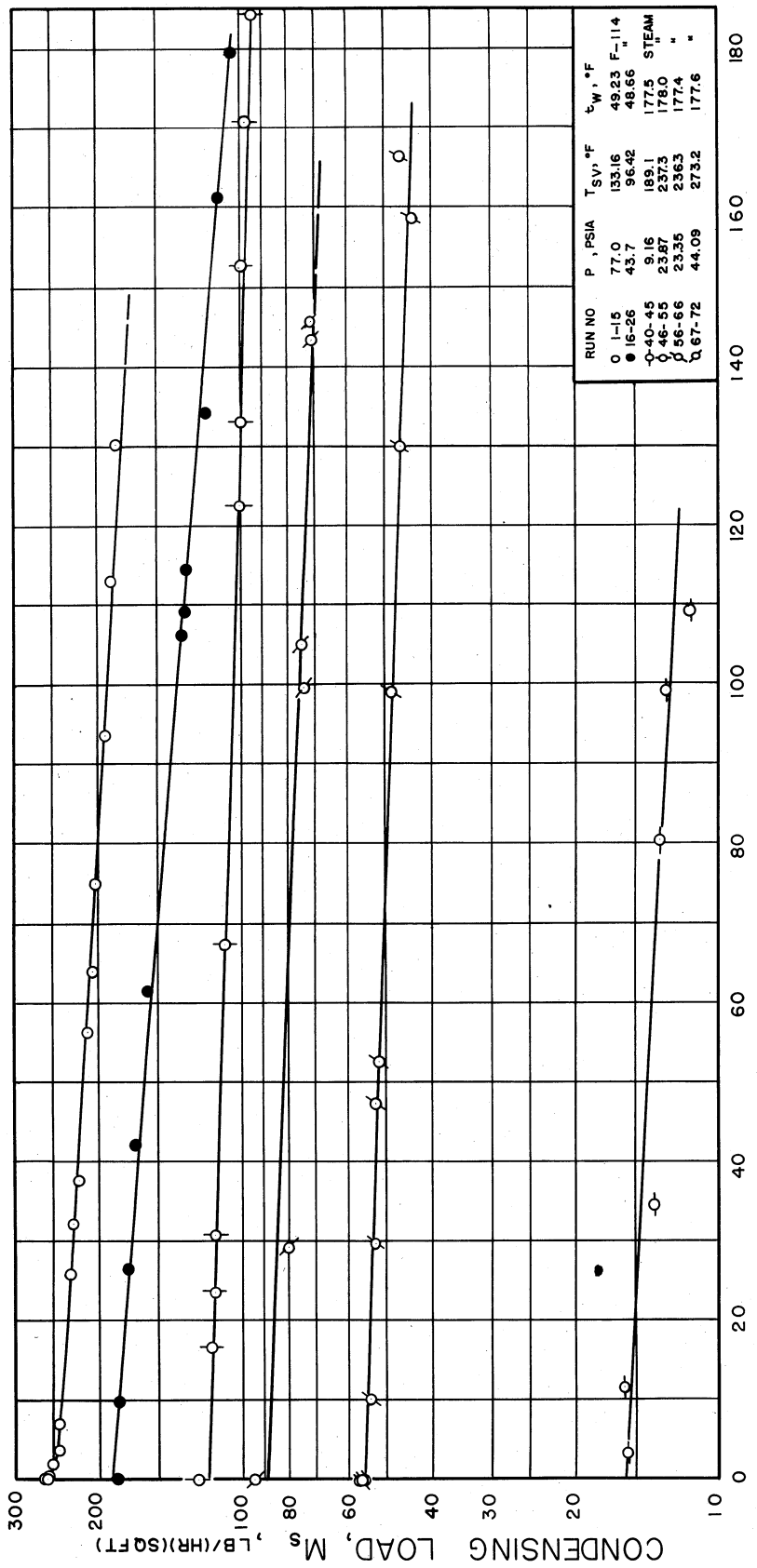

FIGURE 9- EFFECT OF SUPERHEAT ON CONDENSING LOAD FOR CONDENSATION OF FREON-114 AND STEAM

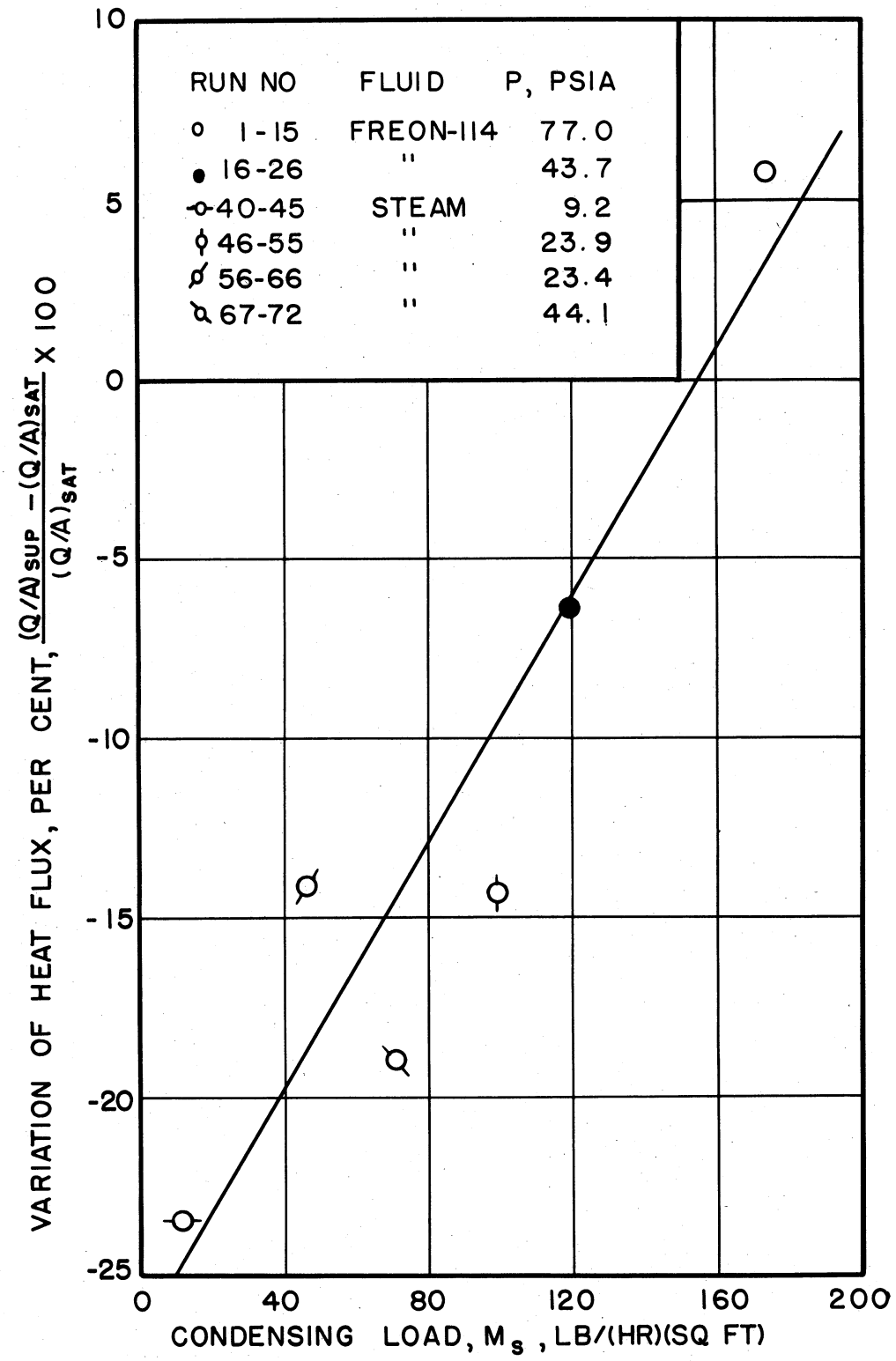

FIGURE 9A— CORRELATION OF THE EFFECT OF SUPERHEAT ON THE HEAT FLUX WITH THE CONDENSING LOAD

vapor-liquid interface between the superheated vapor and the condensate surface. The latter will be referred to as the primary process of heat transfer.

For the ideal case when all desuperheating and condensation of the vapor occurs at the vapor-liquid interface the theory of interphase transfer predicts a lowering of the heat flux with increase in superheat. When heat transfer occurs by both primary and secondary processes then only a portion of the expected lowering in heat flux is actually observed since the effective temperature of the vapors at the vapor-liquid interface is lower than the superheated vapor temperature. This results in a lower temperature difference through the interfacial film and a higher interfacial vapor film coefficient. It follows from this reasoning that at appreciably high condensing loads an increase in the heat flux is possible if the extent of cooling of the superheated vapor by the secondary process is appreciable. This subject is discussed further in the next section concerning the mechanism of mass and energy transfer. The only disagreement of the experimental results with this explanation is the 19.0 per cent lowering in the heat flux at 140°F superheat given by steam condensing at 44.1 lb per sq in. absolute. The present interpretation of results predicts a lower reduction in the heat flux for steam at 44.1 lb per sq in. absolute than the 14.1 per cent decrease indicated by steam condensing essentially filmwise at 23.4 lb per sq in. absolute. This discrepancy may be due to the unstable pattern of condensation which steam exhibits. The apparently constant lowering of the heat transfer rate for steam condensing at 23.4 and 23.9 lb per sq in. absolute corresponding to appreciably different condensing loads is due primarily to the difference in the tube-side water flow rates and the type of condensation obtained.

Heat transfer rates and condensing loads obtained for a constant tube-side water temperature vary according to the condensing pressure, the tube-side water flow rate, and the extent of fouling on the tube side. For steam an additional factor is the type of condensation obtained. The experimental data with measured tube-wall temperatures indicate a gradual fouling. Experimental data, runs 56 through 72, obtained on the original tube (Table I) prior to wall thermocouple installation indicate some fouling on the tube side. The extent of fouling is determined by comparing the performance of the tube at any time with that of the clean tube. The results of the studies on the water-film coefficient inside the experimental tube are discussed and presented as Wilson plots[49] in Appendix B. The equation used to predict the water-film coefficient and enable the calculation of the outside tube surface temperature for runs 56 through 72 is given in Appendix B. The calculated fouling factor is found to be 0.00023 (hr)(°F)(sq ft inside) per Btu.

The conditions under which a superheated vapor does not form a wet film of condensate on the tube surface is important because convection coefficients from a gas to a solid usually give heat transfer rates which are much lower than that obtained during condensation. In the previous section the effect of superheat at reasonable condensing loads is found to be a gradual decrease in the heat flux as compared to the heat flux obtained with the saturated vapor. In the next section this effect is related to the lowering of the condensate surface temperature below that of the saturation temperature. It is important to know the degree of superheat at which the condensate surface temperature decreases sufficiently to attain the limiting value corresponding to the outside tube surface temperature. Under these conditions condensation ceases and the

tube surface becomes dry. At a given pressure and tube-wall temperature the superheated vapor temperature corresponding to the degree of superheat required to attain the dry tube condition represents the "dry point."

During the present studies the degree of superheat required to attain the "dry point" is found to be extremely high. "Dry points" estimated in the next section for Freon-114 are found to be between 625°F and 925°F. Thus, a direct investigation of this problem is presently impossible. A similar problem which can be investigated experimentally is the condensation of superheated vapors at constant superheat and different values of $(T_{sv}-t_o)$. This group represents the difference between the saturation temperature of the vapor and the measured outside tube-surface temperature. Heat flux data obtained while $(T_{sv}-t_o)$ approaches zero describe the manner in which the heat transfer rate, the condensing load and the overall outside coefficient vary in the region where the tube surface temperature approaches the saturation temperature. Table IV gives the results of these experiments (runs 27 through 34) made with superheated steam condensing under vacuum. The group $(T_{sv}-t_o)$ is varied conveniently by maintaining the superheat and the tube surface temperature constant and reducing the condenser pressure until the saturation pressure approaches the tube surface temperature. Beyond a certain degree of approach the experimental heat fluxes are found to be inaccurate because of the very small temperature rise obtained on the tube side.

Figure 10 presents variation of the heat flux and the condensing load obtained for the condensation of steam at pressures varying from 7.5 to 9.0 lb per sq in. absolute and superheats varying from 37.30°F to 46.72°F. The experimental results indicate a gradual decrease in the heat flux and the condensing load as $(T_{sv}-t_o)$ approaches zero. The trend

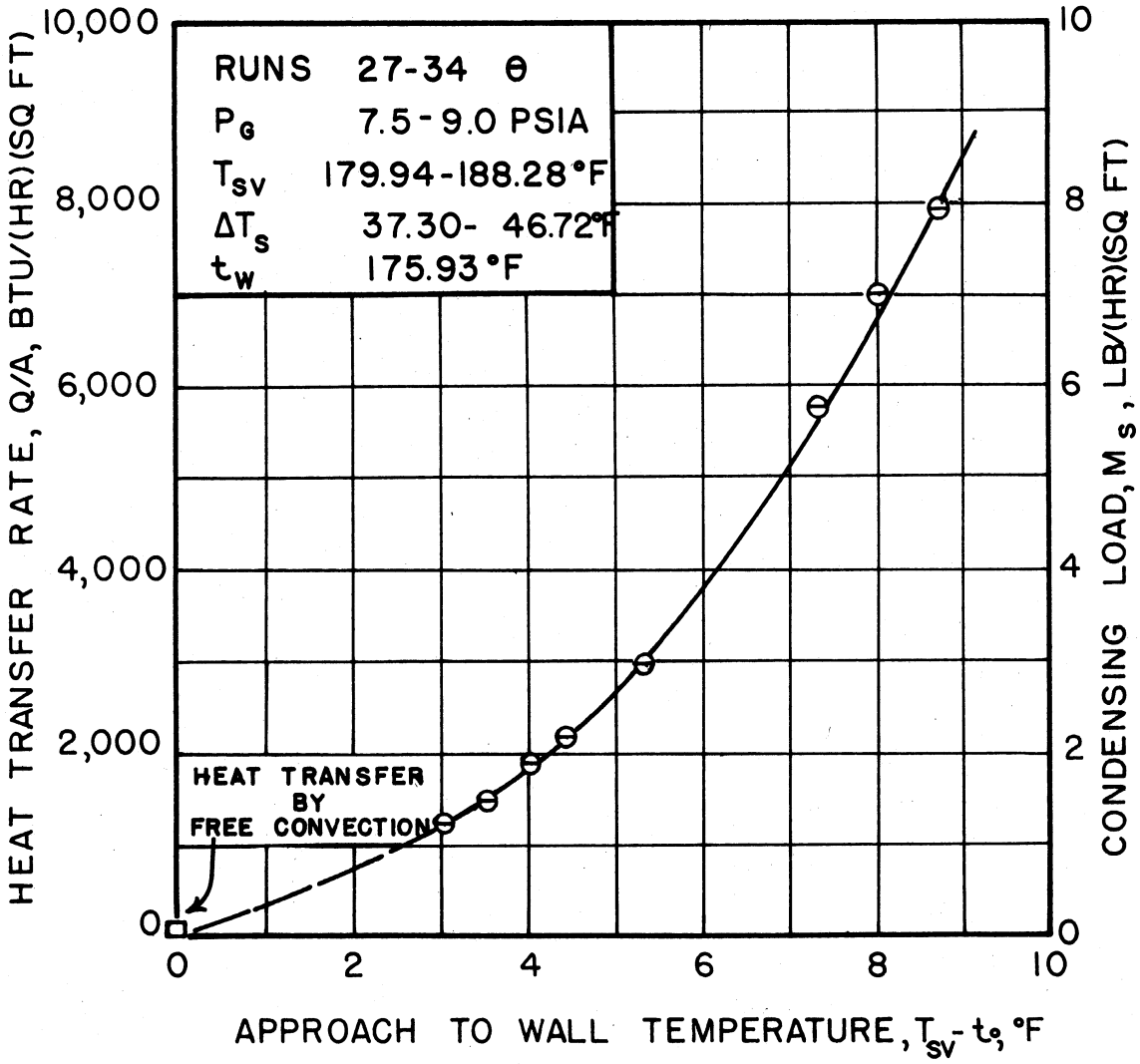

FIGURE 10 – HEAT FLUX AND CONDENSING LOAD FOR CONDENSATION OF SUPERHEATED STEAM WHILE APPROACHING DRY TUBE CONDITIONS

of the curve shows a minimum value for the heat flux when the tube surface is at the saturation temperature. The overall outside film coefficient is calculated from the heat flux and the measured temperatures by the following equation;

$$h_o = \frac{Q}{A(T_g - t_o)} \tag{23}$$

where

h_o = overall outside film coefficient, Btu per (hr)(°F)(sq ft outside)

T_g = temperature of superheated vapor, °F.

Figure 11 presents the variation of the overall outside film coefficient with the temperature difference through the film. The experimental results do not extend to values of $(T_{sv}-t_o)$ where the tube surface is dry, but Figures 10 and 11 indicate that this condition is reached when the tube surface is at the saturation temperature. This is proved by visual observation of the tube surface and the temperature measurements made while $(T_{sv}-t_o)$ becomes zero and negative. These results are tabulated as runs 35 through 39 in Table IV. Small discrepancies in the measured saturation, tube wall, and water temperatures are indicated in column 13. These are due to the difficulty of attaining satisfactory steady-state conditions at the very low heat fluxes involved. Columns 17 and 18 describe the physical condition of the tube. These results substantiate the fact that below the "dry point" a superheated vapor will condense and wet the tube so long as the tube surface temperature is below the dew point of the superheated vapor.

The degree of superheat and the tube surface temperature varies somewhat for runs 27 through 34. In order to determine the overall outside

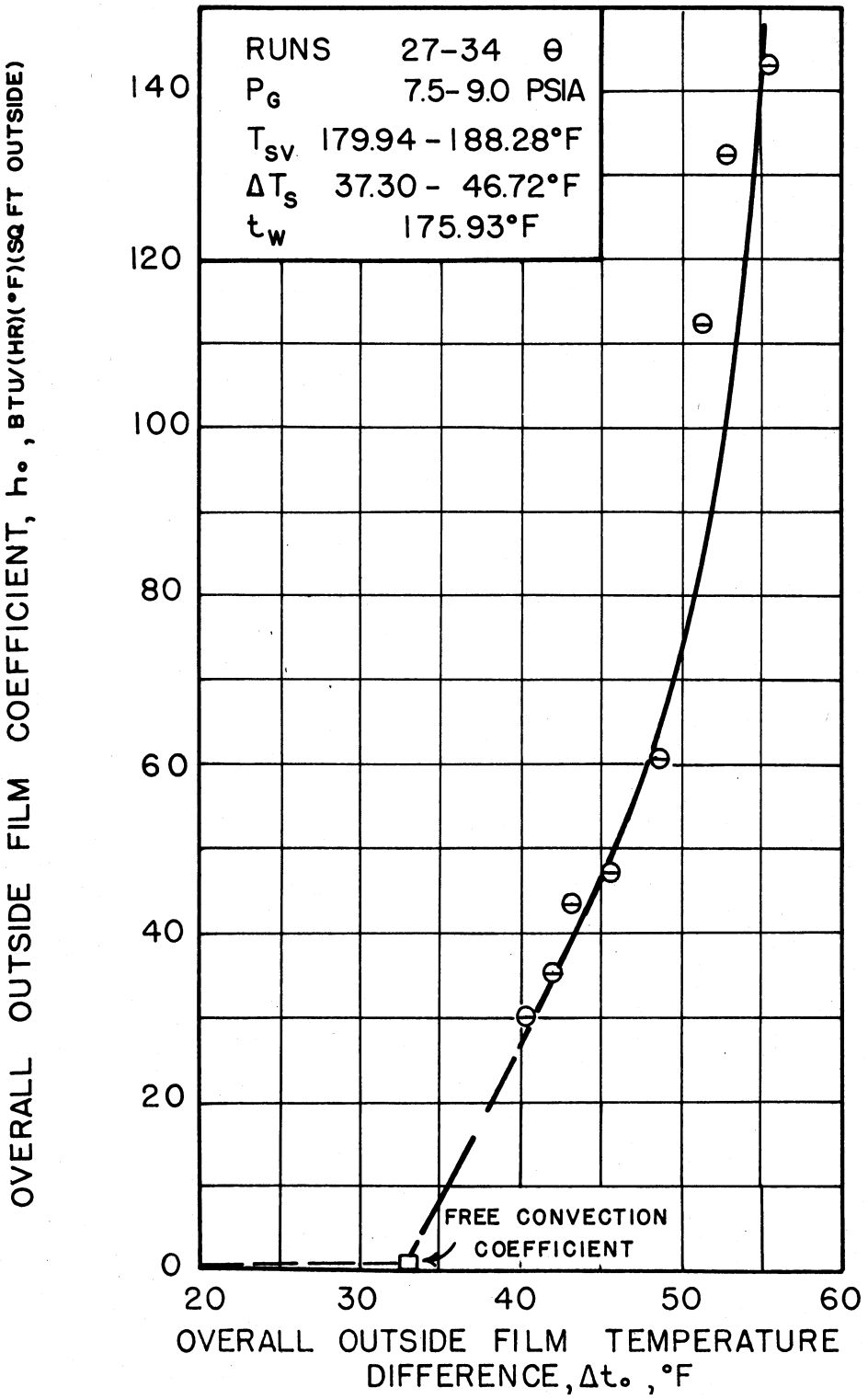

FIGURE 11 — OVERALL OUTSIDE FILM COEFFICIENT FOR CONDENSATION OF SUPERHEATED STEAM WHILE APPROACHING DRY TUBE CONDITIONS

film coefficient at $(T_{sv}-t_o)$ equals zero the experimental superheats and tube surface temperatures are graphically extrapolated to $(T_{sv}-t_o)$ equals zero. Figure 31 of Appendix F indicates that when $(T_{sv}-t_o)$ is zero, the saturation and tube surface temperatures are 176.0°F and the degree of superheat is 33.0°F. The outside film coefficient can be estimated at these conditions by the following equation recommended for the evaluation of the natural convection coefficient on the outside of a horizontal tube:[33]

$$h_o = 0.53 \left[\frac{k_f^3 \, \rho_f^2 \, g \, \beta_f \, C_{pf} \, \Delta t_o}{\mu_f \, D_o} \right]^{1/4} \qquad (24)$$

where

h_o = natural convection coefficient for a horizontal tube, Btu per (hr)(°F)(sq ft outside)

Subscript f refers to vapor or gas properties evaluated at the mean vapor film temperature T_f, °F

$T_f = \frac{T_g + t_o}{2}$, °F

β = coefficient of cubical expansion of vapor or gas, $°R^{-1}$

Δt_o = vapor or gas film temperature difference, (T_g-t_o), °F.

The outside film coefficient calculated from equation 24 is found to be 0.86 Btu per (hr)(°F)(sq ft outside) and is represented by the square point in Figure 11. The corresponding heat flux and condensing load are calculated from equations 23 and 22, respectively. These values are found to be 28.4 Btu per (hr)(sq ft) and 0.0282 lb per (hr)(sq ft outside) and are presented in Figure 10 by the square point.

Figure 12 presents in a conventional way the overall outside film coefficients for superheated Freon-114 and steam calculated from the ex-

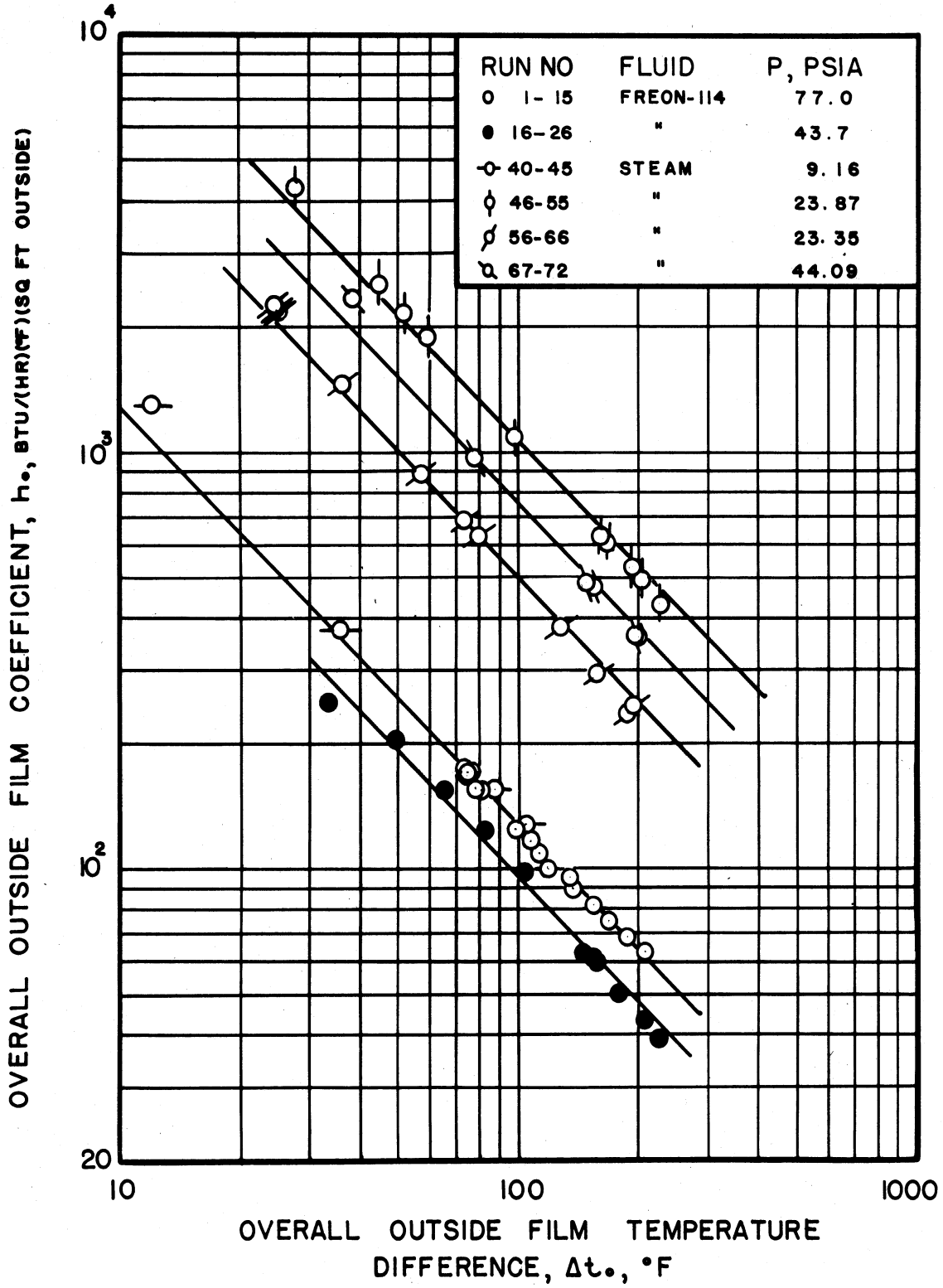

FIGURE 12 — EFFECT OF SUPERHEAT ON OVERALL OUTSIDE FILM COEFFICIENT FOR CONDENSATION OF SUPERHEATED FREON-114 AND STEAM

perimental data by equation 23. The lines representing the data at various pressures have a negative slope of unity. The overall outside film coefficient increases consistently with pressure for both Freon-114 and steam. The apparent discrepancy indicated by the steam data for a condensing pressure of 23.9 lb per sq in. absolute (runs 46 through 55) is due to appreciable dropwise condensation obtained during these runs. These results are further analyzed in the next section to calculate the interfacial coefficient at the vapor-liquid interface.

THEORY OF FILMWISE CONDENSATION OF SUPERHEATED VAPORS

The mechanism of the condensation of superheated vapors is discussed in this section. The applicability of the theory of interphase mass and energy transfer and its limitations are presented for the interpretation of the experimental and calculated results and for an understanding of the condensation of superheated vapors.

The process of condensation of vapors involves the transfer of mass and energy from a vapor phase to a liquid surface. For a saturated vapor the vapor moves onto the liquid surface and condenses. The primary barrier to energy transfer is the layer of condensate through which heat is essentially carried by conduction from the condensate surface to the tube surface. This process attains steady state at constant pressure and tube surface temperature by the build-up of the condensate thickness and with it the resistance to heat transfer. The deviation from equilibrium, if any, is very small at the vapor-liquid phase boundary and the vapor-liquid interface can be assumed to provide no barrier for mass and energy transfer. Both vapor and liquid at the interphase are at the saturation temperature. These assumptions are implied in the derivation of equation 1 discussed in an earlier section and are justified by good agreement between experimental and theoretical results.

The transfer of mass and energy during the condensation of a superheated vapor proceeds much in the same way as that of a saturated vapor. However, the assumption of thermodynamic equilibrium at the vapor-liquid interface seems to be questionable because of the conflicting evidence indicated by experimental results. The temperature and pressure conditions which prevail at the interface are uncertain because of the difficulty of the necessary measurements and the lack of effort evidenced from a review of the literature in this field. Experimental and theoretical studies reported in the literature indicate conflicting opinions and results on the effect of superheat on the heat flux obtained during condensation. The results vary from a large or small increase in the heat flux due to superheat,[33,34,35,47] no effect of superheat on the heat flux,[26] an increase in the heat flux at low heat transfer rates with a subsequent decrease at high heat transfer rates,[24] to a decrease in the heat flux due to superheat.[23] These results tend to indicate that in general the process of condensation of superheated vapors is not adequately understood, and in particular, the nature and importance of the vapor-liquid interface is overlooked.

A thorough understanding of the condensation of superheated vapors requires a theoretical approach to the interphase transfer of mass and energy because the vapor-liquid interface is definitely present. However, an understanding of all processes involving mass and heat transfer is necessary in addition to that which occurs at the phase boundary.

Evidence of the effect of superheat on the process of condensation is the general lack of agreement among the results of different investigators, and the difficulties encountered with superheated vapor condensers designed by conventional methods discussed previously. The heat

transfer rates obtained in condensers designed to handle vapors with excessively high superheats or superheated vapors at pressures considerably below atmospheric are usually below their design capacity. This indicates that in some applications the vapor-liquid interface offers an appreciable barrier to the transfer of mass and energy, whereas in others the assumption of equilibrium at the interface is valid.

In the present investigation an attempt is made to observe the various processes which enable the transfer of mass and heat in order to determine the conditions under which the effect of superheat becomes important. The experimental data cover a wide range of condensing loads which evidently influence the effect of superheat on the heat flux by the secondary process of heat transfer discussed in the previous section.

The experimental results indicate a gradual but definite decrease in the tube surface temperature with increase in the superheat of the condensed vapors (Tables II and III, Figure 12a). It is also shown in Figure 9

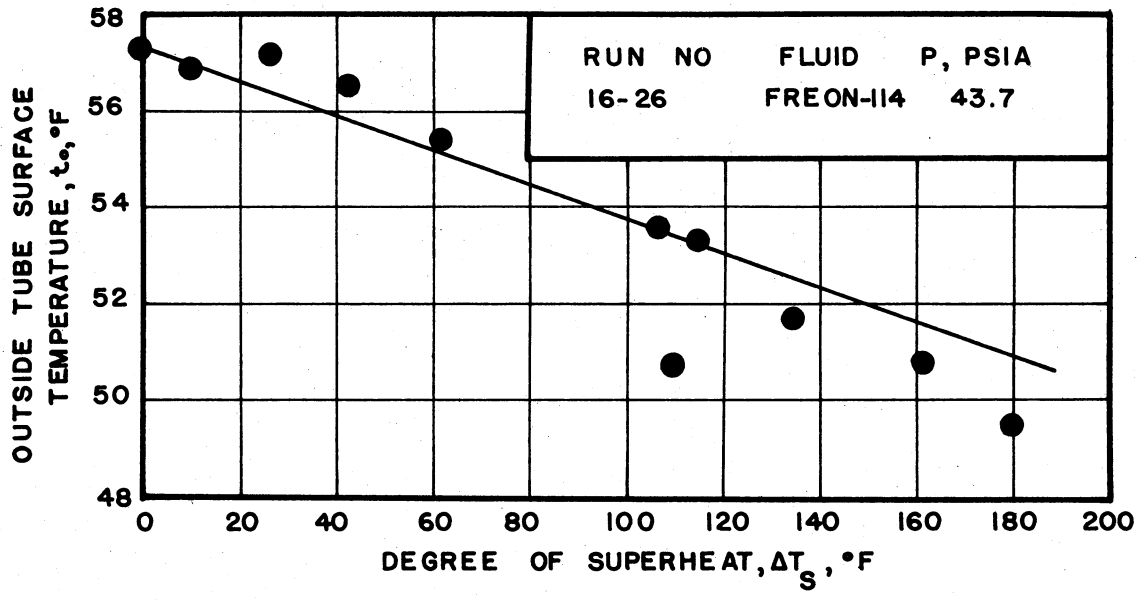

FIGURE 12A — DECREASE OF TUBE SURFACE TEMPERATURE WITH SUPERHEAT

that in all cases with superheated Freon-114 and steam the condensing load decreases with increase in the superheat of the vapor. It follows from these observations that for the heat flux curves (Figures 7 and 8) which indicate a reduction in the rate of heat transfer with increase in the degree of superheat, the condensate surface temperature definitely decreases with increasing superheat. That this is true also for those Freon-114 results which indicate a slight increase in heat flux is shown later (Figure 17). This conclusion results from the fact that the slope of the temperature profile through the condensate film is proportional to the heat flux through the film. If the condensate surface is assumed to be at the saturation temperature during the condensation of the saturated vapor, then it must be at a lower temperature during the condensation of the superheated vapor which gives a lower heat flux (smaller slope) and a lower tube surface temperature.

It is concluded from this discussion that superheat in the condensing vapors affects the temperature and pressure conditions at the vapor-liquid interface. This implies the presence of a phase boundary where the vapor is not in equilibrium with the liquid and the vapor film interface becomes a barrier to the condensation of superheated vapor molecules. The temperature of the liquid and the vapor at the interface is not measured experimentally. A comparison of the experimental condensate film coefficient for the saturated vapor with that calculated from equation 1 shows good agreement for those cases which give stable film condensation. For saturated Freon-114 the calculated condensate film coefficient is 4.1 per cent higher than the experimental value of 170 Btu per (hr)(°F)(sq ft outside) obtained at a pressure of 77.0 lb per sq in. absolute and 17.5 per cent lower than the experimental value of 251 Btu per (hr)(°F)(sq ft outside) obtained at a pressure of 43.7 lb per sq in. absolute.

Since the temperature drop through the condensate film is unknown for condensing superheated vapors, it is more convenient to calculate the condensate film coefficient from the equation using the condensing load which is obtained experimentally. The following is the equation recommended for this calculation[33] and it is equivalent to equation 1:

$$h_c = 1.2 \left(\frac{k_f^3 \, \rho_f^2 \, g}{\mu_f^2} \right)^{1/3} \left(\frac{\mu_f}{2\Gamma'} \right)^{1/3} \qquad (25)$$

where Γ' = condensing load, lb per (hr)(ft of tube length). The use of this equation is simplified by the calculation of the physical property group

$$\left(\frac{k_f^3 \, \rho_f^2 \, g}{\mu_f} \right)^{1/3}$$

as a function of the mean condensate film temperature (T_f). These calculations are illustrated in Appendix C.

The experimental condensate film coefficients obtained during mixed condensation of steam at 9.2 and 23.9 lb per sq in. absolute (runs 40 through 55) are considerably higher than those calculated for film condensation from equations 1 and 25. For these runs the condensate film coefficient for a run with superheated steam is estimated from the experimental film coefficient at saturation by multiplying the latter with the ratio of the condensing loads raised to the one-third power.

It is important to note that any error in the prediction of the condensate film coefficient does not introduce any appreciable error in the interfacial temperature difference finally evaluated. This is shown in Tables II and III by the relative magnitude of Δt_c and Δt_i at various superheats. Above superheats of 10°F the error in the calculated value of the temperature drop at the interface (Δt_i) is negligible. The cal-

culation of the condensate film coefficient by equation 25 involves the determination of the temperature drop through the condensate film (Δt_c) as shown in the sample calculations of Appendix C. The condensate surface temperature is evaluated from the experimental tube surface temperature and the calculated Δt_c by the following equation:

$$T_s = t_o + \Delta t_c \quad . \tag{26}$$

The temperature drop through the interfacial film is obtained from the following equation:

$$\Delta t_i = T_g - T_s \tag{27}$$

where Δt_i = temperature drop through the interfacial film, °F. Equation 27 gives the maximum temperature drop available at the interface and implies that this temperature drop occurs at the vapor-liquid interface. The validity of this assumption is shown by the extent to which experimental results agree with the present theory. Possible deviations from this assumption are discussed later in this section. The interfacial vapor film coefficient is defined as follows:

$$h_i = \frac{Q}{A(T_g - T_s)} \tag{28}$$

where h_i = interfacial vapor film coefficient, Btu per (hr)(°F)(sq ft outside). Since the exact location and area of the interface is unknown, a good approximation is the use of the outside tube area. This assumption is implied in equation 28. The overall outside film, condensate film, and interfacial film coefficients are related by equation 13 presented earlier with the introductory theory. The calculated interfacial film coefficients are given in Tables II and III.

Figure 13 presents the relationship between the calculated inter-

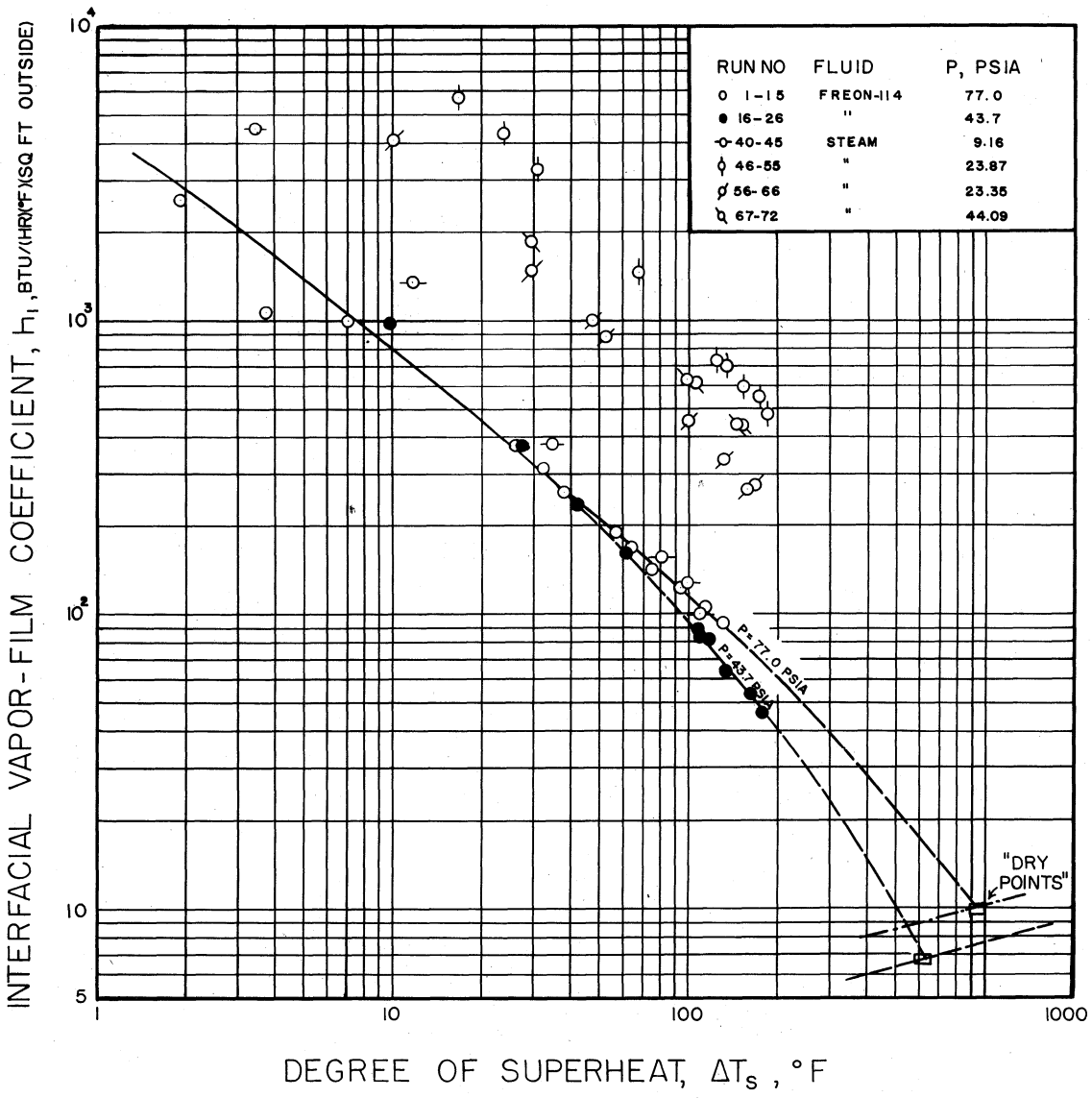

FIGURE 13— EFFECT OF SUPERHEAT ON INTERPHASE VAPOR FILM COEFFICIENT (h_i) FOR CONDENSATION OF FREON-114 AND STEAM

facial film coefficients and the degree of superheat for Freon-114 and steam. For the range of low superheats the spread of the Freon-114 results is reduced in comparison with the trend indicated in Figure 12. The relative spread of the steam results is the same for the experimental outside film coefficients (Figure 12) and the calculated interfacial film coefficients (Figure 13).

The effect of superheat on the overall film resistance, the condensate film resistance, and the interfacial film resistance is shown in Figures 14 and 15. These resistances are defined as the reciprocal of the corresponding film coefficients. Figure 14 presents the individual film and total film resistances for the Freon-114 data. Figure 15 gives the results for Freon-114 at the condensing pressure of 77.0 lb per sq in. absolute on rectangular coordinates. The concept of the individual film resistances is indicated clearly in Figure 15 for the range of experimental results. At saturation the interfacial film resistance is assumed to be zero. As the degree of superheat is increased the condensing load and the condensate film resistance decrease gradually, whereas the resistance of the film at the vapor-liquid interface increases rather sharply. This corresponds to the rapid decrease in the interfacial film coefficient which is infinite at saturation (Figure 13). Up to a superheat of about 30°F the interfacial coefficient of Freon-114 seems to be independent of the pressure.

Figure 13 is useful in predicting conditions of superheat in the region close to the "dry point" defined previously. At the "dry point" the tube surface is dry and the outside film resistance is represented by the interfacial film resistance. The corresponding condensate film resistance is zero. It is also reasonable to assume that at this point the

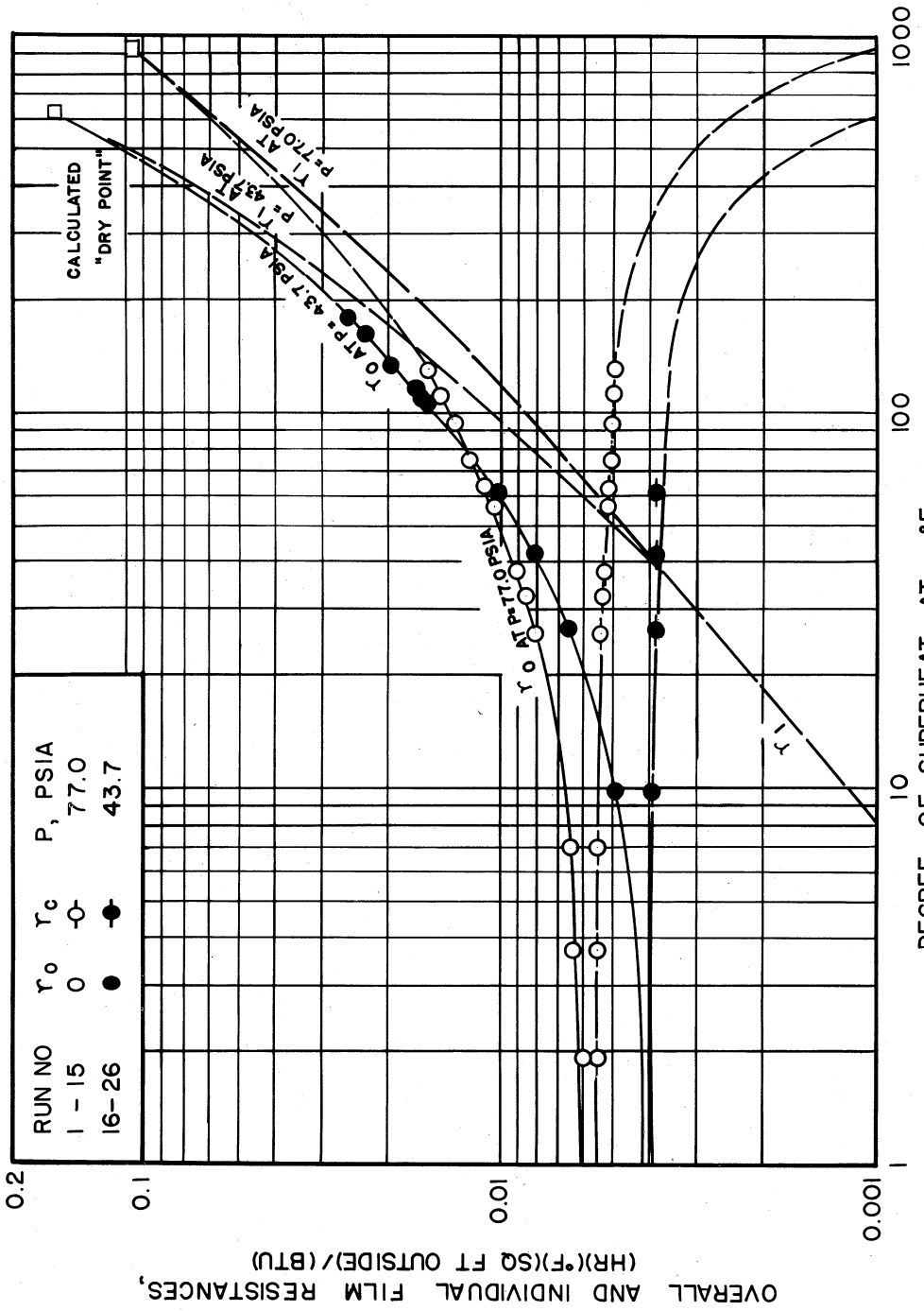

FIGURE 14— EFFECT OF SUPERHEAT ON CONDENSATE AND INTERFACIAL FILM RESISTANCES FOR FREON-114

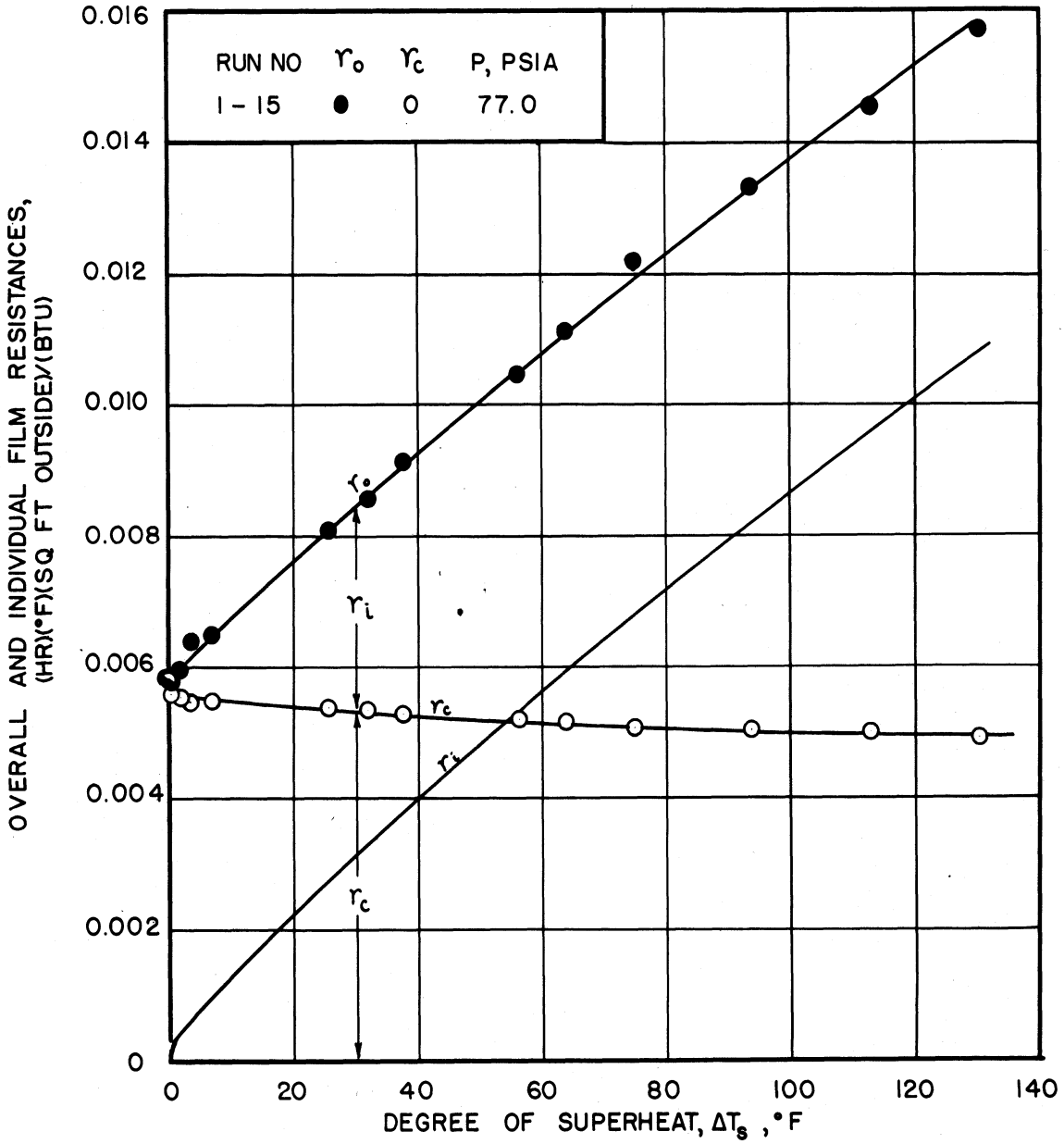

FIGURE 15 — EFFECT OF SUPERHEAT ON CONDENSATE FILM AND INTERFACIAL FILM RESISTANCES FOR FREON-114

interfacial film coefficient is approximately equal to the natural convection coefficient evaluated from equation 24. Lines representing the calculated natural convection coefficients are shown in Figure 13 for Freon-114 condensing at 43.7 and 77.0 lb per sq in. absolute. Intersection of these lines with the extrapolated interfacial film coefficients gives the calculated "dry points" for superheated Freon-114 condensing at a constant pressure and a constant tube surface temperature. The "dry points" shown by the square points in Figure 13 represent a superheated vapor temperature of 1058°F and a superheat of 925°F at a pressure of 77.0 lb per sq in. absolute. The corresponding values at a pressure of 43.7 lb per sq in. absolute are 721°F and 625°F.

It follows from the trend obtained in Figure 13 that as the superheat is increased past the value corresponding to the "dry point," the latter marks a sudden reversal in the variation of the outside film coefficient. However, it is likely that this reversal in trend occurs smoothly and not abruptly as obtained in Figure 13. This is suggested by the experimental results described previously and presented in Figures 10 and 11. The trend of the heat flux curves may be followed beyond the "dry point" by considering the slope of the line in Figure 13 beyond the "dry point." For the range in which radiation effects are not appreciable the heat flux curves would decrease gradually. When heat transfer by radiation becomes controlling the heat flux curve would indicate a reversal in trend and a gradual increase. In Figure 14 the interfacial film resistance curves are extrapolated to the "dry point" values shown by the square points.

Figure 16 describes the variation of the overall outside film coefficient as the superheated vapor temperature attains the "dry point,"

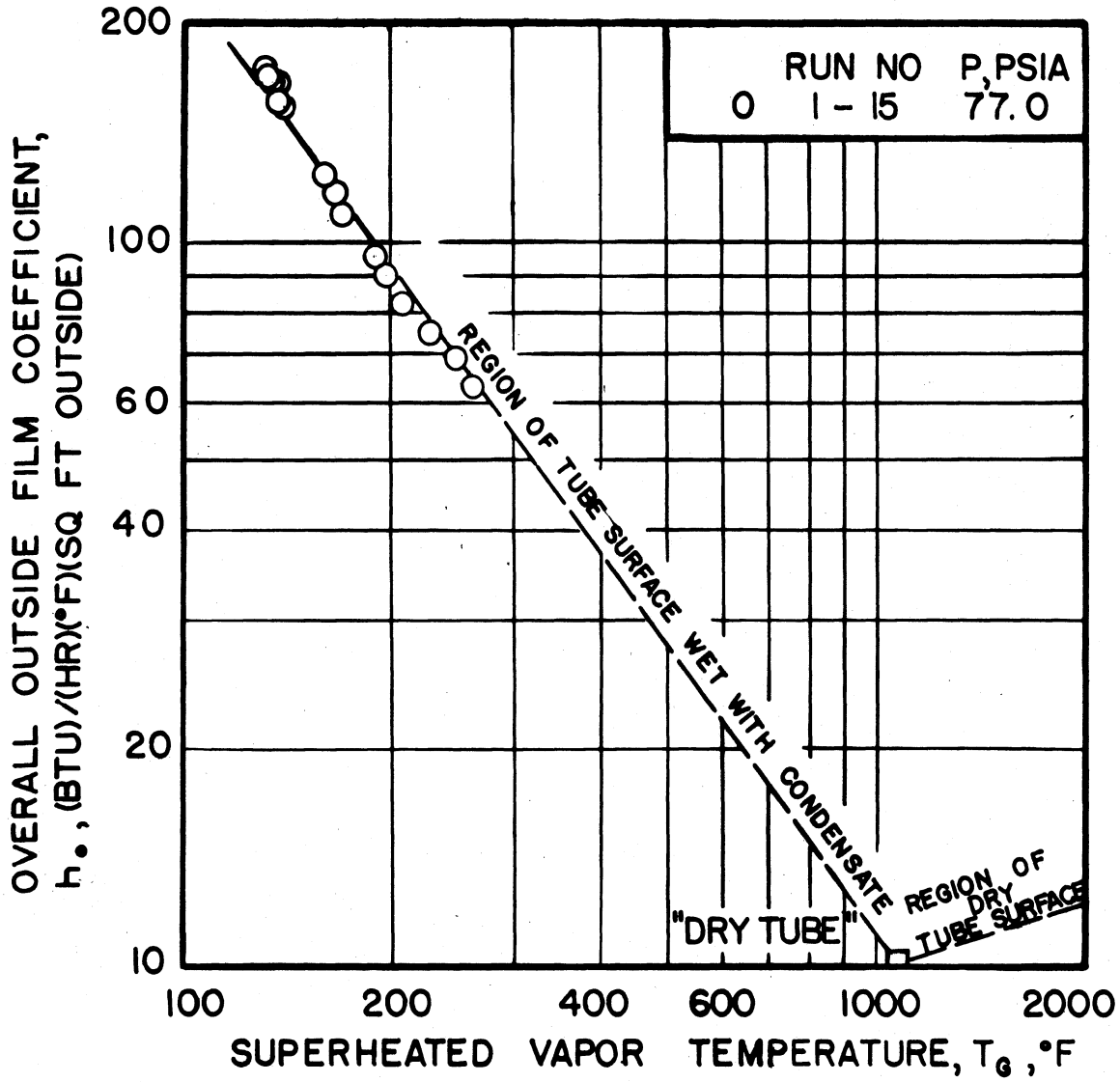

FIGURE 16— EFFECT OF VAPOR TEMPERATURE LEVEL ON OVERALL OUTSIDE FILM COEFFICIENT OF SUPER-HEATED FREON-114

for the Freon-114 data obtained at a pressure of 77.0 lb per sq in. absolute. The general trend is the same as that obtained in Figure 13 because near the "dry point" the value of the interfacial film coefficient approaches that of the overall film coefficient.

At a constant condensing pressure increase in the tube surface temperature reduces the "dry point" of the superheated vapor. For applications involving the condensation of superheated vapors at high superheats and high tube surface temperatures or low values of $(T_{sv}-t_o)$, it is important to evaluate the dry point of the condensing vapors. This requires a knowledge of the interfacial film coefficient as a function of the degree of superheat. The correlation of the calculated interfacial film coefficients on a generalized basis enables this calculation. Such a correlation is presented in the next section.

The calculated interfacial film temperature difference and the corresponding interfacial film coefficient discussed in this section assume that condensation of the superheated vapors occurs entirely by the mechanism of interphase mass and energy transfer. There is evidence that this is true to an uncertain extent. Figure 17 presents the temperature profile for a condensing superheated vapor. The profiles presented qualitatively correspond to runs 6 and 14 for Freon-114 condensing at a pressure of 77.0 lb per sq in. absolute. The degree of superheat is 7.0°F for run 6 and 113.0°F for run 14. The reductions in the tube surface temperature, the condensate film thickness, and the calculated condensate surface temperature with increase in the degree of superheat are shown. The increase in the interfacial film thickness with increasing superheat is shown for the case of interphase mass and energy transfer. The effect of superheat on interphase transfer is lowering of the condensate surface

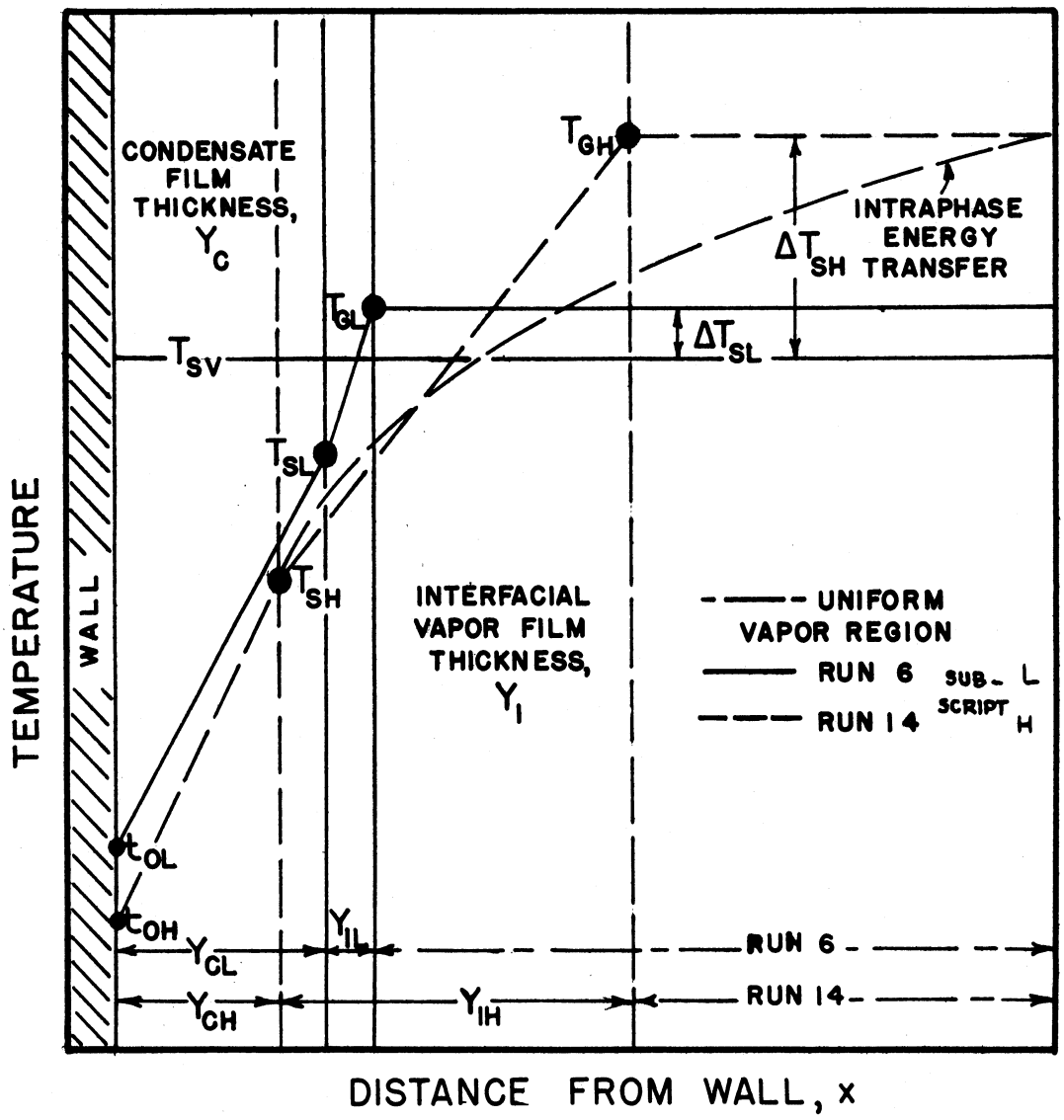

FIGURE 17– TEMPERATURE PROFILE FOR A CONDENSING SUPERHEATED VAPOR

temperature. The general theory of interphase transfer discussed previously predicts this lowering of the condensate surface temperature below the saturation temperature. This assumes that a temperature drop of (T_g-T_s) occurs at the vapor-liquid interface. The order of magnitude of the interface is somewhat less than the mean free path of the superheated vapor molecules. This thickness is exaggerated in Figure 17 in order to clarify the concept of the vapor-liquid interface.

Condensation of superheated vapors involves secondary processes of heat transfer other than interface transfer of mass and energy. Deviations of the behavior of superheated vapors from that predicted by interphase transfer theory are due to heat transfer from the superheated vapor to the subcooled condensate and heat transfer between the vapor molecules adjacent to the interface. The latter is known as intraphase energy transfer. Usually intraphase and interphase transfer operations occur simultaneously and complicate the proper treatment of interphase transfer data. The effect of intraphase energy transfer on the temperature profile is shown by the dashed line in Figure 17. The resulting film temperature drop across the vapor-liquid interface is only a portion of the total temperature drop (T_g-T_s) available. This results in a lowering of the condensate surface temperature which is less than that predicted from interphase transfer theory. The higher condensate surface temperature results in a higher temperature drop and a higher heat flux across the condensate film.

It is seen from this discussion that both intraphase energy transfer and contact of the superheated vapor with the condensate tend to counteract the effect of superheat which tends to lower the rate of interphase mass and energy transfer. Therefore the effect of superheat on the heat

flux depends on the relative importance of these opposing trends. At low tube surface temperatures, high values of $(T_{sv}-t_o)$, moderate superheats, and high condensing loads the secondary process of heat transfer tends to become appreciable because of the large quantity of subcooled condensate which contacts the superheated vapor. Conversely at high tube surface temperatures, low values of $(T_{sv}-t_o)$, high superheats, and low condensing loads interphase mass and energy transfer becomes controlling. It may be concluded from this discussion that condensation of superheated vapors may indicate a higher, the same, or a lower heat transfer rate than the corresponding saturated vapor.

The correlation of the experimental and calculated results on the basis of interphase transfer theory will show the validity of this theory as applied to the condensation of superheated vapors. This attempt is made in the next section.

CORRELATION OF RESULTS

The theory of interphase mass and energy transfer is used for the correlation of experimental and calculated results. The actual heat transfer through the vapor-liquid interface cannot be determined from the experimental results, because of the uncertain amount of heat transfer occurring by secondary processes discussed earlier. This introduces a certain amount of uncertainty in the temperature of the superheated vapor at the vapor-liquid interface. It is assumed that the vapor at the interface is at the condenser temperature. The uncertainty introduced by this assumption is of the same order as that of the calculated condensate surface temperature. The temperature of the condensate surface calculated by the method outlined in the previous section is presented as a function of the degree of superheat in Figure 18. The semilogarithmic plot indi-

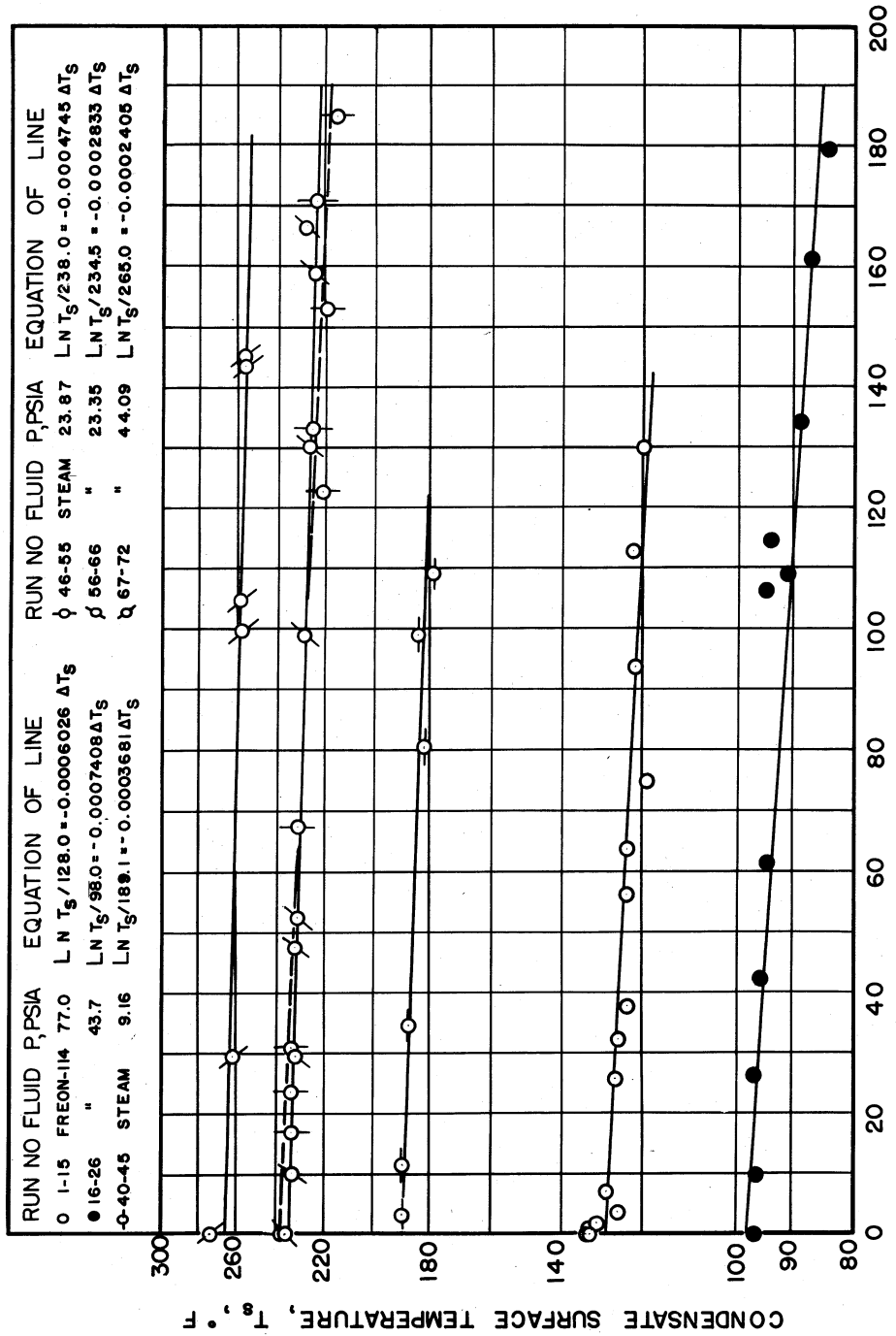

FIGURE 18– CORRELATION OF CALCULATED CONDENSATE SURFACE TEMPERATURE WITH SUPERHEAT FOR CONDENSATION OF FREON-114 AND STEAM

cates a straight-line relationship for Freon-114 and steam. Lines are drawn to represent the best trend indicated by the individual calculated points. The equations of these lines given in Figure 18 show the mean saturation temperature for all the runs in a given set corresponding to the mean condenser pressure. Saturation and condensate surface temperatures used for the correlation of experimental heat transfer rates and condensing loads are obtained from the lines shown in Figure 18. This is justified because of the uncertainty inherent in the calculation of the condensate surface temperature and the unavoidable variation of the saturation pressure and temperature for the runs corresponding to the different degrees of superheat at a given pressure.

The lowering or depression of the condensate surface temperature below the saturation temperature (T_{sv}-T_s) is calculated and shown in Figure 19 as a function of the superheat. These and other calculated results used for the correlation of heat flux and condensing load with superheat are given in Table V. The line shown in Figure 19 represents the best fit for Freon-114 results. The calculated results for superheated steam fall slightly below those for Freon-114. Superheated steam corresponding to a pressure of 24.08 lb per sq in. absolute shows a depression of condensate surface temperature (T_{sv}-T_s) which is about 50 per cent higher than those of Freon-114 and steam at other pressures. This may be due to the pronounced dropwise condensation obtained during these runs (46 through 55) and the greater uncertainty in the calculation of the condensate surface temperature.

The condensation of superheated Freon-114 and steam is studied under conditions which tend to reduce the extent to which processes other than that of interphase mass and energy transfer prevail. The effects of va-

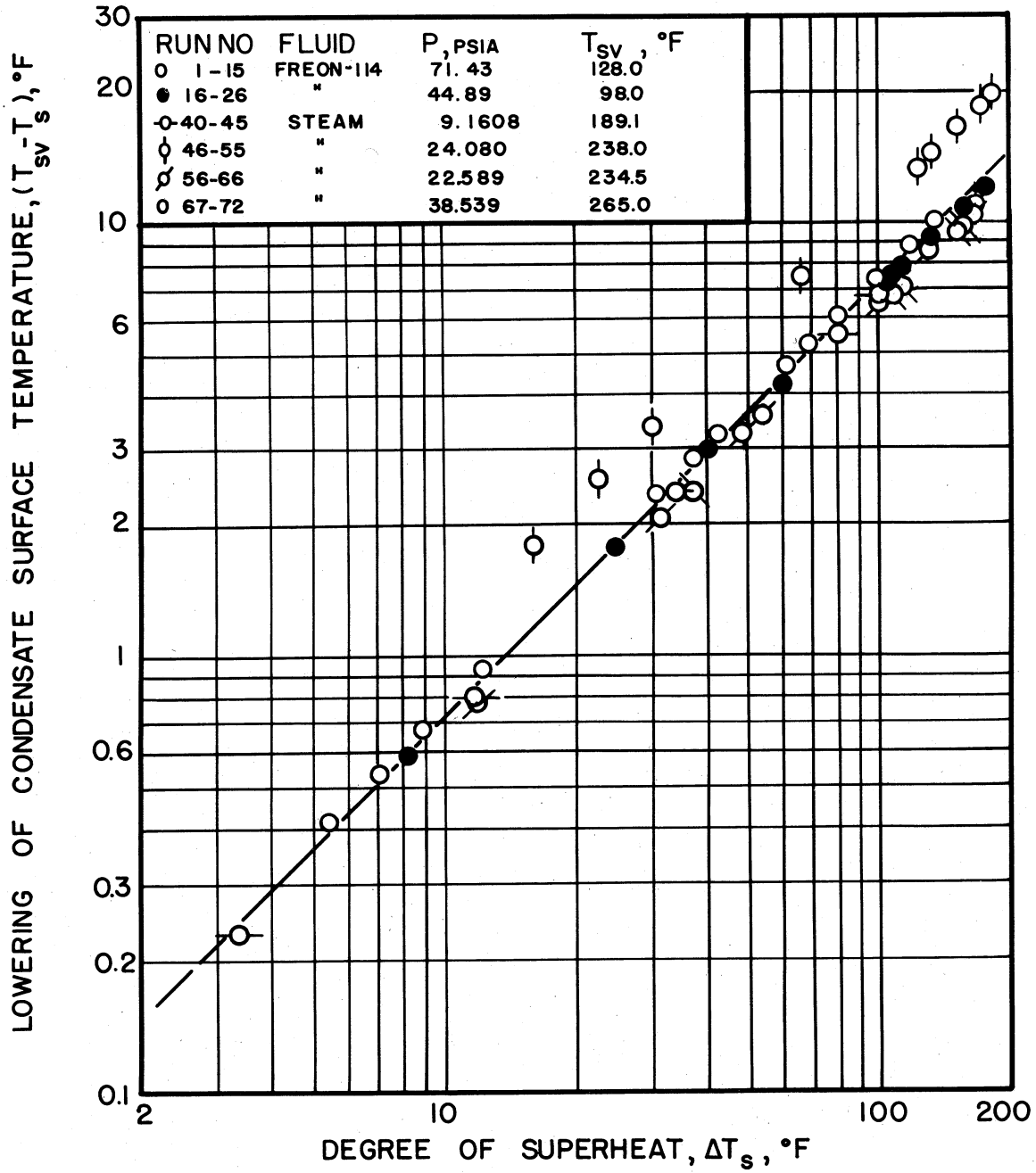

FIGURE 19 – CORRELATION OF CALCULATED CONDENSATE SURFACE TEMPERATURE LOWERING WITH SUPERHEAT FOR CONDENSATION OF FREON-114 AND STEAM

por velocity and intimate contact of the condensate with the superheated vapor are minimized by the experimental condenser shell and tube selected. The small tube provides a low heat transfer area and reduces the condensing load per unit length. The relatively large shell with two inlets reduces the velocity of the vapors moving toward the cooler condensing surface.

Previous discussion of the experimental results indicates a distinct effect of superheat on the temperature and pressure conditions at the interface. The mechanism of condensation of superheated vapors involves the transfer of mass and energy through the vapor-liquid interface. The temperature and pressure conditions are not determined experimentally because of the nature of this study. Based on evidence from the experimental results the validity of the assumed and calculated interfacial conditions is tested by direct application of the equations derived from the theory of interphase mass and energy transfer.[45]

At a given temperature and pressure the net mass transfer rate is related to the interfacial conditions of temperature and pressure by equation 19 presented earlier. This equation is based on the theory of interphase mass and energy transfer discussed earlier in the literature review and is valid for the general case where the vapor and liquid are not in equilibrium ($T_s/T_g \neq 1$) at the interface. In deriving equation 19 the condensation coefficient (f) is assumed to be a function of the state of the surface and the kind of molecules involved.

For a given substance the condensation coefficient decreases with increase in the superheat of the vapor. This observation is explained in this section. The molecular velocity of the vapor and the rate of collision of the molecules with the condensate surface increases with in-

crease of the vapor temperature. The condensation of superheated vapor molecules requires a condensate surface which has a greater potential to absorb molecules than that necessary for the condensation of saturated vapor molecules. This is due to the higher average energy content of a superheated vapor molecule as compared to that of a saturated vapor molecule. Thus, during the condensation of a pure substance the rate of mass transfer or the condensing load is controlled by the rate at which energy or heat is extracted from the superheated vapor and conducted through the liquid film. To increase the probability of condensation of the higher velocity superheated vapor molecules the condensate surface temperature must be lower than that necessary to condense lower-velocity saturated vapor molecules. The lowering of the condensate surface temperature is limited, however, by the mechanism of conduction whereby the heat extracted from the condensed molecule must be transferred to the tube surface. Therefore, the overall rate at which superheated vapor molecules are condensed is less than that of saturated vapor molecules. The increase in the rate of collisions on the one hand and the decrease in the rate of molecules condensed on the other tend to reduce the value of the condensation coefficient (equation 8).

Figure 19 indicates that the effect of superheat on the condensate surface temperature is comparable for different fluids and different pressures. Experimental and calculated results obtained for the film condensation of a pure substance or different substances with similar molecules can be correlated as a function of the condensation coefficient (f) if the latter represents the characteristic variable describing the temperature and pressure conditions at the vapor-liquid interface.

Direct application of equation 19 is complicated because of the cor-

rection factor Γ as indicated earlier. This relationship is simplified by expressing Γ as a simple function of the variable ϕ_g defined by equation 20. Values of $(\Gamma - 1)$ are presented graphically for condensation ($\phi_g < 0$) and evaporation ($\phi_g > 0$) in reference 45 for the range $1 \geq |\phi_g| \geq 10^{-3}$. The major portion of this graph corresponding to the range of $|\phi_g|$ of $0.1 \geq |\phi_g| \geq 0.001$ is represented satisfactorily by a straight line with a slope of unity. The following equation approximates the calculated values of Γ for condensation with a maximum deviation of $\pm$ 4 per cent within the specified range:

$$\Gamma = 1 + 1.85 \, |\phi_g| \quad \text{for} \quad 0.1 \geq |\phi_g| \geq 0.001 \quad . \tag{29}$$

Substituting for the absolute rate of evaporation (m_e) from equation 9 in equation 20 ϕ_g is expressed as:

$$\phi_g = \frac{m_s}{2\pi^{1/2} \, f \, P_g} \sqrt{\frac{2\pi \, RT_s}{g_c M}} \left(\frac{T_g}{T_s}\right)^{1/2} \tag{30}$$

Equation 30 is used subsequently to calculate the range of values of ϕ_g corresponding to the experimental and calculated results obtained in this investigation. Values of $|\phi_g|$ lying within the specified range justify the use of equation 29 for the elimination of Γ in equation 19. Substituting for Γ in equation 19 the linear function given by equation 29 and solving for ϕ_g the following equation is obtained:

$$\phi_g = \frac{1}{1.85} \left(\frac{P_s^*}{P_g}\right) \left(\frac{T_g}{T_s}\right)^{1/2} - \frac{m_s}{1.85 \, f \, P_g} \left(\frac{T_g}{T_s}\right)^{1/2} \sqrt{\frac{2\pi \, RT_s}{g_c M}} - \frac{1}{1.85} \quad . \tag{31}$$

Combining equations 30 and 31 to eliminate ϕ_g the following equation is derived for the condensation coefficient (f):

$$f = \frac{1.52\, m_s \sqrt{\frac{2\pi\, RT_s}{g_c M}}}{\left[P_s^* - P_g \left(\frac{T_s}{T_g}\right)^{1/2}\right]} \qquad (32)$$

Equation 32 is equivalent to equation 19 discussed earlier. The correction factor Γ is eliminated in equation 32 and the condensation coefficient is presented as a function of the condensing load and the temperature and pressure conditions at the vapor-liquid interface.

A relationship similar to equation 32 is presented by Bosnjakovic[11,45] without the correction factor Γ and its equivalent constant coefficient 1.52. He does not define the temperature drop through the interface and the expected deviations from equation 32 because of intraphase film temperature drop. A temperature gradient extending beyond the vapor-liquid interface (shown in Figure 17) indicates intraphase heat transfer. This secondary process of heat transfer affects the predictions made from equation 32 in two ways. Firstly, it reduces the effect of superheat on the condensate surface temperature and results in a higher condensate surface temperature. Secondly, it lowers the superheated vapor temperature at the interface. The overall effect of intraphase heat transfer is a higher value for the ratio (T_s/T_g), a lower value for the terms

$$\left[P_s^* - P_g \left(\frac{T_s}{T_g}\right)^{1/2}\right],$$

and a higher value for the condensation coefficient (f) in equation 32, as compared to the assumption of interphase mass and heat transfer alone.

Substituting for $\sqrt{2\pi R/g_c}$ equation 32 is simplified to:

$$f = \frac{m_s}{19{,}630} \frac{\sqrt{\frac{T_s}{M}}}{\left[P_s^* - P_g \left(\frac{T_s}{T_g}\right)^{1/2}\right]} \qquad (33)$$

where P_s^* and P_g are expressed in lb (force) per sq in. absolute.

The experimental and calculated results are used to calculate f from equation 33 and ϕ_g from equation 31. These calculations indicate values of $|\phi_g|$ of about 0.007 and justify the use of equation 29 to eliminate Γ in equation 19. ϕ_g may be calculated also from equation 30.

Substituting for the molecular weight in equation 33 the following equations are obtained for Freon-114 (M = 170.9) and steam (M = 18.02):

$$f = \frac{m_s \sqrt{T_s}}{256,300} \frac{1}{\left[P_s^* - P_g \left(\frac{T_s}{T_g}\right)^{1/2}\right]} \quad \text{for Freon-114 ;} \tag{34}$$

$$f = \frac{m_s \sqrt{T_s}}{83,300} \frac{1}{\left[P_s^* - P_g \left(\frac{T_s}{T_g}\right)^{1/2}\right]} \quad \text{for steam .} \tag{35}$$

The correlating group defined as

$$G(f) = \frac{m_s \sqrt{T_s}}{\left[P_g \left(\frac{T_s}{T_g}\right)^{1/2} - P_s^*\right]} \tag{36}$$

is used for the correlation of the experimental condensing load and the calculated temperature and pressure conditions at the interface with the degree of superheat. The effect of molecular weight is not included in order to differentiate easily between the Freon-114 and steam results. Table V gives the results of these calculations. The correlating group is plotted against the superheat in Figure 20. Of the two fluids, Freon-114 indicates stable film condensation and is expected to give results which agree better with predictions of interphase theory. This is shown by the satisfactory grouping of the Freon-114 results about the line drawn to represent the best fit. The steam results indicate an appreciable scatter which indicates that the results of more stable film con-

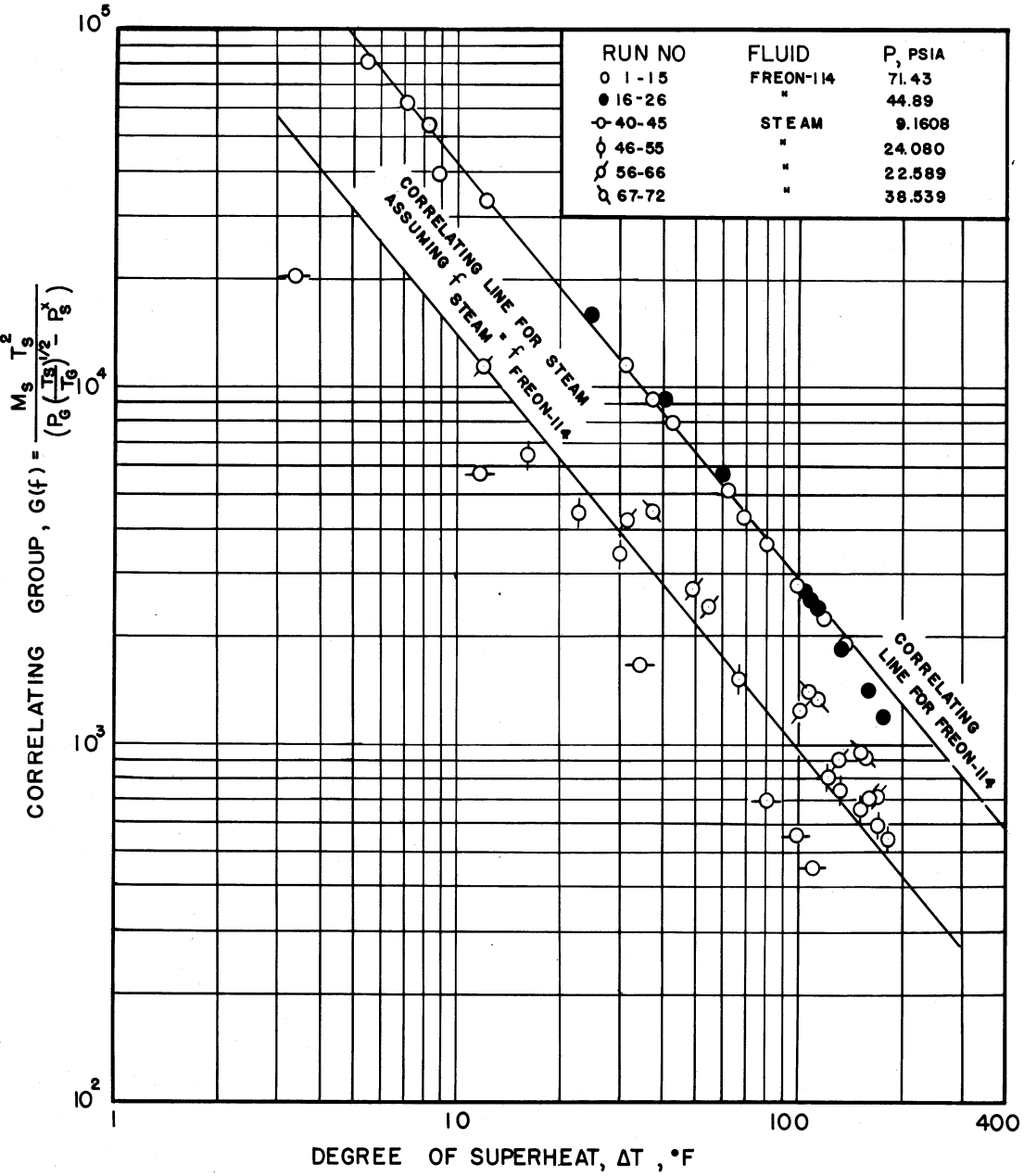

FIGURE 20 – CORRELATION OF CONDENSING LOAD WITH SUPERHEAT AS A FUNCTION OF CONDENSATION COEFFICIENT (f)

densation data (runs 56 through 72) lie above those of the mixed condensation data (runs 40 through 55). Assuming that the condensation coefficient is equal for superheated Freon-114 and steam vapors at the same superheat, the correlating line for the steam results is obtained from the correlating line for Freon-114 and the square root of the molecular weight ratio. The scatter of the steam results from this line is to be accounted for by the mixed condensation obtained with steam. The present theory assumes the existence of a uniform condensate film whereas the pattern obtained with dropwise condensation is widely different from this. It is interesting to note that the present correlation predicts conservative condensing loads for superheated steam condensing filmwise. The maximum deviation of the results is +12 per cent and -20 per cent for Freon-114 and ± 50 per cent for the steam results.

The equation of the correlating line in Figure 20 including the effect of molecular weight is found to be

$$\frac{m_s \sqrt{\frac{T_s}{M}}}{\left[P_g \left(\frac{T_s}{T_g}\right)^{1/2} - P_s^*\right]} = \frac{46{,}700}{\Delta T_s^{1.16}} \qquad (37)$$

where $\Delta T_s = (T_g - T_{sv})$, °F.

Equation 33 is combined with equation 37 to give the following relation between the condensation coefficient (f) and the degree of superheat:

$$f = \frac{2.38}{\Delta T_s^{1.16}} \quad . \qquad (38)$$

The values of the condensation coefficient (f) calculated from equation 38 are not necessarily correct because of the nature of the preceding calculations. However, the condensation coefficient is found to be the important correlating factor for the prediction of the effect of su-

perheat on the filmwise condensation of superheated vapors. Equation 38 may be used to estimate the value of (f) at saturation or zero superheat by calculating the degree of superheat corresponding to f ≡ 1.0. This is found to be 2.11°F. Since the value of f cannot exceed unity by definition, it may be deduced that the value of the condensation coefficient is close to unity for the filmwise condensation of saturated Freon-114 and steam. For quantitative determination of (f) the interfacial conditions must be known accurately by direct or indirect experimental measurement.

The approximate equation 7 discussed earlier is used extensively for the correlation of mass and heat transfer data without clarification of the underlying assumptions. A comparison of equation 7 with equation 32 indicates that in the former the group

$$\left(\frac{T_s}{T_g}\right)^{1/2} \Gamma$$

is assumed to be unity. A function of the condensation coefficient defined as

$$E(f) = \frac{m_s \sqrt{T_s}}{(P_g - P_s^*)} \qquad (39)$$

is calculated and shown in Figure 30 given in Appendix F. These results are given in Table V. Figure 30 indicates a satisfactory correlation for the Freon-114 results. Steam results with both dropwise and filmwise condensation are spread above the correlating line drawn for steam. This inconsistency is accounted for by the assumption of $(T_s/T_g) = 1.0$ which invalidates the use of equation 7 for applications involving a temperature drop through the interfacial film.

Equation 33 is modified to correlate the calculated interfacial film coefficient with the temperature drop through the interface $(T_g - T_s)$ and

the interfacial conditions. The condensing load (m_s) in the correlating group defined by equation 36 is replaced by the representative variables which are the interfacial film coefficient (h_i) and the enthalpy change for the condensed superheated vapor. The resulting group is defined as

$$H(f) = \frac{h_i \sqrt{T_s}}{(-\Delta H)\left[P_g \left(\frac{T_s}{T_g}\right)^{1/2} - P_s^*\right]} \quad . \tag{40}$$

These calculated results are given in Table V and presented in Figure 21 as a function of the temperature drop through the interfacial film. In general the calculated results indicate a pattern similar to that observed in Figure 20. Following the previous assumption of equal condensation coefficients for Freon-114 and steam at the same superheat the correlating line is drawn for the steam results. The use of this line for the prediction of interfacial film coefficients gives conservative results for superheated steam condensing filmwise. The group of variables defined in equation 40 is a direct function of the condensation coefficient (f) and correlates the calculated results satisfactorily for the filmwise condensation of superheated Freon-114 and steam.

The correlating lines drawn in Figure 21 are represented by the following equation:

$$\frac{h_i \sqrt{\frac{T_s}{M}}}{(-\Delta H)\left[P_g \left(\frac{T_s}{T_g}\right)^{1/2} - P_s^*\right]} = \frac{60{,}500}{\Delta t_i^{2.21}} \quad . \tag{41}$$

Equations 37 and 41 and the correlating lines in Figures 20 and 21 are recommended alternately for the prediction of the condensing load and the interfacial film coefficient for the filmwise condensation of Freon-114 and steam. The use of these relationships requires determination of the condensate surface temperature for the specific conditions of superheat

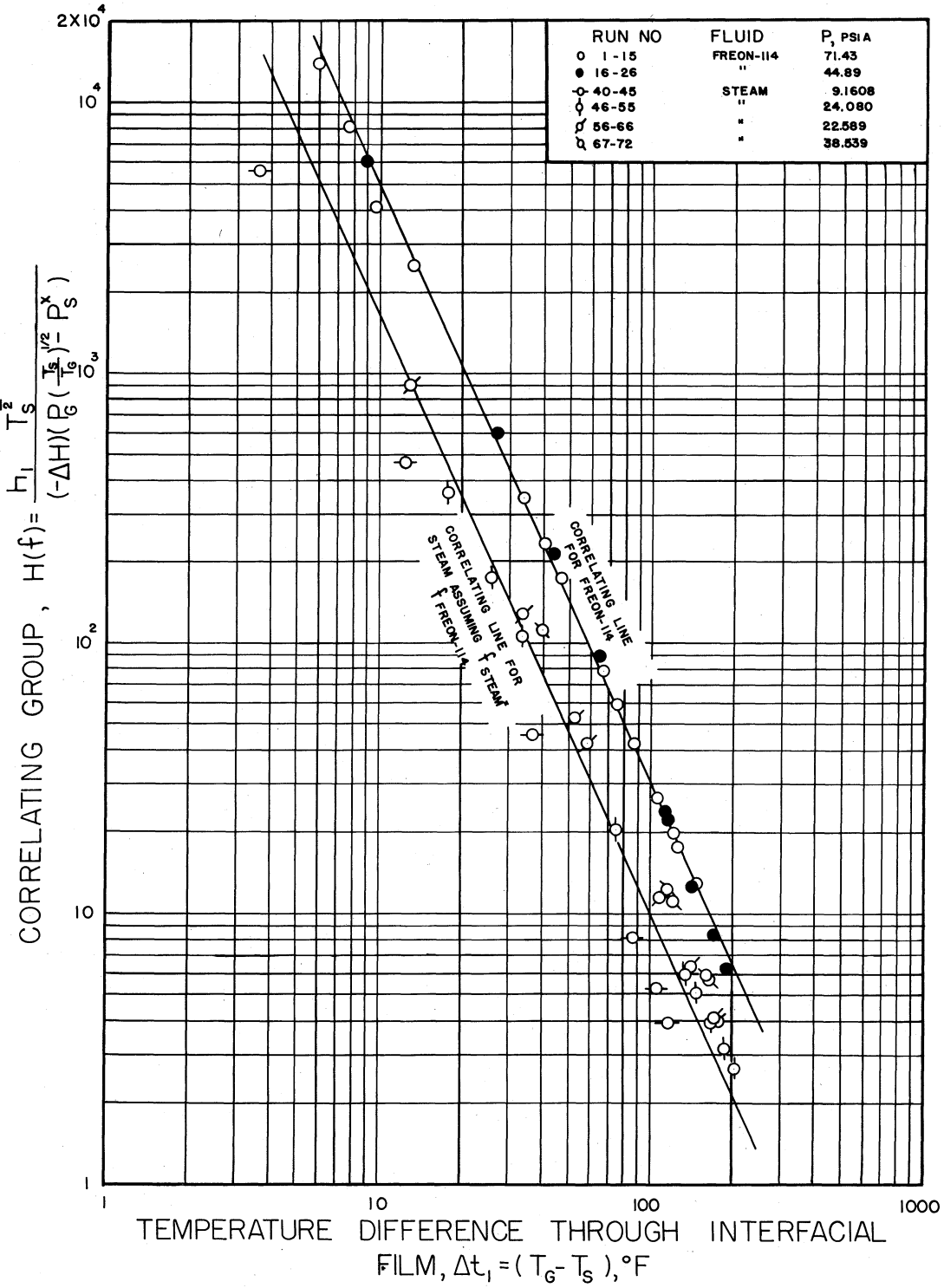

FIGURE 21— CORRELATION OF INTERFACIAL FILM COEFFICIENT(h_1) WITH INTERFACIAL FILM TEMPERATURE DROP AS A FUNCTION OF CONDENSATION COEFFICIENT(f)

and outside tube surface temperature. For tube surface temperatures corresponding to the values given in Tables II and III and the condensing pressures used the degree of lowering of the condensate surface temperature can be obtained from the respective position of the results in Figure 19. The general procedure recommended for the evaluation of the condensate surface temperature is given in the next section.

The correlations derived in this discussion are used in the next section to outline a general procedure for the design of superheated vapor condensers under widely different conditions of superheat, pressure, and outside tube surface temperature.

DESIGN PROCEDURE

The correlation of the experimental and calculated results based on the theory of interphase mass and energy transfer is satisfactory for the experimental results which correspond to the filmwise condensation of superheated Freon-114 and steam. These correlations are recommended for the prediction of variables necessary for the design of superheated Freon-114 and steam condensers. For most applications encountered in industry where vapors with as much as 200°F superheat are condensed filmwise at pressures ranging from one to five atmospheres and the mean tube-side water temperature is about 100°F these correlations may be used for the design of condensers handling fluids with properties similar to those of Freon-114 and steam.

The conventional design procedure based on the condensate film coefficient calculated from equation 1 is discussed earlier. To determine the validity of this method for the range of variables studied in this investigation condensate film coefficients are calculated for comparison with the experimental results for Freon-114. The conventional film co-

efficients (h_c") are calculated from equation 1 by using a ($-\Delta H$) value corresponding to that of the actual run and a constant ($T_{sv}-t_o$) value obtained for the saturated run of each of the two condensing pressures. The film coefficient obtained from the experimental heat transfer rates is calculated on a comparable basis from the following equation:

$$h_c' = \frac{Q}{A(T_{sv}-t_o)} \qquad (42)$$

where h_c' = condensate film coefficient comparable to h_c", Btu per (hr)(°F)(sq ft outside). The calculated results are given in Table II and presented in Figure 22. For Freon-114 condensing at a pressure of 43.7 lb per sq in. absolute the conventional film coefficients are conservative up to a superheat of 90°F but become steadily greater than the corresponding coefficient calculated from the experimental results. For Freon-114 condensing at a pressure of 77.0 lb per sq in. absolute conventional film coefficients are higher than the condensate film coefficients calculated from equation 42. The trend shown by the curves in Figure 22 indicates that conventional film coefficients calculated for design purposes may be 15 to 25 per cent higher than the corresponding actual film coefficients at normal superheats of 100 to 200°F. Even at normal condensing pressures these deviations may be more pronounced at higher superheats.

This discussion shows that at best the use of equation 1 is limited to the estimate of design film coefficients for applications involving normal pressures and superheats. Under peculiar conditions of low pressures, high superheats, and high tube surface temperatures a more fundamental approach is necessary. The general design procedure outlined below is based on the correlations derived in the previous section from considerations of interphase transfer theory. It involves the trial-and-

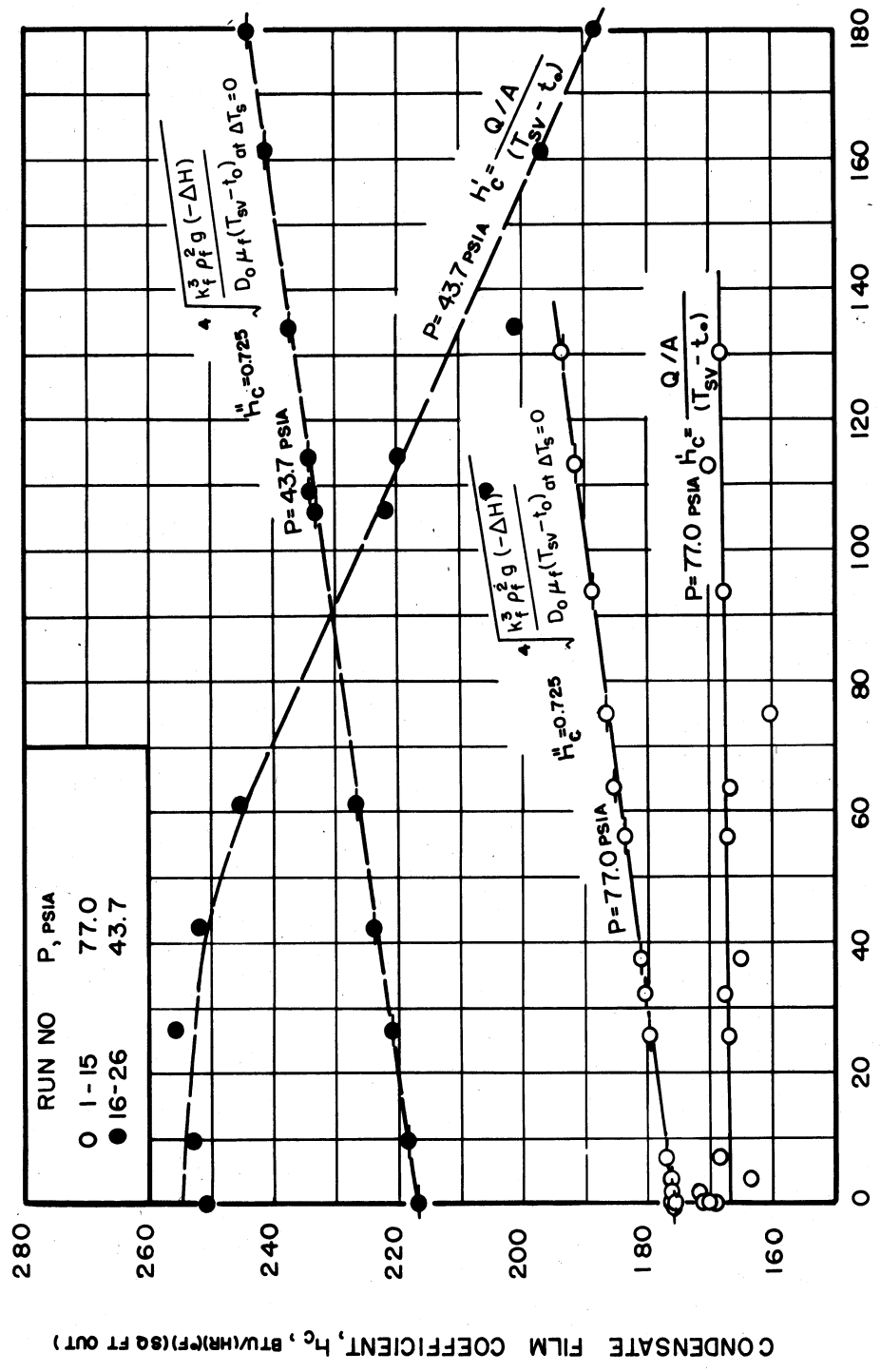

FIGURE 22 — COMPARISON OF CONVENTIONAL DESIGN AND EXPERIMENTAL CONDENSATE FILM COEFFICIENTS FOR SUPERHEATED FREON-114

error determination of the condensate surface temperature for the specified conditions of condensing pressure, superheat, and tube surface temperature. The following procedure is recommended for the evaluation of the condensing load:

1. As a first approximation a reasonable condensate surface temperature (T_s) is assumed, and the corresponding equilibrium pressure (P_s*) is obtained from the vapor pressure of the fluid.

2. The given superheat and condenser pressure, and the assumed variables are substituted in equation 37 and the condensing load is calculated.

3. The heat transfer rate through the interface is calculated from the condensing load and ($-\Delta H$).

4. The condensate film coefficient is calculated from equation 1 using ($-\Delta H$) and the temperature difference ($T_s - t_o$) corresponding to the assumed T_s.

5. The heat transfer rate through the condensate film is calculated from the evaluated condensate film coefficient and the value of ($T_s - t_o$) corresponding to it.

6. The calculated heat flux through the vapor-liquid interface is compared with the calculated heat flux through the condensate film. If the two values deviate appreciably a second trial is made for another assumed value of T_s.

Equation 41 can be used alternately for the design of a superheated vapor condenser. The calculations involved in using equation 41 are more tedious in general and the method outlined above is preferable. The recommended procedure is illustrated for the design of a superheated Freon-114 condenser in Appendix E. It is important to note that the present

method is recommended for the design of superheated vapor condensers in which the vapors condense filmwise on the outside of horizontal tubes. This procedure gives results which are conservative for most normal applications. In general the extent of secondary processes of heat transfer is appreciable in most industrial applications. The intimate contact of the superheated vapor with the condensate lowers the temperature drop through the interfacial film and gives an actual interfacial film coefficient higher than that calculated directly from equation 41 or corresponding to the condensing load determined from equation 37.

The present method is useful for the prediction of interfacial film coefficients and condensing loads under unusual conditions of low pressures, high superheats, and high tube surface temperatures. During the condensation of a superheated vapor at low pressures of 0.1 to 1 inch mercury molecular effects and interfacial film resistances become appreciable. At high superheats and high tube surface temperatures the possibility of the superheated vapor not forming a wet film on the tube can be predicted. This is obtained by evaluating the interfacial film coefficient corresponding to the specified condensing pressure and tube surface temperature for a series of superheats from equation 41. For the same application heat transfer film coefficients for natural convection and radiation are calculated for a series of superheats. The two sets of film coefficients are plotted against the superheat in a manner similar to the results presented in Figure 13. The intersection of the two curves gives the estimated "dry point." A comparison of the specified superheat with that corresponding to the calculated "dry point" indicates the relative severity of the specified conditions.

The design procedure discussed in this section is a fundamental method

of wide applicability. The somewhat tedious calculations inherent to the basic approach are justified by the predictions which these equations enable under varied conditions encountered in the filmwise condensation of superheated vapors outside horizontal tubes.

CONCLUSIONS AND RECOMMENDATIONS

A survey of the literature reveals that the condensation of superheated vapors is not entirely understood. The present study reveals and explains some important phenomena occurring during the condensation of superheated vapors. The various steps used and the conclusions derived from the results of this investigation are outlined as follows.

1. The necessary apparatus including the horizontal tube condenser was constructed and experimental data were obtained for the condensation of superheated Freon-114 at pressures of 43.7 and 77.0 lb per sq in. absolute and superheated steam at pressures of 9.16, 23.35, 23.87, and 44.09 lb per sq in. absolute.

2. A lowering of the tube surface temperature was observed with increase in the superheat of the condensing vapor. Studies showed that superheat causes a lowering of the condensate surface temperature as well. The indicated effect of superheat was a general decrease in the heat flux of as much as 23.4 per cent in comparison to the heat flux of the saturated vapor.

3. The lowering of the heat flux for the different pressures was correlated with the condensing load. The overall performance obtained from the condensation of superheated vapors was explained in terms of the interphase and intraphase mass and heat transfer processes which occurred.

4. The general theory of interphase mass and energy transfer was applied to the condensation of superheated vapors. A mechanism of mass and heat transfer through the vapor-liquid interface based on this theory was introduced to explain satisfactorily the condensation of superheated

vapors. Deviations from the theory were analyzed and explained by intraphase and other mass and heat transfer processes which occur simultaneously with interphase mass and energy transfer. The condensate surface temperature was calculated from the experimental condensing load by the modified Nusselt equation. The interfacial film coefficient was calculated from the experimental results and the calculated condensate surface temperature.

6. The relationship derived from the theory of interphase mass and energy transfer was modified to enable the theoretical analysis of the results. The experimental condensing loads obtained during filmwise condensation were correlated satisfactorily with the degree of superheat and the calculated temperature and pressure conditions at the vapor-liquid interface.

7. The calculated interfacial film coefficients were correlated with the temperature and pressure conditions at the interface as a function of the temperature drop through the vapor-liquid interface.

8. The behavior of superheated vapors in the region close to the "dry point" was explained. The calculated interfacial film coefficients were correlated with the calculated free convection and radiation film coefficients at the "dry point." A method was proposed to estimate the "dry point" of a superheated vapor condensing at a specified pressure, degree of superheat, and tube surface temperature. It was verified experimentally that a superheated vapor below its "dry point" will condense on a surface so long as the latter is at a temperature below the dew point of the superheated vapor.

9. The experimental results were compared with results calculated by the conventional method used for the design of superheated vapor con-

densers. A basic procedure was outlined and illustrated to design condensers for the filmwise condensation of superheated vapors outside horizontal tubes. The use of this method was discussed for applications presenting peculiar conditions of pressures, superheats, and tube surface temperatures.

Further study of the condensation of superheated vapors is necessary to determine the precise nature and importance of the vapor-liquid interface. For a thorough understanding the interfacial temperature and pressure conditions must be obtained accurately from direct or indirect experimental measurements. Difficult as it may be progress in this field indicates the necessity of the measurement of the vapor and liquid temperatures at the interface and the temperature gradient through the superheated vapor region beyond the phase boundary. The applicability of electrical resistivity measurements is suggested for the accurate determination of these temperatures.

APPENDICES

APPENDIX A

DETAILS OF EXPERIMENTAL APPARATUS

The three components of the experimental equipment are the vapor generation and superheating units, the condenser shell and tube, and the water circulating system. The vapors are generated in a reboiler with steam as the source of heat and are superheated in a Chromalox electric heater. The condenser shell has condenser temperature and pressure measurement devices, and six sight glasses for visual observation of the experimental tube. The condenser tube has thermocouples installed in the wall to measure the temperature at four points. The reboiler, superheater, and condenser shell are welded together and heavily insulated with several layers of magnesia and glass-wool insulation. This resulted in a negligible heat loss from the condenser to the surroundings. The water circulating system consists of the mixing reservoir, the water heater, and the pump for the controlled heating and circulation of water through the experimental tube.

VAPOR GENERATION AND SUPERHEATING

The vapors are generated in a reboiler made from a section of 6-inch galvanized pipe 24 inches long as shown in Figure 2. The source of heat is steam at 125 lb per sq in. gage which is condensed inside two parallel U-shaped coils. The coils are made from two 30-inch lengths of 0.750-inch outside diameter copper tubes. The connection at the top of the reboiler with valve B is used to charge the system with distilled water. Valve C

is used to empty the unit. The condensate line is equipped with a steam trap and a by-pass.

A Chromalox electric superheater is used to superheat the vapors. The unit used is GCH - 330, 240 volts, with a capacity of 3 kilowatts, and equipped with a K-3150 three-pole magnetic contactor. The magnetic contactor coupled with a thermostat enables automatic control of the superheater outlet vapor temperature. The temperature of the superheated vapor leaving the superheater varies as much as 5°F with the off-on operation of the heating coil. However, the loss of heat in the connecting lines and the volume of the condenser shell level the temperature fluctuations to about 1°F at the highest superheats used.

CONDENSER SHELL AND EXPERIMENTAL TUBE

Figure 3 indicates the condenser shell and tube details, and Table I summarizes the shell and tube characteristics. The condenser shell is made from a 38-inch length of 6-inch galvanized pipe. The 6-inch pipe is selected to give a very low vapor velocity inside the shell. Two headers with 6 inches diameter are machined for a 2-inch diameter and one-inch deep packing section and packing gland. The left-end header is inserted and welded to the shell whereas the right-end header is removable by the flanged connection shown in Figure 3. Three sight glasses at the top and three at the front enable visual observation of the process of condensation and the external tube condition. The vapor enters the condenser through a manifold which is designed to give a uniform flow and temperature distribution inside the condenser shell.

At the top of the condenser are located the pressure tap, two connections for thermocouples used to measure the condenser temperature, and a

vent A used to evacuate the system with the Duo-Seal vacuum pump prior to charging the system, charge the unit with Freon-114, and purge the system of non-condensables. A one-inch pipe at the center of the shell returns the condensate to the reboiler. Condensate flow is observed through the Jerguson gage in the return line.

The Condenser Temperature is measured with two thermocouples, T_{LC} located close to the left end and T_{MC} located close to the middle. These thermocouples are made from 30 AWG gage iron-Constantan wire with glass wool insulation. The insulated wire is inserted through a length of 15 BWG type 304 stainless-steel tubing, bare lengths of the two wires about 0.0625 inch long are twisted together at the protruding end, and the hot junction is completed by silver soldering the twisted ends to the stainless-steel tubing and filing the solder down to a small point. The hot junction is located 1.25 inches above the condenser tube, i.e. half way between the condenser wall and the tube. Thermocouples T_{LC} and T_{MC} were calibrated at the low range in a constant temperature bath against Bureau of Standards thermometers, and at two points at the high range corresponding to the boiling point of water at barometric pressure and the melting point of tin (231.9°C). The cooling curve method is used to determine the actual thermocouple reading at the melting point of tin.

A similar iron-Constantan thermocouple is installed in the condenser wall at the middle and is calibrated in an identical manner. Thermocouple measurements are made with a Leeds and Northrup portable precision potentiometer graduated in 0.01 millivolt. Potentiometer readings are accurate to ± 0.002 millivolt. The ice point of water is used as the cold junction. All thermocouple calibration corrections are made to the Leeds and Northrup Tables.[30]

The Condenser Pressure is measured with a mercury manometer 30 inches long at pressures below one atmosphere and up to 25 lb per sq in. absolute. A Bourdon type gage graduated at 2 psi intervals up to 100 lb per sq in. gage is used to measure condenser pressures above 25 lb per sq in. absolute. This gage is calibrated against a mercury column at the low range and against a dead-weight tester at the high range. Corrections for liquid leg in the line are shown in Appendix C.

The auxiliary condenser is used to prevent vapor stagnation and damage to the heating coils of the superheater. Vapors are allowed to flow from the two ends of the main condenser and condense on the outside of five 12-inch long finned tubes of 0.50-inch outside diameter. Valve D controls the water flow rate through the auxiliary condenser.

The Selection of the Experimental Tube involved consideration of the following factors. The tube wall temperature is to be measured accurately with thermocouples. Easy installation of thermocouples favors a thick wall whereas reduction of the temperature drop across the tube wall favors a tube with a thin wall and high thermal conductivity metal. The inside diameter is to be such that for a reasonable tube-side water flow rate the temperature rise and the convection film coefficient are sufficiently high. A small outside diameter tends to reduce circumferential tube wall temperature gradients due to the gradual build-up of the condensate thickness. On the basis of these considerations a plain copper tube of 0.750-inch outside diameter, 0.1095-inch wall thickness is selected. The length of the tube is 35.4375 inches long with a 4-inch long brass collar silver soldered to the left end and a 3-inch-long brass collar silver soldered to the right end. When placed in the condenser the brass collars protrude 0.5625 inch into the condensing chamber at each end. This corresponds to

a total outside heat transfer area of 0.6372 sq ft used for the preliminary run numbers 56 to 72 summarized in Table III. For all subsequent runs with measured tube-wall temperatures the brass collar ends protruding into the condenser are thermally insulated with Teflon sleeves and washers thus exposing a 34.4375-inch length of tube to heat transfer. The corresponding outside heat transfer area is 0.565 sq ft. The tube wall temperature is measured at four points by copper-Constantan thermocouples which are described in detail in this section.

The experimental tube is placed symmetrically in the condenser as shown in Figure 3, Chevron type 530 packing is used to seal the ends and the whole unit is made leak proof by tightening gently on the packing glands. To minimize longitudinal heat conduction a 4-inch length of one-inch rubber hose and clamps (No. 15 in Figure 2) are used to connect the condenser tube with the circulated water line.

The Measurement of Tube-Wall Temperatures is a convenient way of determining the individual resistances to heat transfer offered by the shell-side and tube-side fluid and fouling films. Thermocouples installed properly in the tube wall enable this type of measurement. It is desirable to have a sturdy hot junction the location of which is known exactly. The selection of materials and method must be such that the conduction of heat along the leads is minimized and the temperature distribution at the hot junction is essentially the same as that in other geometrically similar locations. The temperature at the hot junction may be in error because of an abrupt change in the thermal conductivity of the metal at that point. In applications where a vapor condenses on the outside of a horizontal tube a slight hump or depression would also introduce errors in the measured wall temperature.

Various methods of installing wall thermocouples are available in the literature.[8,33,42] Baker and Mueller[7] suggest a convenient groove design, but the method of installation is erroneous since the hot junction well is filled with solder. They also discuss the circumferential variation of wall temperature with various fluids condensing at high and low temperature differences. Considering the condensate flow pattern around a horizontal tube the highest wall temperature is expected to be at the top and the lowest temperature at the bottom. The results of Baker and Mueller[7] and of Katz *et al.*[25] on the condensation of steam and n-hexane indicate this trend. A discussion of the wall temperature variation is given by Bromley.[13]

The thick-walled tube with a small diameter minimizes variation of the tube wall temperature specially at small temperature differences. Copper-Constantan wire of 30 AWG gage is used for the thermocouples to minimize the errors due to conduction along the leads. This error estimated by the method of Rizika and Rohsenow[41] is found to be very small. Figure 4 indicates details of thermocouple installation used in this investigation. A longitudinal groove is cut in the wall 0.076-inch wide, 0.076-inch deep, and 0.50-inch long. Beginning at the end of the groove and perpendicular to it a hole is drilled such that its bottom is at the desired hot junction at the middle of the wall. This hole is 0.055 inch in diameter and 0.1875 inch deep. The 30 AWG insulated duplex thermocouple wire is inserted through the desired length of 15 BWG type 304 stainless-steel tubing 0.072 inch in outside diameter so that it extends about 0.5 inch at the other end. The hot junction is prepared by removing all insulation from the protruding insulated wire in excess of 0.3125 inch, twisting the two bare wires together and cutting the length of twisted

junction in excess of 0.0625 inch. The twisted junction is soldered, then placed in the hole, and the stainless-steel tube placed in the groove. The groove and the top of the hole is sealed with solder and all excess solder filed off to obtain a smooth surface. The hot junction is thus free from solder and condensate flow is uniform. The steel tube is taken out of the condenser through holes drilled through the 3-inch-long brass collar at the right end and soldered to the collar. This prevents leakage of vapor or liquid through the thermocouple assembly. Four thermocouples are installed in the tube wall with locations as shown in Figure 3. The two thermocouples at 0° (top) and at 90° at the left end do not indicate an appreciable wall temperature variation. These thermocouples were calibrated in place, and the correction is applied to the 38 calibration in reference 30.

WATER HEATING AND CIRCULATING SYSTEM

The water heating and circulating section of the apparatus is designed to heat city water to any desired temperature up to 200°F and circulate the hot water through the experimental condenser tube at velocities up to 20 feet per second in order to maintain the condenser tube wall at any desired temperature. A 55-gallon-capacity drum equipped with a stirrer is used for hot-water storage. The water is withdrawn from the storage tank (Figure 2) by a centrifugal pump and is circulated through the test section. The water heater 12 consists of a single-tube and single-shell pass condenser with steam condensing inside the tubes. It has a 3-feet-long bundle with 40 finned tubes of 0.870 inch in outside diameter and 16 fins per inch, and a total outside area of 65.6 sq ft.

Figure 2 indicates the piping used to obtain flexibility and control of operation. During normal operation valves G, K, L, and O are closed. Valve E is used to control the water flow rate through the test section and Valve J is used to vary the flow of by-passed water in order to maintain a steady water temperature in the storage tank. The water heater capacity is varied by the quantity of by-passed water and the steam flowing through the two valves. Small adjustments necessary to maintain a constant reservoir water temperature are enabled by valve F which controls the capacity of the water cooler 13 by varying the quantity of the city water flowing through the tube side. Water cooler 13 is assembled from a 1.5-inch pipe shell and four 12-inch-long finned tubes of 0.5-inch outside diameter.

The Water Flow Rate through the experimental tube is measured by a Fischer-Porter flowrator located upstream to the test section. The flowrator has a maximum capacity of 21.1 gallons per minute and is calibrated by measuring the length of time necessary to collect a desired quantity of water for a constant flowrator reading. During this operation valves H, J, K, and N are turned off, valves G and M are fully open, and valve E is used to control the flow of water coming from the main line through valve L. The temperature of the water is recorded as read on thermometers T_1 and T_2. For water temperatures different than that used for the flowrator calibration a correction is made by use of the following equation:[14]

$$W_{t(actual)} = W_{t(calibration)} \sqrt{\frac{[\rho(\rho_f - \rho)]_a}{[\rho(\rho_f - \rho)]_c}} \qquad \text{(A-1)}$$

where

ρ = density of water
ρ_f = density of stainless-steel float
subscript a refers to properties at the actual temperature
subscript c refers to properties at the calibration temperature.

The flowrator calibration is checked several times throughout the duration of the experimental work.

The Ambient Room and Water Temperatures are measured with mercury-in-glass thermometers. The inlet and outlet water temperatures are measured with thermometers T_1 and T_2, respectively, shown in Figure 2. Thermometers T_1 and T_2 are graduated in 0.1°, from 0°C to 100°C and calibrated to ± 0.01°C against a platinum resistance thermometer used with a Mueller bridge. The accuracy of the readings made during the experimental runs with the help of a magnifying glass is ± 0.02°C.

APPENDIX B

EXPERIMENTAL STUDIES ON TUBE-SIDE WATER FILM COEFFICIENT

The inside and outside film coefficients of heat transfer between the tube-side fluid and the inner tube surface and between the outer tube surface and the shell-side fluid, respectively, can be determined directly from the experimental heat flux if the mean tube wall temperature is measured. For the preliminary data (runs 56 through 72) obtained during this investigation the wall temperature is not measured. The possibility of determining the individual film coefficients by a method presented by Wilson[49] is examined in this section. A procedure is outlined and illustrated for the calculation of the inside and outside film coefficients from Wilson-plot type data. The validity of this procedure is proved by good agreement between the calculated water film coefficient and that determined directly from experimental data obtained with measured tube wall temperatures after installation of tube wall thermocouples. A brief discussion of the observed temperature gradient along the tube is given at the end of this section.

DETERMINATION OF TUBE-SIDE WATER FILM COEFFICIENT

The convection coefficient for water flowing through a tube is correlated with the tube diameter, water flow rate, and the fluid properties by the Dittus-Boelter equation. Over the range of temperatures from 40°F to 220°F the following simplified equation is recommended by McAdams:[33]

$$h_w = 150\,(1 + 0.011\,t_w)\,\frac{V_t^{0.80}}{d_i^{0.20}} \qquad \text{(B-1)}$$

where

h_w = convection coefficient for water, Btu per (hr)(°F)(sq ft ins.)

t_w = average water temperature, °F

V_t = water velocity through the tube, ft per sec

d_i = inside diameter of tube, inches.

Equation B-1 predicts reliable film coefficients of water for applications in which the following conditions prevail:

1. The temperature and velocity proviles of the flowing stream are established and flow is fully developed.
2. The degree of turbulence in the flowing stream is not increased due to an excessive roughness of the tube wall or various pipe fittings located upstream within a distance less than about fifty tube diameters.

Assumptions 1 and 2 presented above are not valid for most applications in which the experimental apparatus is relatively small and heat transfer to water occurs in a short length of tube. Deviations from assumption 1 referred to as "end effects" and additional turbulence in the flowing stream tend to increase the coefficient (c) and the exponent (n) of the water velocity term in equation B-1. Such effects are reported in the literature.[42]

For a given experimental tube equation B-1 may be written as:

$$h_w = c\ (1 + 0.011\ t_w)\ \frac{V_t^{\,n}}{d_i^{(1-n)}} \qquad \text{(B-2)}$$

where the simple expression $(1 + 0.011\ t_w)$ presenting the variation of the fluid properties with temperature is assumed to be valid for conditions in which $\underline{n}$ is different from 0.80.

The overall resistance to heat transfer consists of the various film

resistances between the shell-side and tube-side fluids. Using equation B-2 to express the water-film coefficient and assuming no fouling of the outer tube surface the overall resistance is defined by the the following equation:

$$\frac{1}{U_o} = \frac{1}{h_o} + r_m + f_i \frac{A_o}{A_i} + \frac{d_i^{(1-n)} A_o}{c(1 + 0.011 t_w) V_t^n A_i} \qquad (B-3)$$

where

U_o = overall coefficient of heat transfer, Btu per (hr)(°F)(sq ft outside)

r_m = tube wall resistance, (hr)(°F)(sq ft outside) per Btu

f_i = inside fouling factor, (hr)(°F)(sq ft inside) per Btu

A_o = outside tube surface area, sq ft per ft

A_i = inside tube surface area, sq ft per ft.

The metal resistance (r_m) is defined as follows:

$$r_m = \frac{Y_m A_o}{k_m A_m}$$

where

Y_m = tube wall thickness, ft

k_m = thermal conductivity of tube metal, Btu per (hr)(°F)(ft)

A_m = mean metal heat transfer area, sq ft per ft, $A_m = \pi d_m/12$

d_m = mean metal diameter, inches

$$d_m = \frac{d_o - d_i}{\ell n \frac{d_o}{d_i}}$$

d_o = tube outside diameter, inches.

During the condensation of a saturated vapor the overall coefficient is defined by the following equation:

$$U_o = \frac{Q}{A(T_{sv}-t_w)} \quad . \tag{B-4}$$

It follows from equations B-3 and B-4 that the overall coefficient calculated from data obtained in a manner in which the water flow rate is varied whereas the other three terms on the right side of equation B-3 are maintained individually constant presents the effect of the water film coefficient on the overall coefficient. In actual practice the metal and fouling resistances under stable tube surface conditions are approximately constant. Wilson[49] presents a method in which it is assumed that the outside film resistance is constant if the saturated vapors are condensed at a constant pressure while the average water temperature is maintained constant and the flow rate varied. On the basis of this assumption a plot of $1/U_o$ against

$$\frac{1}{(1 + 0.011\ t_w)\ V_t^{0.80}}$$

is expected to give a straight line. The intercept of this line on the ordinate corresponds to an infinite water velocity and film coefficient and gives the sum of the other three resistances. The outside film coefficient can be evaluated from the value of this intercept and the known metal resistance if the tube is clean or the extent of fouling is known.

In practice even if the condenser temperature is maintained constant the condensing load and the corresponding outside film temperature drop vary with varying water flow rates. The best approximation to a constant outside film resistance is obtained when the overall temperature difference and the condensing load are maintained constant. However, the main objection to the use of the Wilson method in many applications is the fact that the value of n = 0.80 is not valid and the results obtained from the

Wilson plot with the assumed value of 0.80 are erroneous.

If Wilson-plot type data are obtained in which all resistances other than that of the water film are approximately constant, the calculated results for a Wilson plot can be used to determine the exponent n for the particular apparatus used for the studies. This method is presented and illustrated in this section for the derivation of equation B-2 valid for the calculation of the tube surface temperature for runs 56 through 72 with filmwise condensation of steam.

Runs 73 through 84 in Table VI present the Wilson plot type data obtained with saturated steam condensing at a temperature of 248.59°F with a mean water temperature of 86.49°F. The Wilson plot ordinate and abscissa are calculated for these runs with the assumed value n = 0.80. The calculated results are given in Table VI and presented in Figure 23. The trend indicated by the calculated results deviates appreciably from a straight line and presents a curve concave upwards. This trend depends on the value of the exponent n used in the calculations and shows that the actual exponent must be greater than the assumed value of 0.80. Since the mean water temperature is maintained very closely constant at about 86.49°F, the effect of temperature on fluid properties may be omitted and the equation of the straight line desirable for the correlation of Wilson-plot type data presented by the following equation:

$$y = a + bx \qquad \text{(B-5)}$$

where

$y = \frac{10^4}{U_o}$, (hr)(°F)(sq ft outside) per Btu

$x = \frac{10^4}{W_t^n}$

a = Wilson plot intercept

b = slope of the corresponding straight line.

TABLE VI

EXPERIMENTAL DATA AND CALCULATED RESULTS FOR TUBE-SIDE WATER FILM COEFFICIENTS

(Saturated Steam-Mixed Condensation)

1	2	3	4	5	6	7	8	9	10	11	12	13	14	15	16	17	18	19	20	21	22	23
Run No.	Condenser Temp., t_c, °F	Tube-Side Water Flow Rate, W_t, lb/hr	Avg. Water Temp., t_w, °F	Water Temp. Rise Δt_t, °F	Total Heat Transferred Q, Btu/hr	Heat-Transfer Rate Q/A, Btu/hr-sq ft out	Overall Temp. Difference ΔT_{OA}, °F	Overall Heat-Transfer Coefficient U_O, Btu/hr-°F-sq ft out	$y = \frac{10^4}{U_O}$	Wilson Plot Abscissa Group $\frac{10^4}{(1+0.011\ t_w)\ W_t^{0.80}}$	$\frac{10^4}{(1+0.011\ t_w)\ W_t^{0.91}}$	Determination of n in Equation $h_w = C(1+0.011\ t_w)\ W_t^n$ by the Method of Least Mean Squares: n = 0.80, $x = \frac{10^4}{W_t^{0.80}}$	n = 0.85, $x = \frac{10^4}{W_t^{0.85}}$	n = 0.90, $x = \frac{10^4}{W_t^{0.90}}$	n = 0.95, $x = \frac{10^4}{W_t^{0.95}}$	n = 1.00, $x = \frac{10^4}{W_t}$	Outside Tube Surface Temp. t_o, °F	Condensate Film Temp. Difference Δt_c, °F	Condensate Film Coefficient h_c, Btu/hr-°F-sq ft out	Inside Tube Surface Temp. t_i, °F	Water Film Temp. Difference Δt_w, °F	Water Film Coefficient h_w, Btu/hr-°F-sq ft ins.
Tube Fouled Inside																						
73	248.44	2,060	86.44	29.49	60,760	107,600	162.00	664.0	15.060	9.58	4.95	22.331	15.249	10.411	7.107	4.854						
74	248.82	3,210	8 .54	22.45	72,050	127,400	162.28	786.0	12.723	7.98	3.30	15.659	10.458	6.969	4.664	3.115						
75	248.66	4,030	86.52	19.04	76,700	135,800	162.14	837.3	11.943	6.65	2.68	13.055	8.621	5.692	3.758	2.481						
76	248.60	5,380	86.59	15.405	82,900	146,800	162.01	905.8	11.040	5.30	2.075	10.361	6.743	4.388	2.856	1.859						
77	248.62	6,500	86.32	13.38	86,950	154,000	162.30	948.3	10.545	4.558	1.732	8.905	5.741	3.701	2.387	1.538						
78	248.44	7,230	86.11	12.245	88,430	156,200	162.33	964.7	10.366	4.158	1.580	8.177	5.244	3.364	2.157	1.383						
79	248.72	7,572	86.41	12.15	91,990	162,800	162.31	1003	9.970	4.025	1.523	7.880	5.043	3.226	2.064	1.321						
80	248.59	8,850	86.89	10.67	95,500	169,000	161.70	1045	9.569	3.541	1.302	6.959	4.417	2.804	1.780	1.130						
81	248.16	8,900	86.30	10.44	92,900	164,200	161.86	1016	9.843	3.55	1.302	6.925	4.396	2.789	1.771	1.124						
82	248.78	9,720	86.36	9.65	93,800	166,000	162.42	1023	9.775	3.30	1.213	6.456	4.078	2.577	1.628	1.029						
83	248.78	10,630	86.82	8.91	94,780	167,800	161.96	1037	9.643	3.058	1.110	6.010	3.779	2.378	1.495	0.9407						
84	248.47	11,840	86.53	7.998	94,600	167,500	161.94	1035	9.662	2.82	1.012	5.513	3.448	2.157	1.350	0.8446						
Avg. Value	248.59		86.49																			
Clean Tube																						
85	248.03	2,080	85.90	39.70	82,600	146,200	162.13	901	11.10	11.32	4.950						202.43	45.60	3200	195.25	109.35	1,882
86	247.77	3,070	85.90	34.80	107,000	189,200	161.87	1170	8.55	8.32	3.460						193.90	53.87	3515	184.66	98.76	2,700
87	248.07	4,045	85.85	29.77	120,200	212,600	162.22	1312	7.63	6.65	2.685						183.48	64.59	3890	173.08	87.23	3,440
88	248.46	5,340	87.20	25.90	138,200	244,500	161.26	1515	6.60	5.32	2.080						180.77	67.69	3610	168.83	81.63	4,220
89	248.07	6,620	86.20	24.54	165,000	292,000	161.87	1802	5.55	4.494	1.714						178.36	75.71	3860	158.12	71.92	5,740
90	247.94	7,820	86.70	23.15	181,000	320,200	161.24	1984	5.04	3.903	1.570						170.92	77.42	4150	154.92	68.22	6,620
91	244.42	9,330	86.10	20.80	194,000	343,500	158.32	2165	4.61	3.405	1.255						164.29	80.13	4290	147.55	61.45	7,890
92	238.76	12,035	88.00	16.92	204,000	361,300	150.76	2400	4.17	2.750	0.984						156.43	82.33	4395	138.85	50.85	10,000
Avg. Value	246.44		86.48																			
Clean Tube																						
93	225.76	2,760	87.10	31.80	87,840	155,300	138.63	1122	8.91	9.0	3.775						181.80	43.93	3540	174.20	87.10	2,520
94	225.86	4,470	86.10	26.00	116,200	206,000	139.76	1472	6.80	6.14	2.44						169.74	56.12	3670	159.70	73.60	3,940
95	225.79	6,280	86.10	22.24	139,800	247,500	139.69	1772	5.64	4.665	1.792						161.66	64.13	3860	149.62	63.52	5,490
96	225.69	7,670	87.40	19.43	149,000	264,000	138.29	1910	5.24	3.96	1.486						157.74	67.95	3884	144.90	57.50	6,470
97	225.63	8,820	87.00	17.92	158,000	280,0	138.63	2020	4.95	3.55	1.322						155.65	69.98	4000	142.03	55.03	7,160
98	225.56	9,470	87.00	17.42	165,000	292,000	138.56	2110	4.75	3.364	1.234						152.75	72.81	4010	138.53	51.53	7,990
99	225.89	10,480	86.60	16.60	173,800	307,500	139.29	2203	4.54	3.12	1.13						150.86	75.03	4100	135.86	49.26	8,800
100	225.92	12,300	86.60	15.33	188,800	334,000	139.32	2400	4.16	2.725	0.971						148.52	77.40	4315	132.28	45.68	10,300
Avg. Value	225.76		86.74																			
Pump and Stirrer Used — Tube Fouled Inside																						
101	227.38	2,083	181.2	14.27	29,700	52,500	45.58	1150	8.70	7.35	3.20						215.20	12.18	4310	212.62	30.82	2,400
102	227.31	3,245	181.2	11.58	37,600	66,550	46.11	1442	6.94	5.16	2.13						212.11	15.20	4380	208.85	27.65	3,390
103	227.14	4,206	182.0	9.80	41,200	73,000	45.14	1612	6.20	4.184	1.682						209.12	18.02	4050	205.54	23.54	4,370
104	227.04	5,400	182.2	8.25	44,550	78,900	44.84	1760	5.69	3.41	1.352						206.81	20.23	3890	202.95	20.75	5,360
105	227.34	6,100	181.8	7.68	46,850	82,900	45.54	1820	5.50	3.10	1.196						205.39	21.95	3780	201.33	19.53	5,980
Avg. Value	227.24		181.7																			

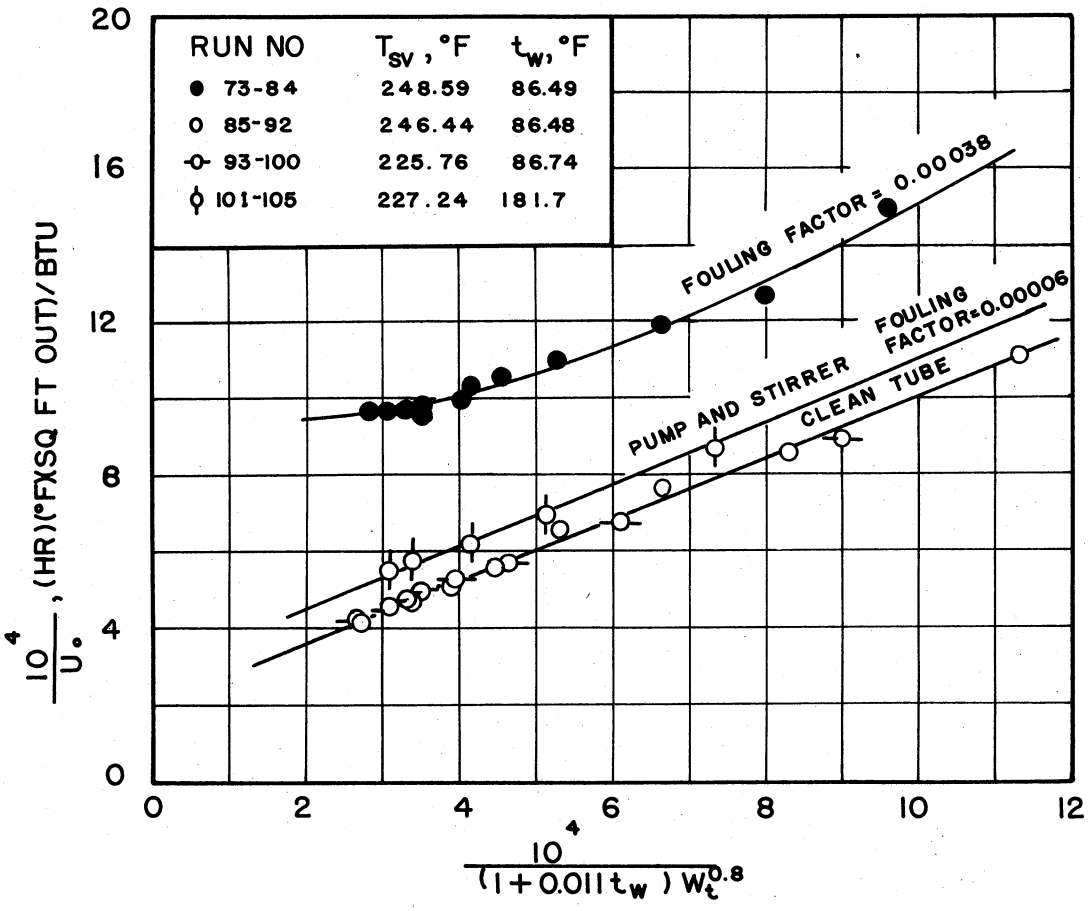

FIGURE 23 — WILSON PLOT WITH WATER FLOW RATE EXPONENT OF 0.80

Equation B-5 is used for the determination of the correct exponent n for this application by the method of least mean squares. Values of x and y calculated for runs 73 through 84 corresponding to assumed values of n of 0.80, 0.85, 0.90, 0.95, and 1.00 are given in Table VI. The least mean square deviation of all the runs is determined for each assumed value of n and the correct value of n is selected as that which gives the minimum least mean square deviation for the experimental results. Derivation of the equation expressing the least mean square deviation as a function of x and y is given in this section. The deviation of a run from the best line obtained by the determination of a and b in equation B-5 is defined as

$$e = y - a - bx \tag{B-6}$$

where e = deviation of a run from best line.

The least mean square deviation is defined by the following equation:

$$\sum e^2 = \sum (y - a - bx)^2 \quad . \tag{B-7}$$

It follows from equation B-7 that $\sum e^2$ is a minimum for the best straight-line fit when

$$\frac{\delta \sum e^2}{\delta a}$$

and

$$\frac{\delta \sum e^2}{\delta b}$$

are zero. Differentiating $\sum e^2$ in equation B-7 with respect to a and b, equating the resulting two equations to zero and solving for a and b the following equations are obtained:

$$a = \frac{\sum y - b\sum x}{N} \tag{B-8}$$

$$b = \frac{\sum xy - \frac{\sum x \sum y}{N}}{\sum x^2 - \frac{\left(\sum x\right)^2}{N}} \tag{B-9}$$

where N = number of runs in the set, twelve for runs 73 through 84.

Substituting for b from equation B-9 into equation B-8

$$a = \frac{\sum y}{N} - \frac{\sum x}{N}\left(\frac{\sum xy - \frac{\sum x \sum y}{N}}{\sum x^2 - \frac{\left(\sum x\right)^2}{N}}\right) . \tag{B-10}$$

Substituting for a and b from equations B-10 and B-9 into equation B-7:

$$\sum e^2 = \sum \left[y - \frac{\sum y}{N} - \frac{\sum x}{N}\left(\frac{\sum xy - \frac{\sum x \sum y}{N}}{\sum x^2 - \frac{\left(\sum x\right)^2}{N}}\right) - x\left(\frac{\sum xy - \frac{\sum x \sum y}{N}}{\sum x^2 - \frac{\left(\sum x\right)^2}{N}}\right)\right]^2 \tag{B-11}$$

Simplifying the relationship given in equation B-11 the following equation is obtained for the least mean square deviation as a function of the calculated experimental results x and y:

$$\sum e^2 = \sum y^2 - \frac{\left(\sum y\right)^2}{N} - \frac{\left(\sum xy - \frac{\sum x \sum y}{N}\right)^2}{\sum x^2 - \frac{\left(\sum x\right)^2}{N}} \qquad \text{(B-12)}$$

Equation B-12 is used to determine the least mean square deviation for the values of x and y given in Table VI for five values of the exponent n varying from 0.80 to 1.00. The calculated deviations are given in Table VII.

TABLE VII

DETERMINATION OF EXPONENT BY THE METHOD OF LEAST MEAN SQUARES (Runs 73 through 84)

Assumed Value of n	Least Mean Square Deviation, $\sum e^2$	$\frac{\Delta \sum e^2}{\Delta n}$
0.80	0.23905	
		- 0.2762
0.85	0.22524	
		- 0.1162
0.90	0.21943	
		+ 0.0734
0.95	0.22310	
		+ 0.2582
1.00	0.23601	

Figure 24 presents the variation of the deviation with the assumed value for the exponent n. In order to determine the value of n where

$$\sum e^2$$

is a minimum the average slope of the curve is obtained between consecutive values of n. These calculated slopes are given in Table VII and presented in Figure 25. A curve is drawn through the incremental levels such that

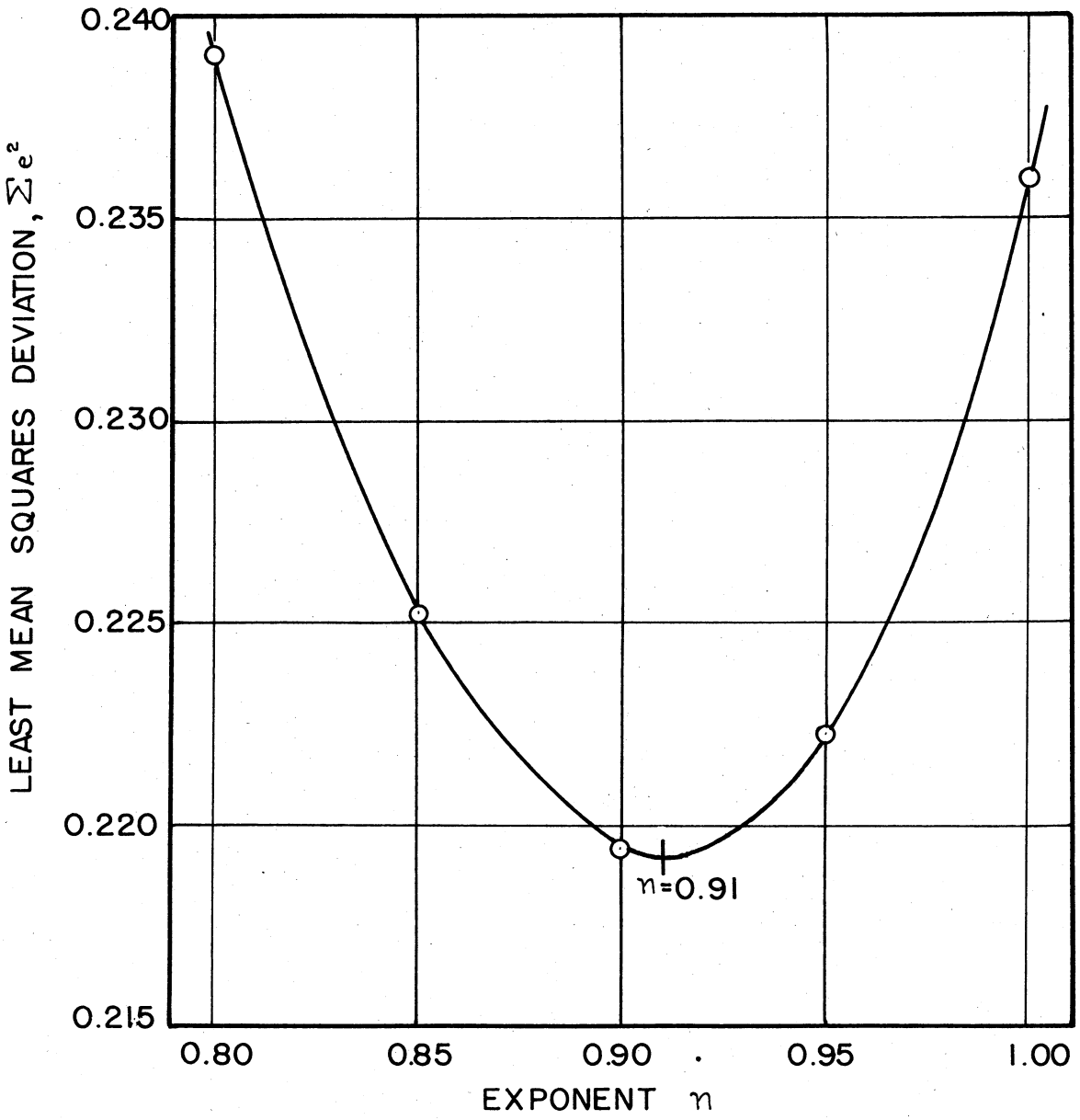

FIGURE 24—DETERMINATION OF WATER FLOW RATE EXPONENT BY THE METHOD OF LEAST MEAN SQUARES

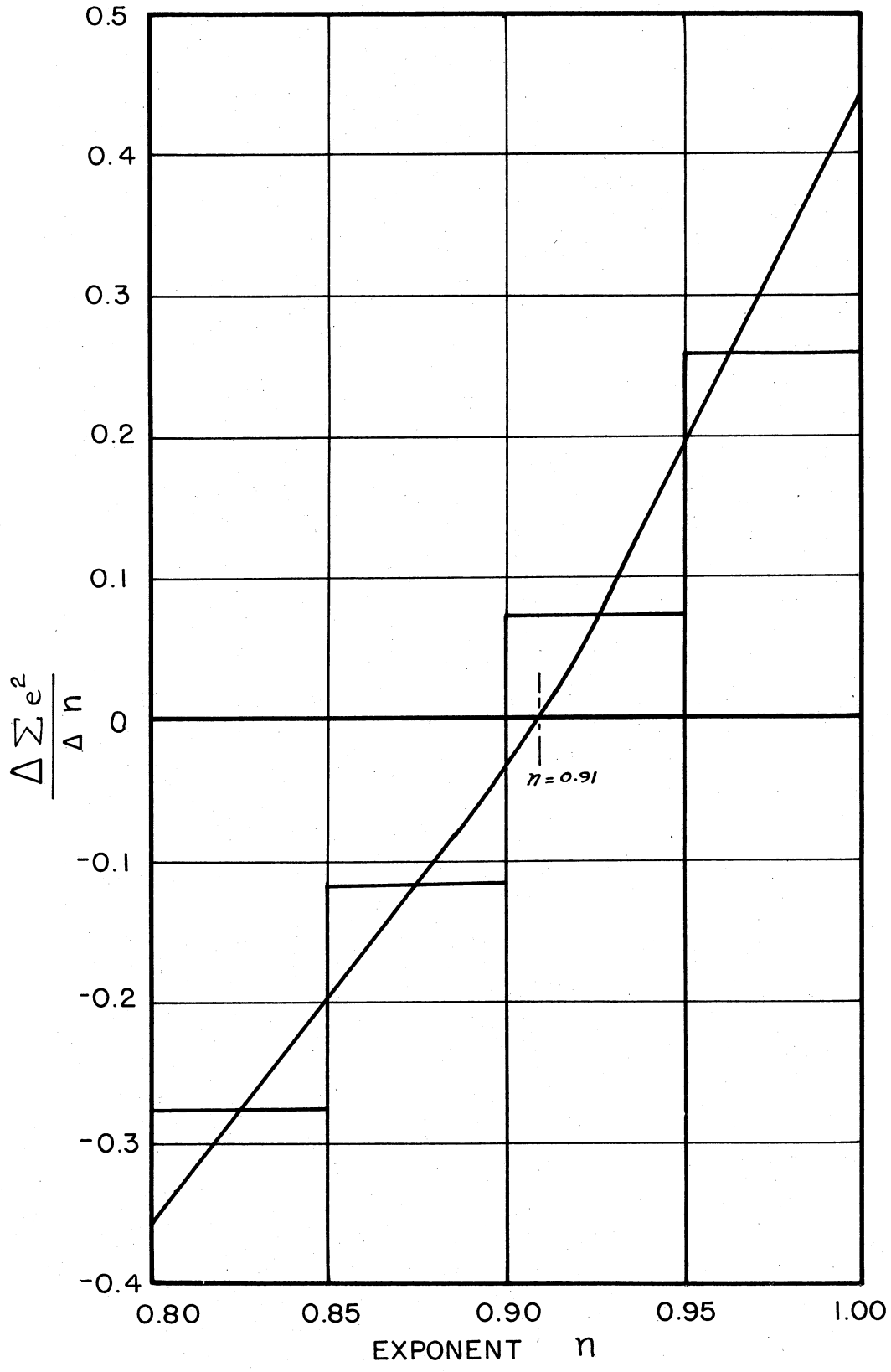

FIGURE 25— EQUAL AREA CURVE FOR DETERMINATION OF WATER FLOW RATE EXPONENT

the area of the curve below the zero line is equal to the area above it. This curve intersects the zero line where the least mean square deviation is a minimum at n = 0.91. This point is also shown in Figure 24. The actual value of n = 0.91 obtained by this analytical procedure is used to prepare the Wilson plot presented in Figure 26. It is interesting to note that the curved trend indicated previously by runs 73 through 84 (Figure 23) is eliminated by using the proper value of n.

In order to prove the validity of this procedure additional Wilson-plot type data were obtained with saturated steam condensing at 246.44°F (runs 85 through 92) and 225.76°F (runs 93 through 100) after installation of tube-wall thermocouples. The calculated results for these data with a clean tube are tabulated in Table VI. Wilson-plot results are computed for the assumed value of n = 0.80 and the calculated value of n = 0.91 and presented in Table VI, and Figures 23 and 26. In both figures no appreciable effect of condensing pressure on the overall coefficient is observed. This is due to the mixed condensation of steam discussed further in a later section. The experimental water film coefficient is calculated from the heat flux and the measured temperature drop through the water film by the following equation:

$$h_w = \frac{Q}{A(t_i - t_w)} \frac{A_o}{A_i} \qquad \text{(B-13)}$$

where t_i = inside tube surface temperature, °F. The calculated water film coefficients are given in Table VI and presented in Figure 27 as a function of the water flow rate. Water film coefficients calculated from the Dittus-Boelter equation simplified for water (equation B-1) are indicated in Figure 27 for comparison purposes. The experimental coefficients are considerably higher than those predicted from equation 1. This increase varies

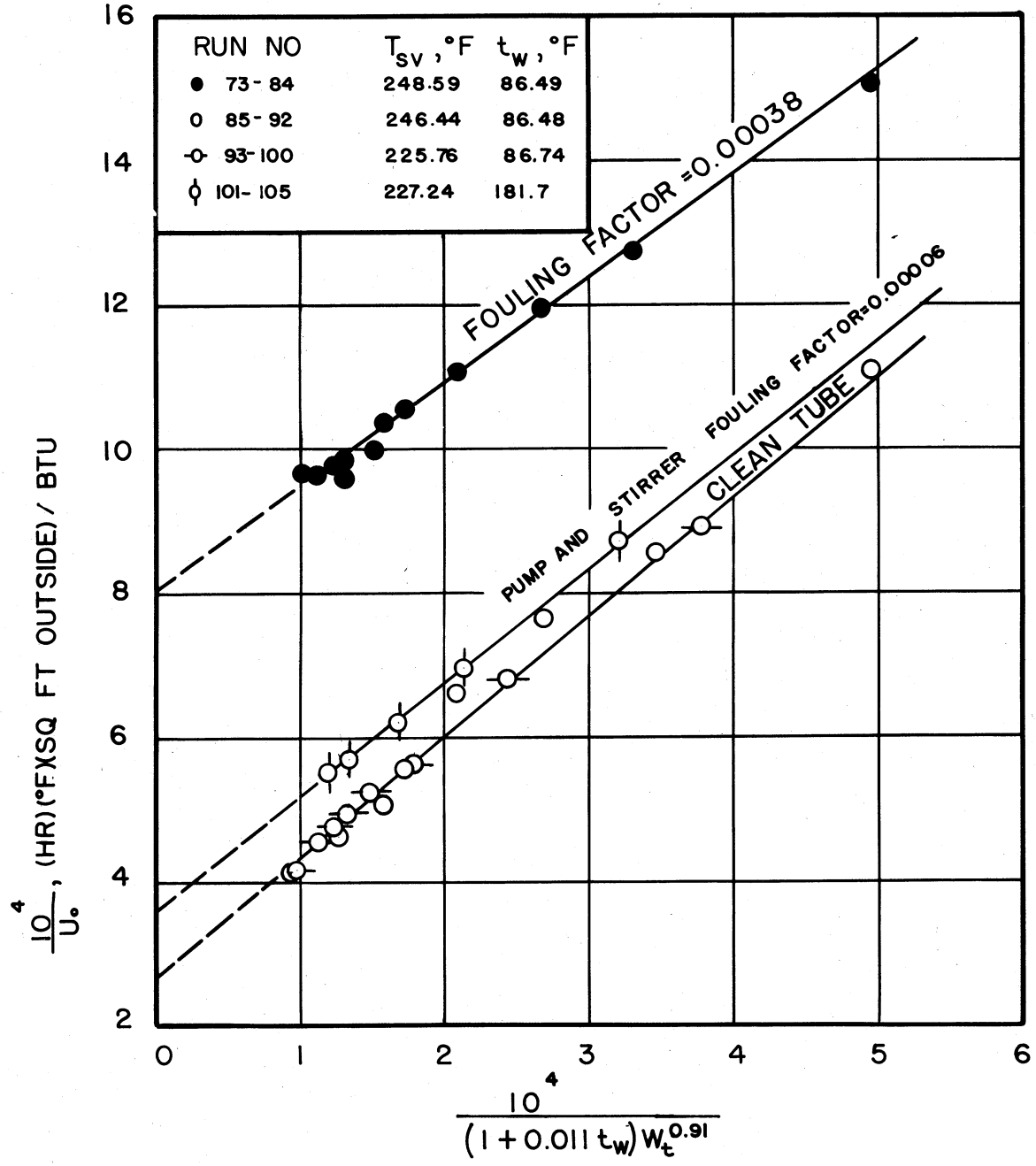

FIGURE 26 — WILSON PLOT WITH WATER FLOW RATE EXPONENT OF 0.91

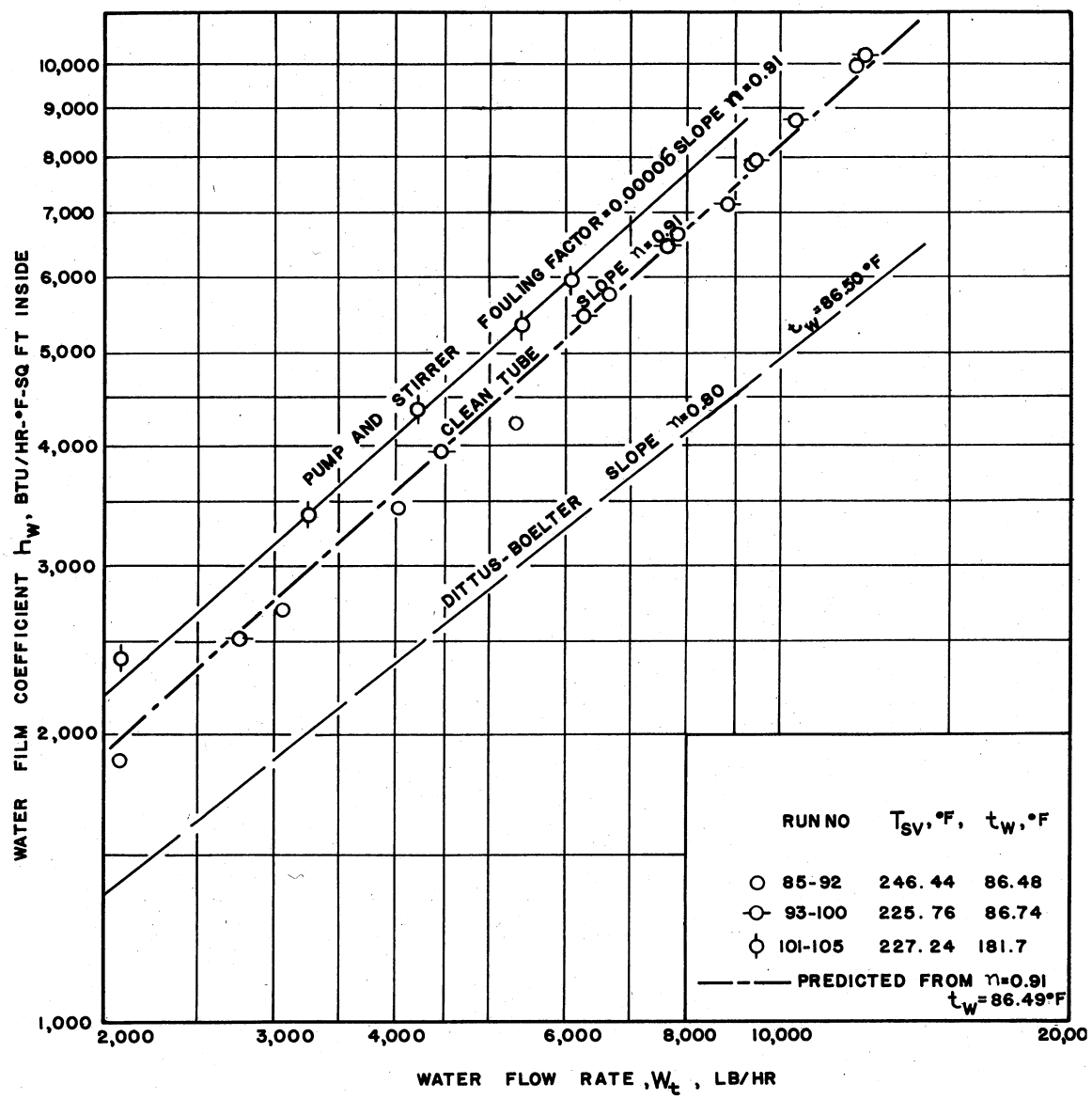

FIGURE 27 – COMPARISON OF PREDICTED AND EXPERIMENTAL TUBE-SIDE FILM COEFFICIENT FOR WATER

from 34.6 per cent at a water flow rate of 2000 lb per hr to 75.5 per cent at 12,000 lb per hr. This deviation is due to the excess turbulence caused by fittings in the flow conduit and the end effects in the condenser and accounts for the abnormal temperature gradient observed along the tube. This subject is discussed in a later section in Appendix B.

The intercept of the Wilson plot for runs 85 through 100 is shown in Figure 26 to be 0.00027 (hr)(°F)(sq ft outside) per Btu. It follows from equation B-3 that the outside film resistance can be evaluated by subtracting that portion of the resistance due to the metal wall [0.000049 (hr)(°F)(sq ft outside) per Btu from Table I] since these results were obtained with a clean tube. The resulting film resistance for the saturated steam is 0.000221 (hr)(°F)(sq ft outside) per Btu and the corresponding condensate film coefficient (h_c) is 4530 Btu per (hr)(°F)(sq ft outside). Comparison of this value with the experimental values (runs 85 through 100) given in Table VI for the range of water flow rates used indicates an increase of 28.3 to 41.5 per cent in the value of the condensate film coefficient. In general with increasing water flow rate and heat flux the condensate film coefficient is expected to decrease. This discrepancy is due to the mixed condensation of steam and the gradual increase in the extent of dropwise condensation with increasing heat flux. This explanation is proved by the order of magnitude of these coefficients which are about twice the value of the coefficients predicted from equation 1 for filmwise condensation. It is interesting to note that the values of these film coefficients agree with those of runs 40 and 46 (Table III) obtained under similar conditions of mixed condensation.

The intercept of the Wilson-plot line for runs 73 through 84 can now be used to evaluate the constant c in equation B-2. The validity of the

resulting equation based on the exponent of 0.91 calculated by the method of least mean squares is checked by comparing the film coefficients calculated from this equation with the experimental coefficients obtained for runs 85 through 100 and presented in Figure 27. The relative location of the lines in Figure 26 indicates a certain amount of fouling for the results from runs 73 through 84. Using the condensate film resistance obtained previously by extrapolation of the clean-tube data and the intercept from the line for runs 73 through 84 (Figure 26) the extent of fouling is determined as follows from equation B-3:

$$f_i = \frac{1}{1.41} (0.00080 - 0.000049 - 0.000221)$$

$$f_i = 0.000376 \text{ or } 0.00038 \frac{(\text{hr})(^\circ\text{F})(\text{sq ft inside})}{\text{Btu}} .$$

The slope of the line for runs 73 through 84 is found to be 1.452 in Figure 26. The resulting water film coefficient equation is:

$$h_w = 0.97 (1 + 0.011 t_w) W_t^{0.91} . \qquad \text{(B-14)}$$

Values of h_w calculated from equation B-14 are indicated in Figure 27 by the dashed line identified with a slope of 0.91. It is seen that the equation derived by the outlined procedure for the determination of n predicts water film coefficients which agree satisfactorily with experimentally determined values. The deviations of the calculated results from the experimental are within the range of the experimental errors involved in the measurements and vary from +4.4 per cent at the low range to -3.2 per cent at the high range. Introducing the water velocity and tube diameter variables into equation B-14 the following relationship is obtained:

$$h_w = 185.2 (1 + 0.011 t_w) \frac{V_t^{0.91}}{d_i^{0.09}} . \qquad \text{(B-15)}$$

Results predicted by equation B-15 deviate from those of equation B-1 about as much as the experimental film coefficients shown in Figure 27 and discussed earlier.

Runs 101 through 105 are made to find out the possible effect of the water circulating pump and stirrer (Nos. 10 and 14 in Figure 2) on the water film coefficient. The experimental results are given in Table VI and are shown as Wilson plots in Figures 23 and 26. Film coefficients presented in Figure 27 are compared with the clean-tube data. No effect of pump and stirrer is observed due to the various straightening sections between the pump and the experimental tube (Figures 1 and 2). Comparison of the water film coefficients with values predicted from equation B-14 indicates a slight fouling of 0.00006 (hr)(°F)(sq ft ins.) per Btu.

The validity of equation B-14 for the prediction of water film coefficients follows from the foregoing discussion. Equation B-14 is used to calculate the water film coefficient for runs 56 through 72 shown in Table III. These results constitute the only data on the filmwise condensation of superheated steam and are obtained prior to wall thermocouple installation. Equation 1 is used to calculate the condensate film coefficient for the saturated runs (runs 56, 57, 58, and 67). The water film coefficient determined from equation B-14 is combined with the condensate film coefficient and the experimental overall coefficient to calculate the extent of tube-side fouling. The inside fouling factor evaluated by this method is found to be 0.00023 (hr)(°F)(sq ft ins.) per Btu and is used along with equation B-14 to determine the tube surface temperature for runs 59 through 66 and 68 through 72 obtained with filmwise condensation of superheated steam.

TEMPERATURE DISTRIBUTION ALONG CONDENSING TUBE

The importance of end effects on the water film coefficient is observed from the experimental results and is discussed in the previous section. Figure 27 indicates that the average water film coefficient may be as much as 75.5 per cent higher than the normal value predicted from equation B-1. It is important to note that this increase is due primarily to the very high water film coefficients which prevail in the region extending from the right end of the tube where the water inlet is located. The effect of this phenomenon is an apparently abnormal temperature gradient along the tube. If the entrance effect is neglected the wall temperature is expected to indicate an almost linear variation along the tube being lowest at the water inlet end and highest at the water outlet end. The experimental wall temperatures for runs 101 through 105 are shown in Table VIII and presented in Figure 28. For all water flow rates the wall temperature is lowest at the water inlet, higher at the water outlet, and highest at the middle of the tube. The difference between the wall temperature (t_M-t_L) at the middle of the tube and at the water outlet is also shown in Table VIII and presented in Figure 29 as a function of the water

TABLE VIII

TEMPERATURE DISTRIBUTION ALONG CONDENSING TUBE

Run No.	Measured Wall Temperature			Temperature Difference, (t_M-t_L), °F
	Water Outlet End, t_L, °F	Middle t_M, °F	Water Inlet End, t_R, °F	
101	215.33	215.59	210.82	0.26
102	212.00	212.70	206.74	0.70
103	208.67	209.74	203.59	1.07
104	206.00	207.59	201.04	1.59
105	204.07	206.26	199.76	2.19

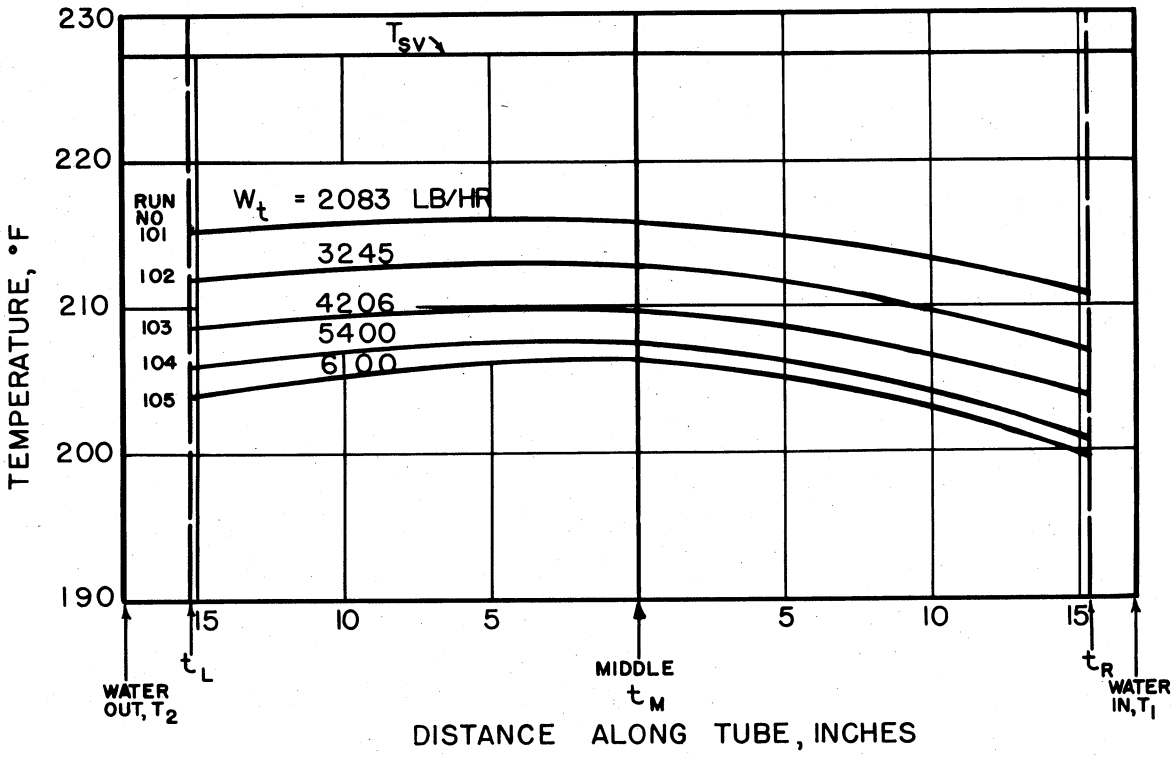

FIGURE 28 — TEMPERATURE DISTRIBUTION ALONG CONDENSING TUBE

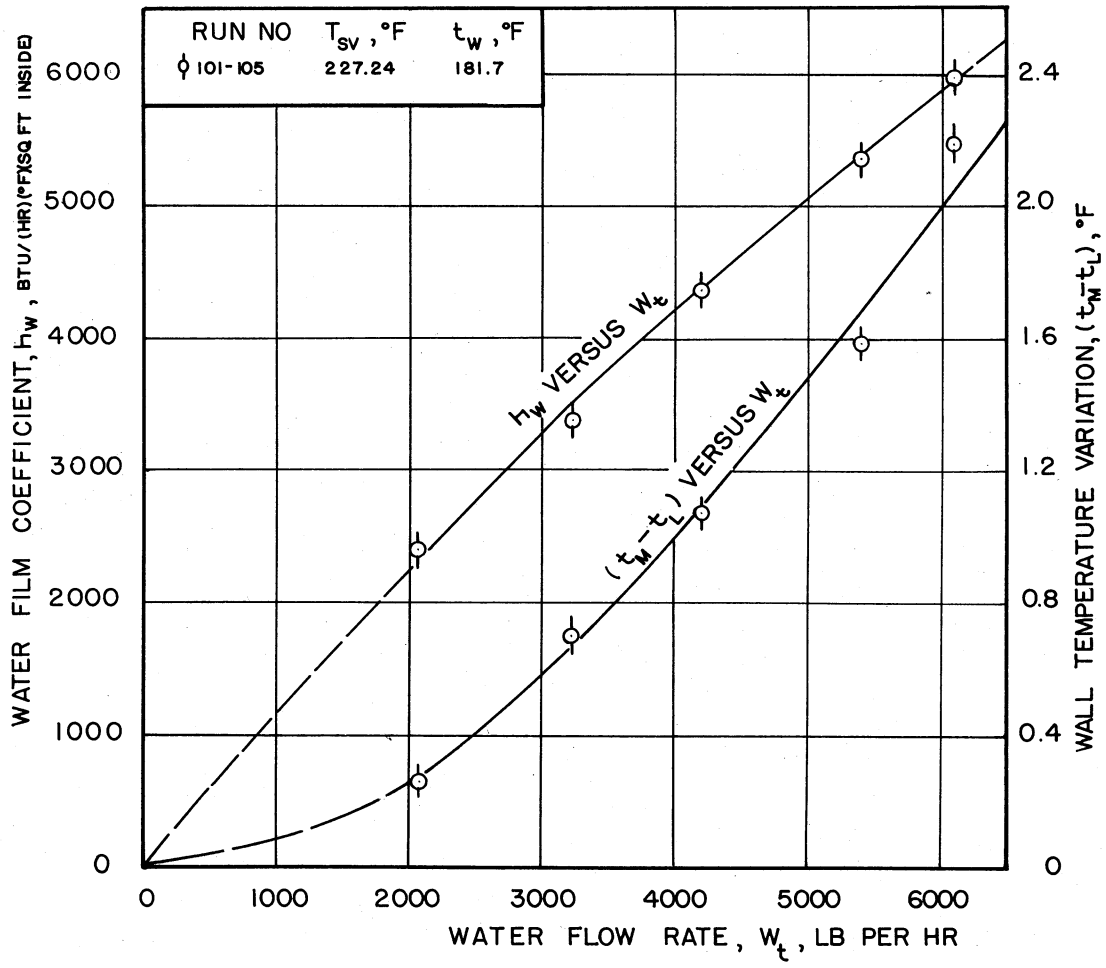

FIGURE 29 — EFFECT OF WATER FLOW RATE ON WATER FILM COEFFICIENT AND TEMPERATURE DISTRIBUTION ALONG CONDENSING TUBE

flow rate. Figures 28 and 29 indicate that the temperature rise at the middle above that at the water outlet varies with the water flow rate and the mean water film coefficient. It may be concluded from these observations that the peculiar temperature distribution is due to entrance effects which are more pronounced at high than at low Reynolds numbers or water flow rates. The $(t_M - t_L)$ curve in Figure 29 is extrapolated to the origin to show that theoretically the middle and water outlet temperatures will be equal when there is no heat flux and therefore no entrance effects.

APPENDIX C

SAMPLE CALCULATIONS

A sample of the original data and calculations are presented in this section for run 21 with superheated Freon-114 condensing at a pressure of 43.74 lb per sq in. absolute.

Table IX presents the original data.

TABLE IX

ORIGINAL DATA SHEET

Run No. 21

Condensing fluid: Freon-114

Cooling fluid: Water

Temperatures:

Room	78.0°F
Inlet water, T_1	8.64°C
Outlet water, T_2	9.80°C
Condenser, middle, T_{MC}	5.038 mvolts
left end, T_{LC}	5.000 mvolts
Tube wall, left end, 0° t_{LO}	0.460 mvolts
left end, 90° t_{L90}	0.418 mvolts
middle, 0° t_M	0.462 mvolts
right end, 0° t_R	0.418 mvolts

Pressures:

Condenser	29.7 psig
Barometric at 29.5°C	29.52 in. Hg
Rotameter reading	23.5 per cent

(1) Condenser Pressure, P_g:

$$P_g = P(\text{barometer}) + P(\text{gage}) + \text{calibration} - \frac{(17.5)\ (\rho \text{ fluid})}{(12)\ (144)}$$

P(gage) = 29.7 lb per sq in. gage

Calibration = -0.21 lb per sq in.

$$P(\text{barometer}) = \frac{(29.52)\ (13.53)\ (62.4)}{(12)\ (144)} = 14.40 \text{ lb per sq in.}$$

Assume vapor in gage line is saturated at $P_g \sim 44$ lb per sq in.

absolute ρ fluid = 1.38 lb cu ft

$$-\frac{(17.5)\ (1.38)}{(12)\ (144)} = -0.014 \text{ lb per sq in.}$$

$\therefore P_g = 14.40 + 29.7 - 0.21 - 0.01 = 43.88$ lb per sq in. absolute

From tables of thermodynamic properties[9]

$T_{sv} = 96.61°F$

The saturation temperature is assumed to be that for run 16 because of its proximity to the more reliable saturation temperature measured by thermocouples for run 16.

$\therefore T_{sv} = 96.42°F$ and $P_g = 43.74$ lb per sq in. absolute

(2) Overall Performance:

From the rotameter calibration at 23.5 per cent, $W_t = 2570$ lb per hr.

The correction to the thermometer readings T_1 and T_2 is negligible for this range. The following are a few values from the thermometer calibration chart:

Observed Temperature °C	Correction to T_1	Correction to T_2
25	0.10	0.05
30	0.41	0.36
40	0.23	0.25
60	0.39	0.44
80	0.62	0.66

Inlet water temperature = 8.64°C

Water temperature rise, Δt_t = 9.80 - 8.64 = 1.16°C

= (1.16) (1.8) = 2.086°F

Mean water temperature = 8.64 + 0.58 = 9.22°C

= (9.22) (1.8) + 32 = 48.60°F

Total heat transferred = $W_t\ C_p\ \Delta t_t$

Q = (2570) (1.0) (2.086) = 5360 Btu per hr

Heat transfer rate, $\frac{Q}{A} = \frac{5360}{0.565} = 9500\ \frac{\text{Btu}}{(\text{hr})(\text{sq ft})}$

(3) Condenser Temperature:

The correction to all potentiometer readings is 0.002 mvolts.

$\therefore$ uncorrected T_{LC} = 5.000 + 0.002 = 5.002 mvolts and

uncorrected T_{MC} = 5.038 + 0.002 = 5.040 mvolts.

Mean uncorrected temperature =

$$\frac{5.002 + 5.040}{2} = 5.021 \text{ mvolts}$$

Correction to condenser thermocouples = - 0.020 mvolts

Corrected thermocouple reading =

5.021 - 0.020 = 5.001 mvolts

From Leeds and Northrup Tables[30]

Condenser temperature, T_g = 202.67°F

Degrees superheat in vapor = $T_g - T_{sv}$

= 202.67 - 96.42 = 106.25°F

Overall temperature difference

$\Delta T_{oa} = (T_g - t_w) = 202.67 - 48.60 = 154.07°F$

Overall coefficient, $U_o = \frac{Q}{A(T_g - t_w)}$

$$U_o = \frac{9500}{154.07} = 61.6\ \frac{\text{Btu}}{(\text{hr})(°\text{F})(\text{sq ft outside})}$$

(4) Condensing Load, m_s:

From Figure 36 in Appendix F or reference 9

at P_g = 43.74 psia and T_g = 202.67°F

Enthalpy of superheated Freon-114

H = 103.16 Btu per lb

at P_g = 43.74 psia

Enthalpy of saturated liquid

h = 31.60 Btu per lb

Heat removed, $(-\Delta H)$ = 103.16 - 31.60 = 71.56 Btu/lb

Total vapors condensed, $W_s = Q/-\Delta H$

$$W_s = \frac{5360}{71.56} = 75.0 \text{ lb per hr}$$

Condensing load, $m_s = W_s/A$

$$m_s = \frac{75.0}{0.565} = 132.8 \text{ lb per (hr)(sq ft)}$$

(5) Tube Wall Temperature, t_m:

Uncorrected t_{LO} = 0.460 + 0.002 = 0.462 mvolts

Uncorrected t_{L90} = 0.418 + 0.002 = 0.420 mvolts

Uncorrected t_M = 0.462 + 0.002 = 0.464 mvolts

Uncorrected t_R = 0.418 + 0.002 = 0.420 mvolts

Mean uncorrected $t_L = \frac{0.462 + 0.420}{2}$ = 0.441 mvolts

t_L calibration correction = 0.020 mvolts

Corrected t_L = 0.441 + 0.020 = 0.461 mvolts

t_M calibration correction = 0.019 mvolts

Corrected t_M = 0.464 + 0.019 = 0.483 mvolts

t_R calibration correction = 0.014 mvolts

Corrected t_R = 0.420 + 0.014 = 0.434 mvolts

Mean tube wall temperature,

$$t_m = \frac{0.461 + 0.483 + 0.434}{3} = 0.459 \text{ mvolts}$$

From Leeds and Northrup Tables for 38 Calibration[30]

$$t_m = 53.32°F$$

(6) Metal Resistance, r_m:

At $t_m = 53.32°F$

$$k_m{}^{38} = 222.7 \text{ Btu per (hr)(°F)(ft)}$$

From Table I

Log-mean diameter, $d_m = 0.636$ inch

Outside diameter, $d_o = 0.750$ inch

Wall thickness, $Y_m = \frac{0.1095}{12}$ ft

$\therefore$ metal resistance $r_m = \frac{Y_m d_o}{k_m A_m}$

$$r_m = \frac{(0.1095)(0.750)}{(12)(222.7)(0.636)}$$

$$= 0.000048 \frac{\text{(hr)(°F)(sq ft outside)}}{\text{Btu}}$$

Temperature drop through metal wall

$$\Delta t_m = \frac{Q}{A} r_m = (9500)\ (0.000048) = 0.46°F$$

(7) Outside Tube Surface Temperature, t_o:

$$t_o = t_m + \frac{\Delta t_m}{2}$$

$$t_o = 53.32 + \frac{0.46}{2} = 53.55°F$$

(8) Overall Outside Film Coefficient, h_o:

Overall outside film temperature drop

$$\Delta t_o = T_g - t_o = 202.67 - 53.55 = 149.12°F$$

$$h_o = \frac{Q}{A(T_g - t_o)} = \frac{9500}{149.12} = 63.7 \frac{\text{Btu}}{(\text{hr})(^\circ\text{F})(\text{sq ft outside})}$$

(9) Condensate Surface Temperature, T_s:

The following equations are obtained from equations 1 and 25 by substituting for the tube characteristics.

$$h_c = 1.45 \left(\frac{k_f^3 \rho_f^2 g}{\mu_f}\right)^{1/4} \left(\frac{-\Delta H}{\Delta t_c}\right)^{1/4} \qquad \text{(C-1)}$$

$$h_c = \frac{1.352}{(W_s)^{1/3}} \left(\frac{k_f^3 \rho_f^2 g}{\mu_f}\right)^{1/3} \qquad \text{(C-2)}$$

For steam runs 56 through 72 the following equation is used instead of C-2:

$$h_c = \frac{1.41}{(W_s)^{1/3}} \left(\frac{k_f^3 \rho_f^2 g}{\mu_f}\right)^{1/3} \qquad \text{(C-3)}$$

Assume $\Delta t_c = 41.0^\circ\text{F}$.

The mean condensate film temperature,

$$T_f = t_o + \frac{\Delta t_c}{2} = 53.55 + \frac{41.0}{2} = 74.05^\circ\text{F}$$

From Figure 38 in Appendix F

$$\text{at } T_f = 74.05^\circ\text{F} \left(\frac{k_f^3 \rho_f^2 g}{\mu_f}\right)^{1/3} = 721.0$$

$$W_s^{1/3} = (75.0)^{1/3} = 4.21$$

From equation C-2

$$h_c = \frac{(1.352)(721.0)}{(4.21)} = 231.5 \frac{\text{Btu}}{(\text{hr})(^\circ\text{F})(\text{sq ft outside})}$$

Corresponding

$$\Delta t_c = \frac{Q}{A\, h_c} = \frac{9500}{231.5} = 41.0^\circ\text{F}$$

which checks the assumed value of 41.0°F.

$$T_s = t_o + \Delta t_o = 53.55 + 41.0 = 94.55°F$$

(10) Interfacial Vapor-Film Coefficient, h_i:

Temperature drop through the vapor-liquid interface

$$\Delta t_i = T_g - T_s = 202.67 - 94.55 = 108.12°F$$

$$h_i = \frac{Q}{A(T_g - T_s)} = \frac{9500}{108.12} = 87.9 \frac{\text{Btu}}{(\text{hr})(°\text{F})(\text{sq ft outside})}$$

Items 1 through 10 are given in Tables II and III.

(11) Saturation and Condensate Surface Temperatures Obtained from Correlating Line Drawn in Figure 18

Derivation of Equation of $\ell n\ T_s$ versus ΔT_s —

The slope of the line is determined from two sets of coordinates:

at $\Delta T_s = 0°F$ $\quad T_s = T_{sv} = 98.0°F$

$\Delta T_s = 115.0°F$ $\quad T_s = 90.0°F$

$$\text{slope} = \frac{\ell n \frac{T_{s1}}{T_{s2}}}{\Delta T_{s1} - \Delta T_{s2}} = \frac{\ell n \frac{98.0}{90.0}}{0-115.0}$$

$\log 98.0 = 1.99123$

$\log 90.0 = 1.95424$

$\log 98.0 - \log 90.0 = 0.03699$

$\log (\log 98.0 - \log 90.0) = 8.56808 - 10$

$\log 2.303 = 0.36229$

$$\log \left(\ell n \frac{98.0}{90.0}\right) = 8.56808 - 10 + 0.36229$$

$$= 8.93037 - 10$$

$$\log 115.0 = 2.06070$$

$$\log\left(\frac{\ell n \frac{98.0}{90.0}}{115.0}\right) = 8.93037 - 10 - 2.06070$$

$$= 6.86967 - 10$$

$$\text{slope} = \frac{\ell n \frac{98.0}{90.0}}{-115} = -0.00074075$$

The equation expressing T_s as a function of ΔT_s is

$$\ell n \frac{T_s}{98.0} = -0.00074075\ \Delta T_s \qquad \text{(C-4)}$$

At $T_{sv} = 98.0°F$, $P_g = 44.89$ lb per sq in. absolute.

Corresponding degrees of superheat

$$\Delta T_s = 202.67 - 98.0 = 104.67°F$$

From equation C-4 the calculated condensate surface temperature is

$$T_s = 90.69°F$$

The equilibrium vapor pressure is obtained from reference 9

at $T_s = 90.69°F$, $P_s^* = 39.755$ psia

Lowering of the condensate surface temperature due to superheat,

$$T_{sv} - T_s = 98.0 - 90.69 = 7.31$$

(12) Interfacial Film Coefficient Based on Correlated Condensate Surface Temperature:

$$\Delta t_i = T_g - T_s = 202.67 - 90.69 = 111.98°F$$

$$h_i = \frac{Q}{A(T_g - T_s)} = \frac{9500}{111.98} = 84.9 \text{ Btu per (hr)(°F)(sq ft outside)}$$

(13) Calculation of Correlating Group

$$G(f) = \frac{m_s \sqrt{T_s}}{P_g \left(\frac{T_s}{T_g}\right)^{1/2} - P_s^*}$$ In Table V:

$T_s = 90.69 + 460 = 550.69°R$

$T_g = 202.67 + 460 = 662.67°R$

$\frac{T_s}{T_g} = \frac{550.69}{662.67} = 0.8310$

$\left(\frac{T_s}{T_g}\right)^{1/2} = (0.8310)^{1/2} = 0.9116$

$P_g \left(\frac{T_s}{T_g}\right)^{1/2} = (44.89)(0.9116) = 40.92 \text{ psia}$

$P_g \left(\frac{T_s}{T_g}\right)^{1/2} - P_s^* = 40.92 - 39.755 = 1.165 \text{ psi}$

$\sqrt{T_s} = \sqrt{550.69} = 23.46$

From Item 4, $m_s = 132.8 \frac{\text{lb}}{(\text{hr})(\text{sq ft})}$

$\therefore G(f) = \frac{(132.8)(23.46)}{(1.165)} = 2680$

(14) Calculation of Correlating Group

$$H(f) = \frac{h_i \sqrt{T_s}}{(-\Delta H)\left[P_g \left(\frac{T_s}{T_g}\right)^{1/2} - P_s^*\right]}:$$

From Item 4, $-\Delta H = 71.56$ Btu/lb

$\therefore H(f) = \frac{(84.9)(23.46)}{(71.56)(1.165)} = 23.9$

APPENDIX D

CALCULATION OF A TYPICAL VALUE OF ϕ_g

The value of ϕ_g is calculated for run 15 to check the validity of the specified range of $0.1 \geq |\phi_g| \geq 0.001$ necessary for the elimination of Γ from equation 19.

The following equations may be used:

$$\Gamma = 1 + 1.85 \, |\phi_g| \text{ for } 0.1 \geq |\phi_g| \geq 0.001 \tag{29}$$

$$\phi_g = \frac{m_s}{2\pi^{1/2} f P_g} \sqrt{\frac{2\pi RT_s}{g_c M}} \left(\frac{T_g}{T_s}\right)^{1/2} \tag{30}$$

$$\phi_g = \frac{1}{1.85}\left(\frac{P_s^*}{P_g}\right)\left(\frac{T_g}{T_s}\right)^{1/2} - \frac{m_s}{1.85 f P_g}\left(\frac{T_g}{T_s}\right)^{1/2}\sqrt{\frac{2\pi RT_s}{g_c M}} - \frac{1}{1.85} \tag{31}$$

$$f = \frac{1.52 \, m_s \sqrt{\frac{2\pi RT_s}{g_c M}}}{\left[P_s^* - P_g\left(\frac{T_s}{T_g}\right)^{1/2}\right]} \cdot \tag{32}$$

From Table V:

For run 15

$P_s^* = 61.523$ psia

$P_g = 71.43$ psia

$\left(\frac{T_s}{T_g}\right)^{1/2} = (0.7990)^{1/2} = 0.8939$

$\left[P_g\left(\frac{T_s}{T_g}\right)^{1/2} - P_s^*\right] = 2.327$ psi

(1) Calculation of ϕ_g from equations 31 and 32:

Substituting for f from equation 32 into equation 31 ϕ_g is defined as

$$\phi_g = \frac{1}{1.85}\left(\frac{P_s^*}{P_g}\right)\left(\frac{T_g}{T_s}\right)^{1/2} - \frac{\left[P_s^* - P_g\left(\frac{T_s}{T_g}\right)^{1/2}\right]}{(1.85)\,(1.52)\,P_g}\left(\frac{T_g}{T_s}\right)^{1/2} - \frac{1}{1.85} \quad . \qquad \text{(D-1)}$$

Solving for the value of ϕ_g:

$$\phi_g = \frac{(61.523)}{(1.85)(71.43)(0.8939)} - \frac{(-2.327)}{(1.85)(1.52)(71.43)(0.8939)} - \frac{1}{1.85}$$

$$\phi_g = 0.521 + 0.013 - 0.541 = -0.007 \quad .$$

(2) Calculation of ϕ_g from equations 30 and 32:

Substituting for f from equation 32 into equation 30 ϕ_g is defined as:

$$\phi_g = \frac{\left[P_s^* - P_g\left(\frac{T_s}{T_g}\right)^{1/2}\right]}{(2\pi^{1/2})(1.52)(P_g)}\left(\frac{T_g}{T_s}\right)^{1/2} \quad . \qquad \text{(D-2)}$$

Solving for the value of ϕ_g:

$$\phi_g = \frac{(-2.327)}{(2\pi^{1/2})(1.52)(71.43)(0.8939)} = -0.0068 \quad .$$

(3) Calculation of Γ:

From equation 29, at $|\phi_g| = 0.0068$

$$\Gamma = 1 + (1.85)(0.0068) = 1.0126 \quad .$$

APPENDIX E

EXAMPLE DESIGN OF A SUPERHEATED FREON-114 VAPOR CONDENSER

The design procedure outlined previously is illustrated in this section for the design of a condenser involving filmwise condensation of superheated Freon-114 outside horizontal tubes.

Problem: 1000 lb per hr of superheated Freon-114 vapors are to be condensed on the shell side of a horizontal tube condenser with water flowing inside the tubes. The superheated vapors enter the condenser at 400°F and condense at a pressure of 60.0 lb per sq in. absolute. The water flow rate and temperature are such that the mean outside tube surface temperature is 85.0°F. The required total outside heat transfer area is to be determined.

The following conditions are specified:

a. Tubes with 1-inch outside diameter are to be used.

b. No fouling occurs on the shell side.

c. Condensate leaving the unit is saturated.

(1) Overall Heat Duty:

From reference 9 the enthalpy of the vapor at 60 psia and 400°F is

$H = 140.39$ Btu per lb

$T_{sv} = 116.30°F$

Enthalpy of saturated liquid is $h = 36.42$ Btu per lb.

Heat removed, $-\Delta H = 140.39 - 36.42 = 103.97$ Btu/lb.

Overall heat duty, $Q = W_s(-\Delta H)$

$Q = (1000)(103.97) = 103,970$ Btu/hr.

(2) Degree of Superheat, ΔT_s:

$$\Delta T_s = T_g - T_{sv}$$

$$T_g = 400°F, \quad \Delta T_s = 400 - 116.30 = 283.70°F$$

(3) Film Coefficient Equations:

The condensate film coefficient is calculated from equation 1

$$h_c = 0.725 \sqrt[4]{\frac{k_f^3 \rho_f^2 g (-\Delta H)}{D_o \mu_f \Delta t_c}} \qquad (1)$$

To simplify the use of equation 1 define

$$Z^{1/4} = \left(\frac{k_f^3 \rho_f^2 g}{\mu_f}\right)^{1/4}$$

Values of $Z^{1/4}$ are presented in Figure 38 in Appendix F as a function of the mean condensate film temperature, T_f.

For the 1-inch outside diameter tubes used in this application equation 1 becomes:

$$h_c = \frac{(0.725)(103.97)^{1/4}}{(1.0/12)^{1/4}} \left(\frac{Z}{\Delta t_c}\right)^{1/4}$$

$$h_c = 4.3 \left(\frac{Z}{\Delta t_c}\right)^{1/4} . \qquad (E\text{-}1)$$

Equation 37 is used to determine the condensing load (m_s) and the condensate surface temperature (T_s) by trial and error. The calculated condensate surface temperature is used to obtain the temperature drop through the interfacial film (Δt_i) and the corresponding interfacial film coefficient (h_i).

$$\frac{m_s \sqrt{\frac{T_s}{M}}}{\left[P_g \left(\frac{T_s}{T_g}\right)^{1/2} - P_s^*\right]} = \frac{46,700}{\Delta T_s^{1.16}} \qquad (37)$$

For Freon-114, M = 170.9, $\sqrt{M}$ = 13.073. For this application equation 37 becomes

$$\frac{m_s \sqrt{\frac{T_s}{170.9}}}{\left[P_g \left(\frac{T_s}{T_g}\right)^{1/2} - P_s^*\right]} = \frac{46{,}700}{(283.70)^{1.16}}$$

$$m_s = 876 \frac{\left[P_g \left(\frac{T_s}{T_g}\right)^{1/2} - P_s^*\right]}{\sqrt{T_s}} . \qquad \text{(E-2)}$$

(4) Trial-and-Error Determination of Condensate Surface Temperature, T_s:

a. First trial —

Assume T_s = 100.0°F

Assumed $\Delta t_c = T_s - t_o = 100.0 - 85.0 = 15.0°F$

From reference 9, P_s^* = 46.39 psia

$T_s = 100.0 + 460 = 560.0°R$

$\sqrt{T_s} = \sqrt{560.0} = 23.66$

$T_g = 400.0 + 460 = 860.0$

$\left(\frac{T_s}{T_g}\right) = \frac{560.0}{860.0} = 0.651$

$\left(\frac{T_s}{T_g}\right)^{1/2} = (0.651)^{1/2} = 0.807$

$P_g \left(\frac{T_s}{T_g}\right)^{1/2} = (60.0)(0.807) = 48.44$ psia

$\left[P_g \left(\frac{T_s}{T_g}\right)^{1/2} - P_s^*\right] = 48.44 - 46.39 = 2.05$ psi

Substituting the calculated values in equation E-2:

$$m_s = \frac{(876)(2.05)}{(23.66)} = 75.9 \frac{\text{lb}}{(\text{hr})(\text{sq ft})}$$

Heat flux, $\frac{Q}{A} = (75.9)(103.97)$

$$\frac{Q}{A} = 7890 \frac{\text{Btu}}{(\text{hr})(\text{sq ft})}$$

The assumed value of T_s and the corresponding assumed value of Δt_c is checked by calculating the condensate film coefficient from equation E-1 and the calculated Δt_c.

Mean condensate film temperature,

$$T_f = t_o + \frac{\Delta t_c}{2} = 85.0 + \frac{15.0}{2} = 92.5°F$$

From Figure 38 in Appendix F,

at $T_f = 92.5°F$, $Z^{1/4} = 135.2$

$\Delta t_c{}^{1/4} = (15.0)^{1/4} = 1.968$

Substituting these values in equation E-1:

$$h_c = \frac{(4.3)(135.2)}{(1.968)} = 295.5 \frac{\text{Btu}}{(\text{hr})(°F)(\text{sq ft outside})}$$

Calculated

$$\Delta t_c = \frac{Q}{A\, h_c}$$

$$\Delta t_c = \frac{7890}{295.5} = 26.66°F$$

The calculated value of Δt_c is higher than the assumed value of 15°C. A value of Δt_c higher than 15°C is assumed in the second trial.

b. Second trial —

Assume $T_s = 102.0°F$ $P_s{}^* = 47.92$ psia

Assumed $\Delta t_c = 102.0 - 85.0 = 17.0°F$

$T_s = 102.0 + 460 = 562.0°R$

$\sqrt{T_s} = \sqrt{562.0} = 23.77$

Substituting in equation E-2,

$$m_s = \frac{(876)\left[60.0\left(\frac{562}{860}\right)^{1/2} - 47.92\right]}{(23.77)}$$

m_s = 21.4 lb per (hr)(sq ft)

Q/A = (21.4)(103.97) = 2222 Btu per (hr)(sq ft)

At $T_f = 85 + \frac{17.0}{2} = 93.5°F$ $\quad Z^{1/4} = 135.0$

$\Delta t_c^{1/4} = (17.0)^{1/4} = 2.03$

From equation E-1

$$h_c = \frac{(4.3)(135.0)}{(2.03)} = 286 \frac{\text{Btu}}{(\text{hr})(°\text{F})(\text{sq ft outside})}$$

Calculated $\Delta t_c = \frac{2222}{286} = 7.79°F$

The calculated value of Δt_c is lower than the assumed value of 17.0°F. The assumed and calculated values of Δt_c and T_s are indicated in Figure 29a. These results indicate that the condensate surface temperature and the corresponding Δt_c may be approximated by the values obtained from the intersection of the two lines in Figure 29a. This is shown by the third trial.

c. Third trial —

From the intersection of the assumed and calculated values shown in Figure 29a,

T_s = 101.12°F $\quad P_s^*$ = 47.25 psia

Δt_c = 101.12 - 85.0 = 16.12°F

T_s = 101.12 + 460 = 561.12°F

$\sqrt{T_s} = \sqrt{561.12} = 23.74$

From equation E-2

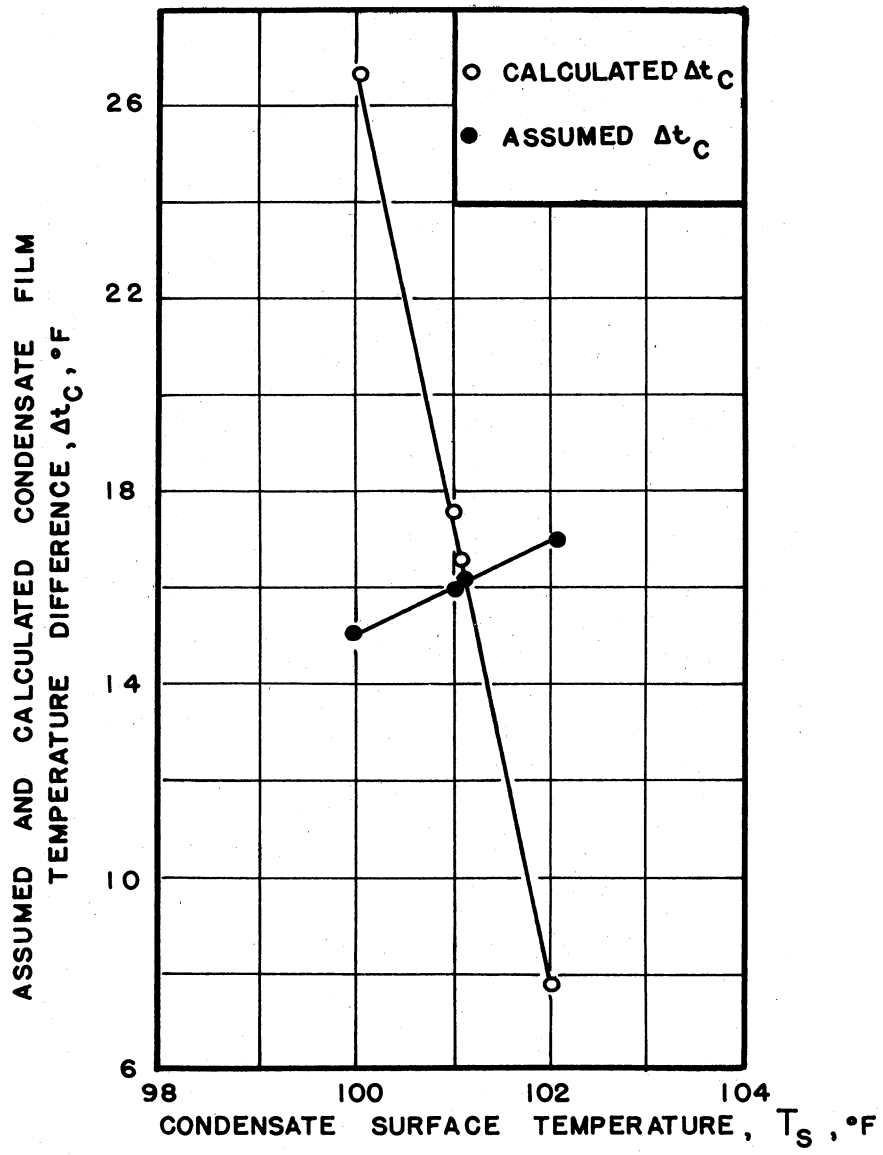

FIGURE 29A TRIAL-AND-ERROR METHOD FOR DETERMINATION OF CONDENSATE SURFACE TEMPERATURE, T_s, °F

$$m_s = \frac{(876)\left[60.0\left(\frac{561.12}{860.0}\right)^{1/2} - 47.25\right]}{(23.74)}$$

m_s = 46.1 lb per (hr)(sq ft)

$\frac{Q}{A}$ = (46.1)(103.97) = 4800 Btu per (hr)(sq ft)

At $T_f = 85 + \frac{16.12}{2} = 93.06°F$ $\quad Z^{1/4} = 135.1$

$\Delta t_c{}^{1/4} = (16.12)^{1/4} = 2.008$

From equation E-1

$$h_c = \frac{(4.3)(135.1)}{(2.008)} = 289.5 \frac{\text{Btu}}{(\text{hr})(°\text{F})(\text{sq ft outside})}$$

Calculated $\Delta t_c = \frac{4800}{289.5} = 16.6°F$

Comparison of these results with the trend shown in Figure 29a indicates that the correct condensate surface temperature is very close to the assumed value at the intersection. The correct value of Δt_c indicated is slightly higher than 16.12°F, and it may be taken to be

$\Delta t_c = 16.15°F$

$T_s = 85.0 + 16.15 = 101.15°F$

(5) Total Outside Area Required, A:

Heat flux, $\frac{Q}{A} = h_c \Delta t_c$

$\frac{Q}{A}$ = (289.5)(16.15) = 4670 Btu per (hr)(sq ft)

$m_s = \frac{(4670)}{(103.97)} = 45.0$ lb per (hr)(sq ft)

Required outside area, A

$A = \frac{W_s}{m_s} = \frac{1000}{45.0} = 22.2$ sq ft

The temperature drop through the interfacial film (Δt_i) and the corresponding interfacial film coefficient (h_i) are

$$\Delta t_i = T_g - T_s = 400.0 - 101.15 = 298.85°F$$

$$h_i = \frac{Q}{A(T_g - T_s)}$$

$$h_i = \frac{(4670)}{(298.85)} = 15.6 \text{ Btu per (hr)(°F)(sq ft)}$$

The correlating groups used in Figures 20 and 21 are calculated for this application:

$$G(f) = \frac{(45.0)(23.74)}{(1.25)} = 855 \text{ at } \Delta T_s = 283.7°F$$

$$H(f) = \frac{(15.6)\ (23.74)}{(103.97)(1.25)} = 2.845 \text{ at } \Delta t_i = 298.85°F$$

These values agree with the correlating lines corresponding to Freon-114 and presented in Figures 20 and 21.

APPENDIX F

PROPERTY CHARTS

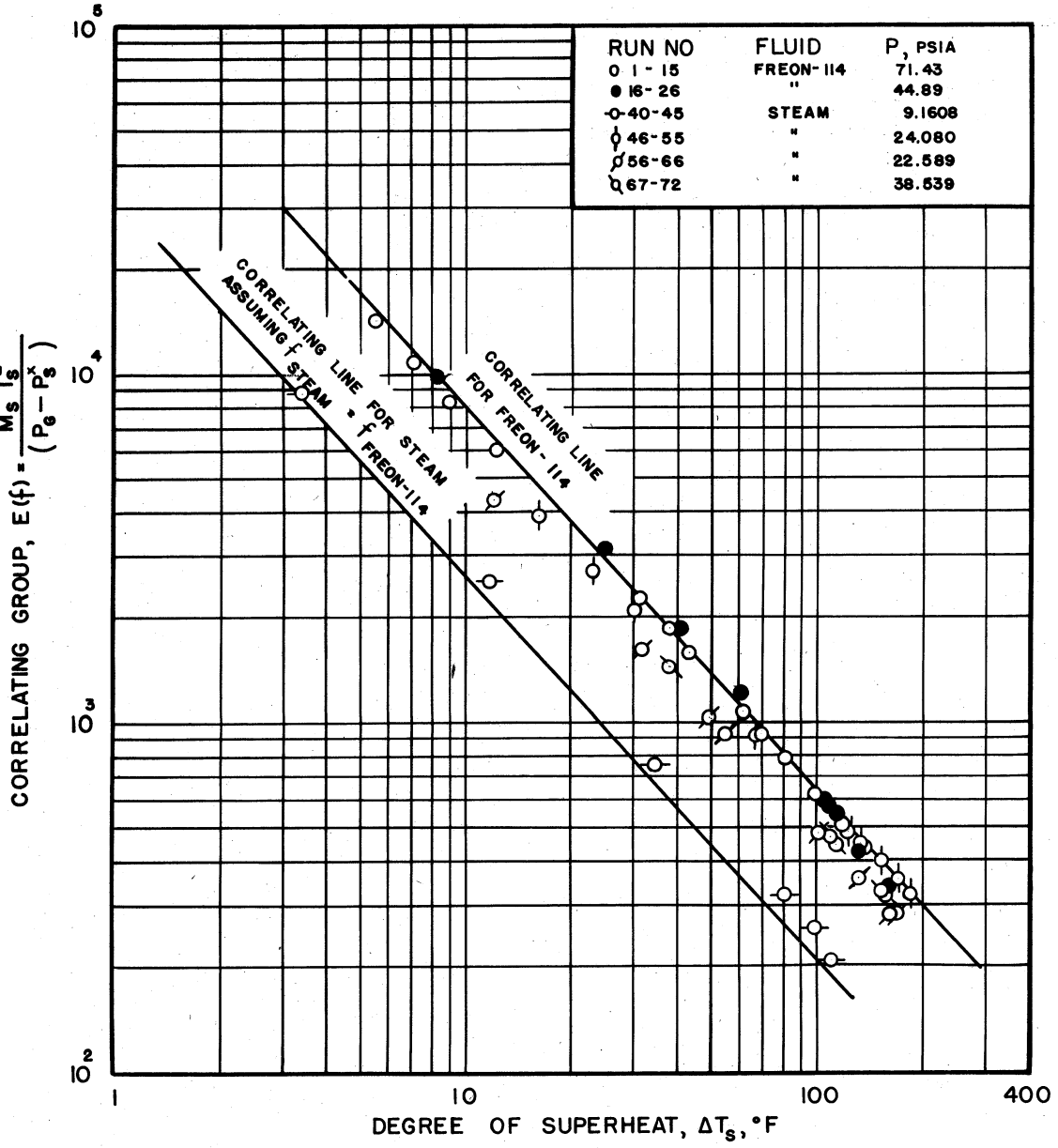

FIGURE 30— CORRELATION OF CONDENSING LOAD WITH SUPERHEAT AS A FUNCTION OF CONDENSATION COEFFICIENT(f). Γ AND T_S/T_G ASSUMED = 1.0

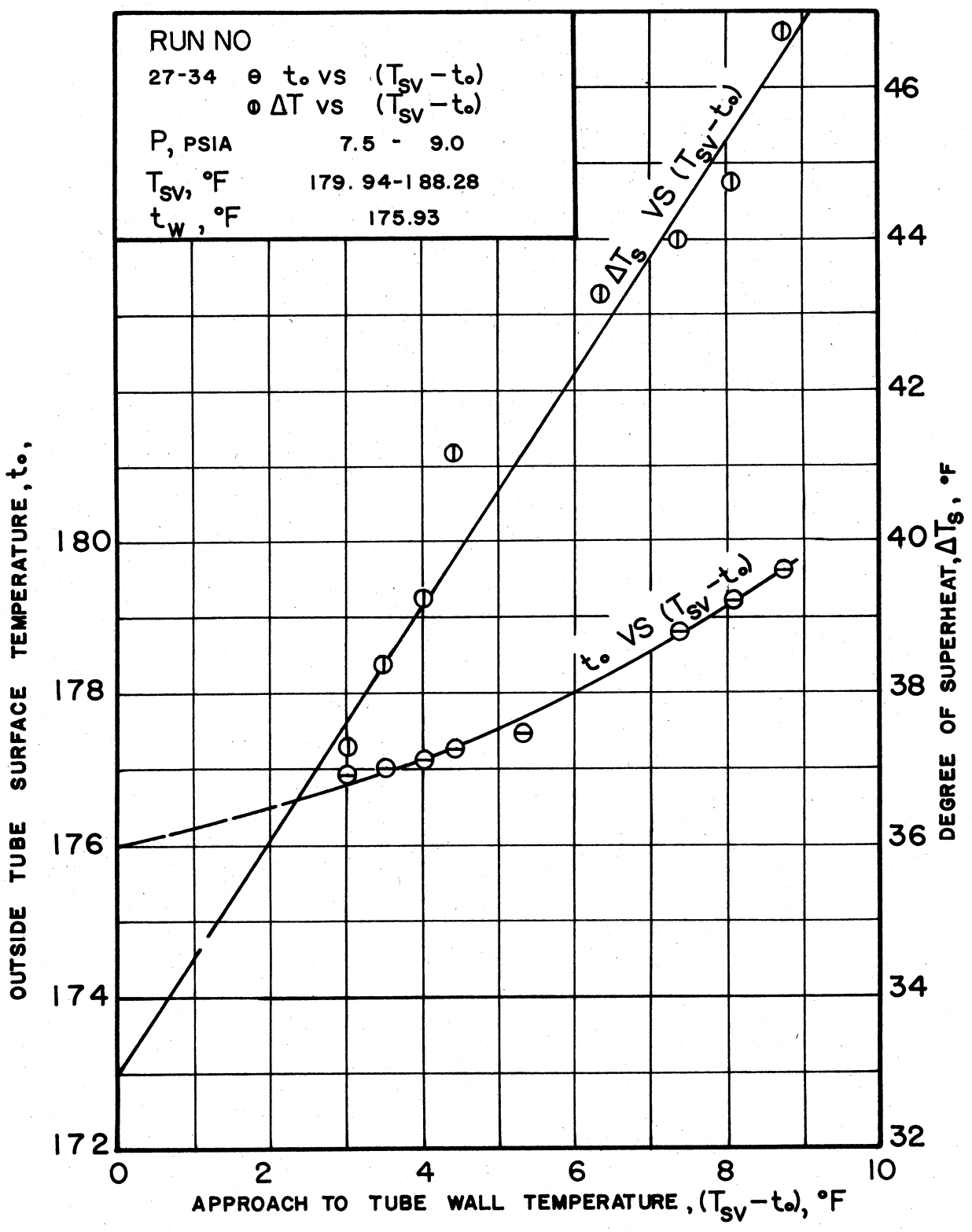

FIGURE 31 — DRY TUBE CONDITION FOR CONDENSING SUPERHEATED STEAM

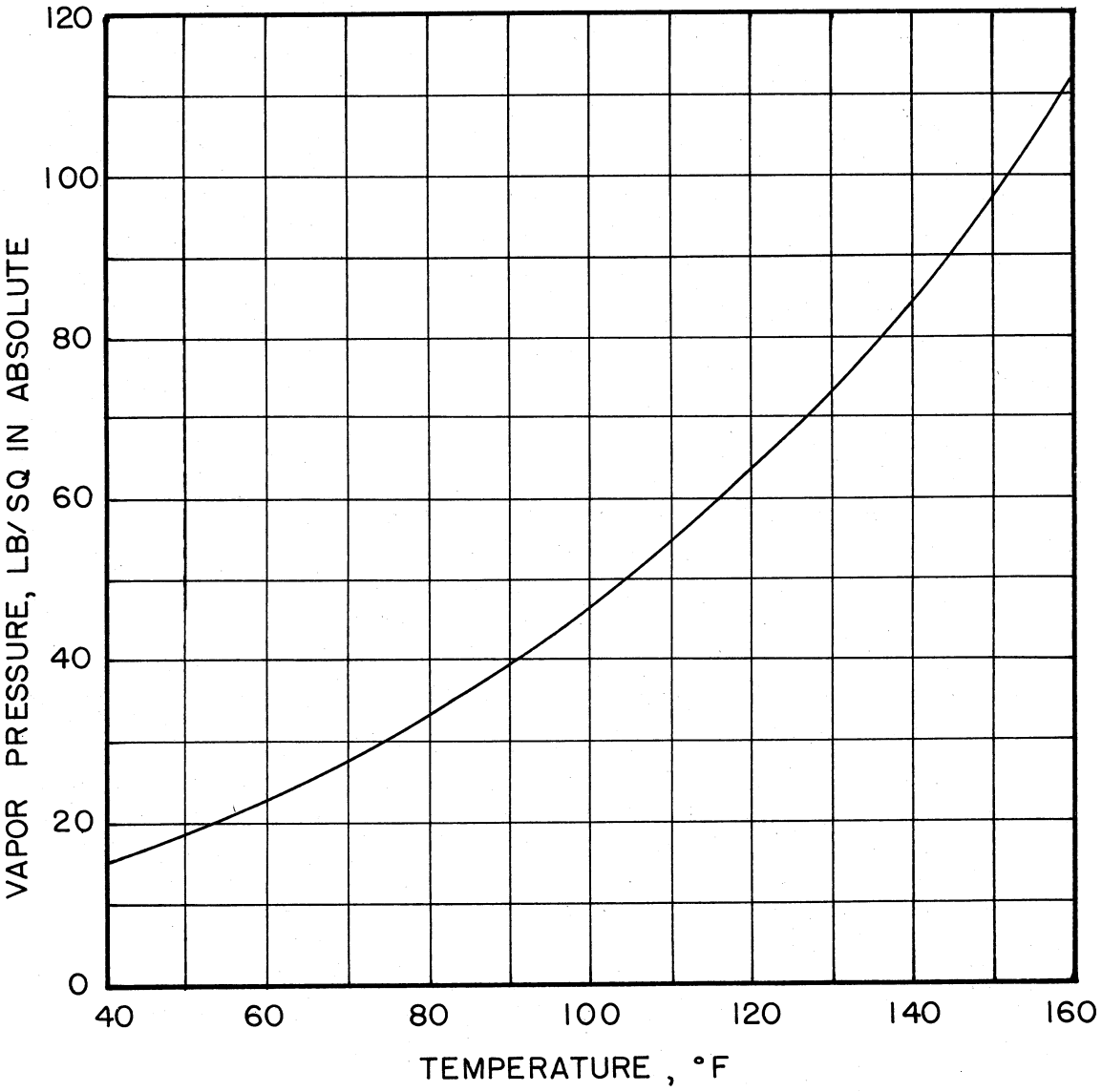

FIGURE 32— VAPOR PRESSURE OF FREON-114

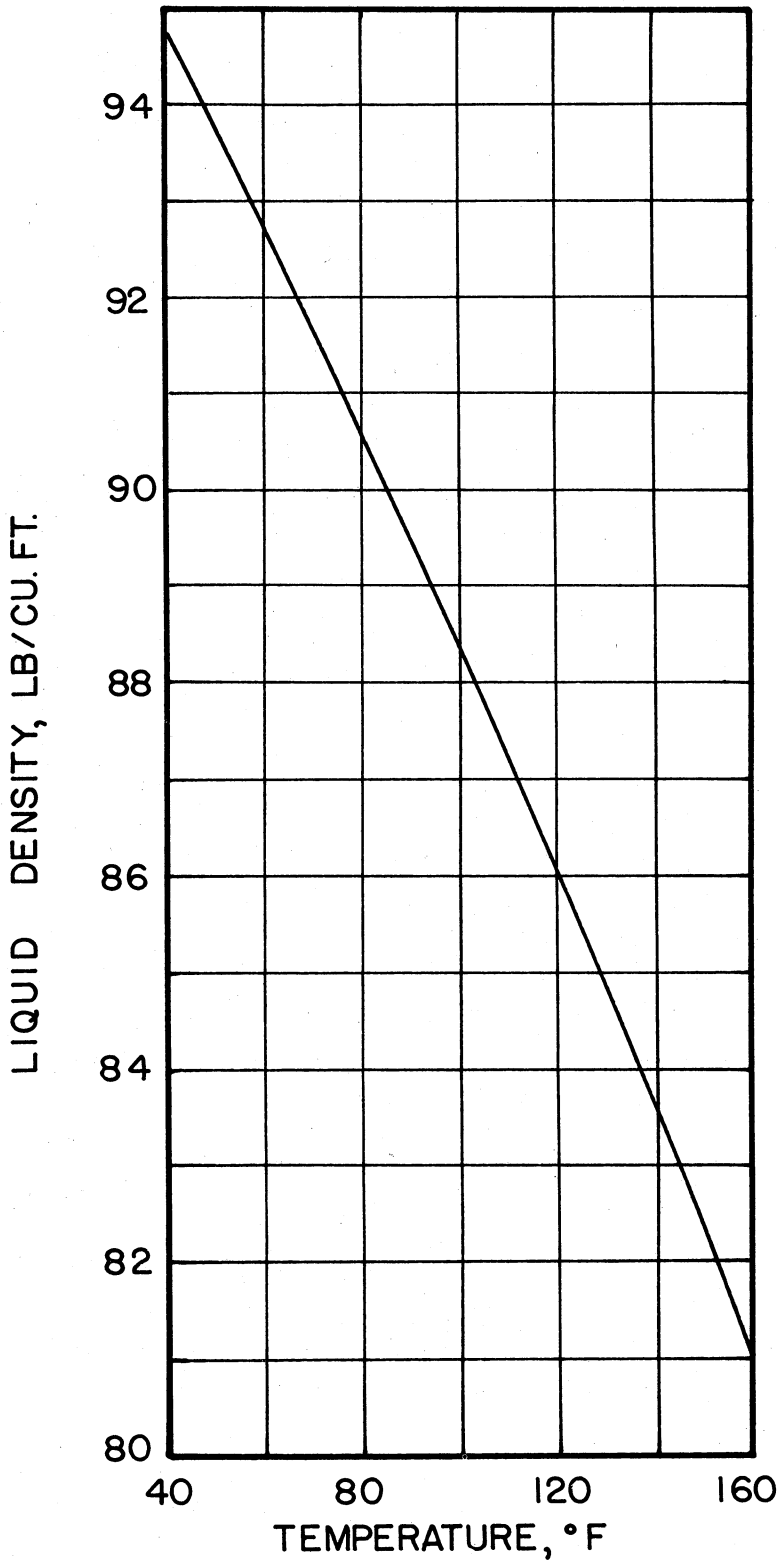

FIGURE 33 - DENSITY OF LIQUID FREON-114

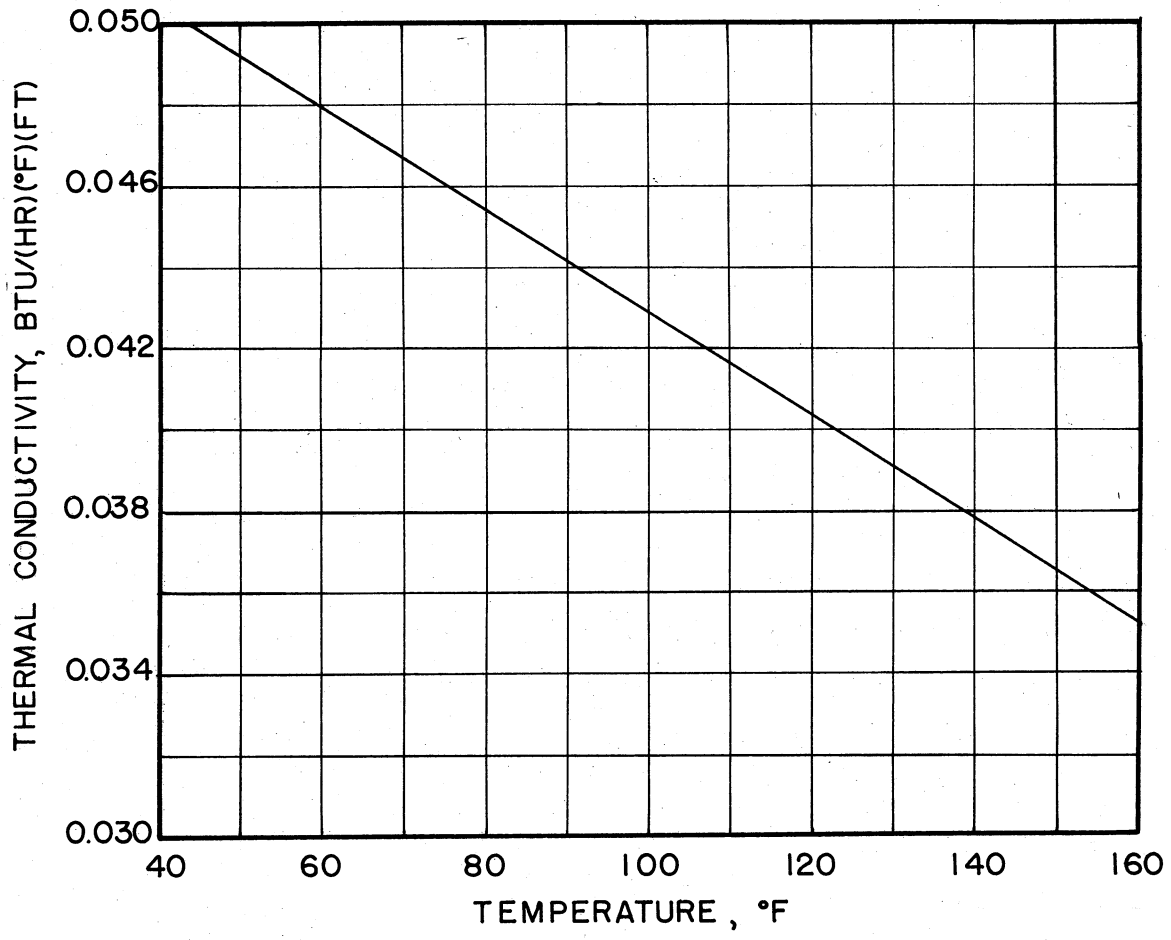

FIGURE 34— THERMAL CONDUCTIVITY OF LIQUID FREON-114

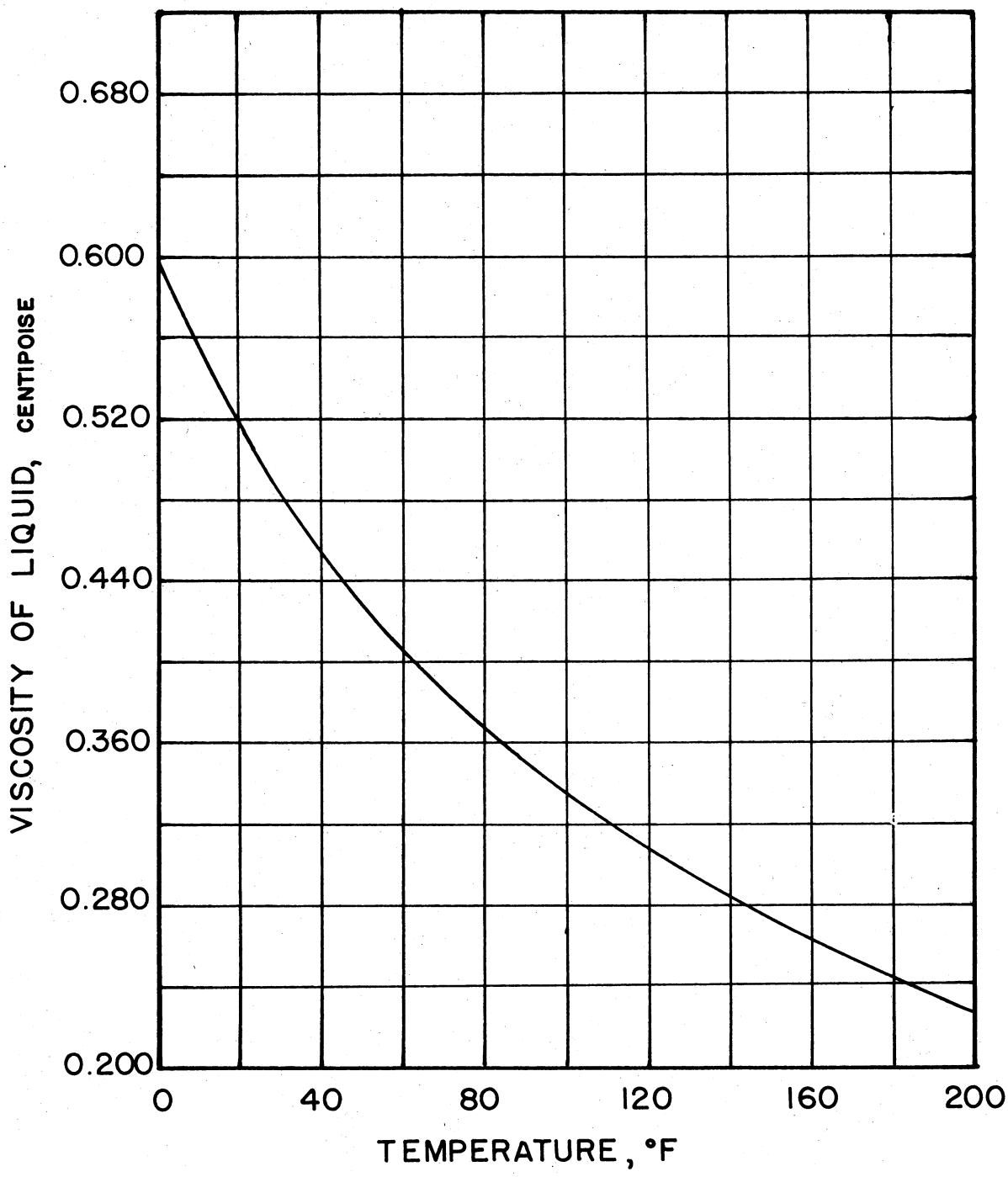

FIGURE 35— VISCOSITY OF LIQUID FREON-114

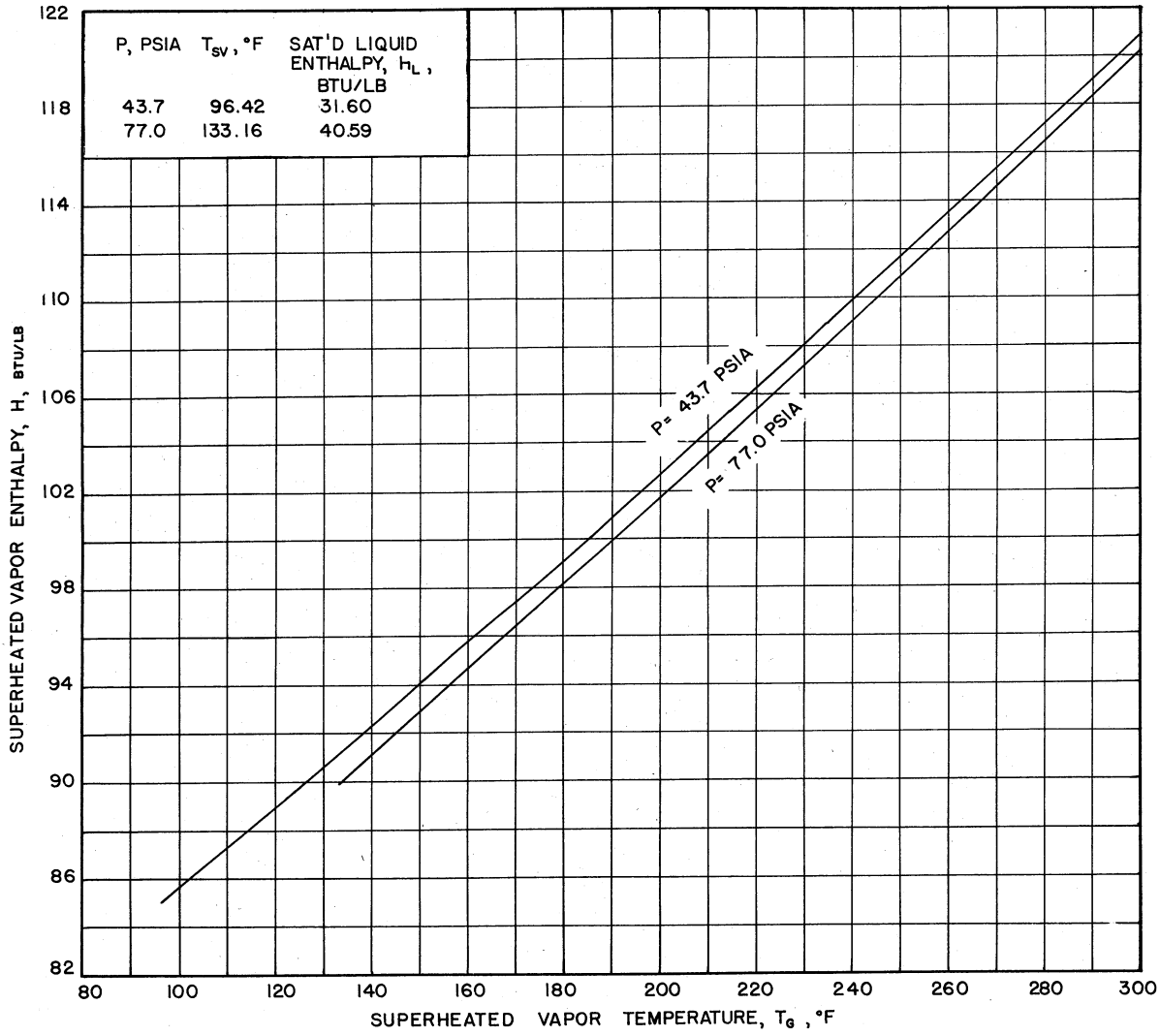

FIGURE 36 – ENTHALPY OF SUPERHEATED FREON-114 VAPOR

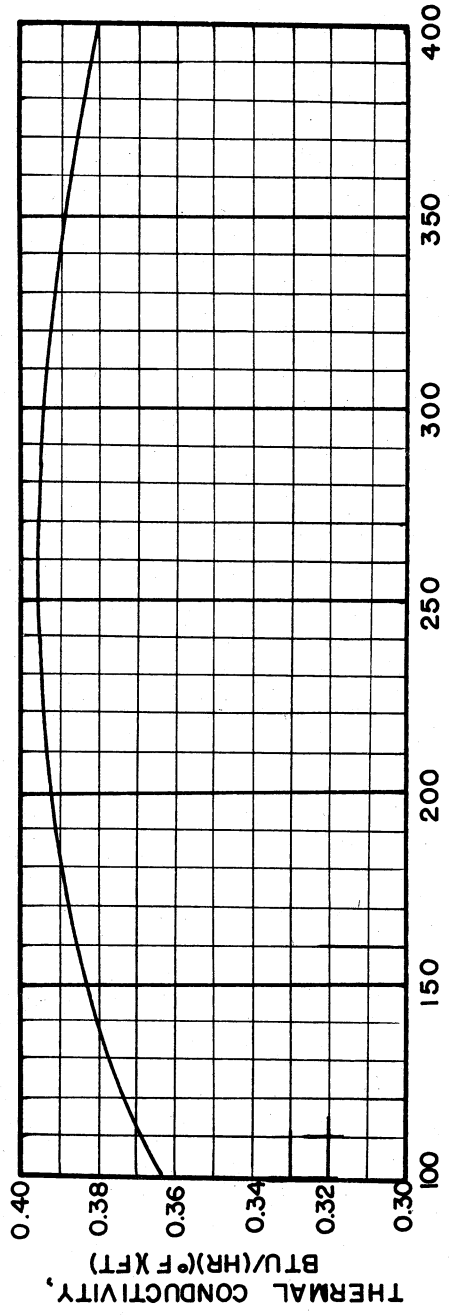

FIGURE 37 — THERMAL CONDUCTIVITY OF WATER (REF. 48)

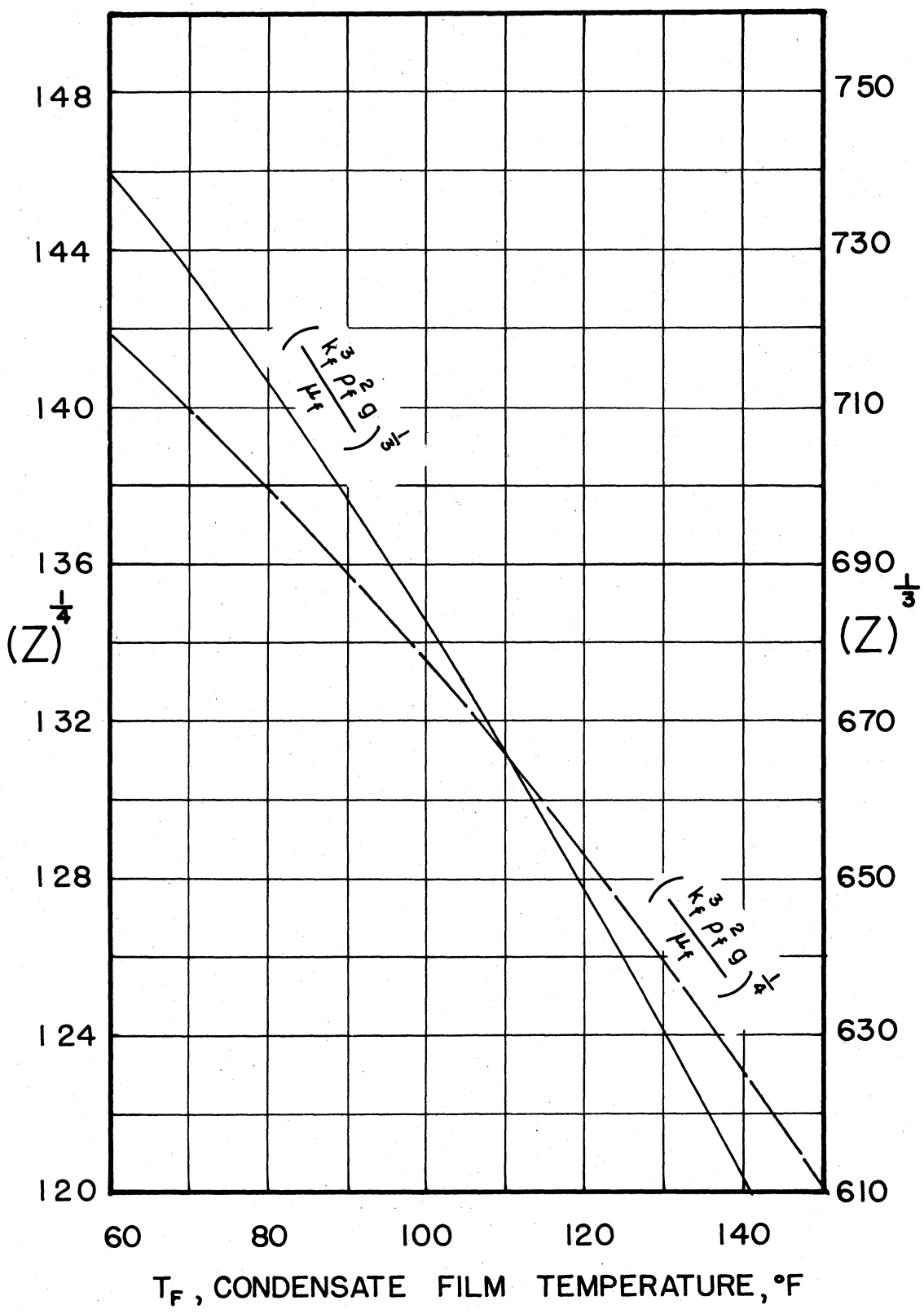

FIGURE 38 - NUSSELT PHYSICAL PROPERTY GROUP FOR FREON-114

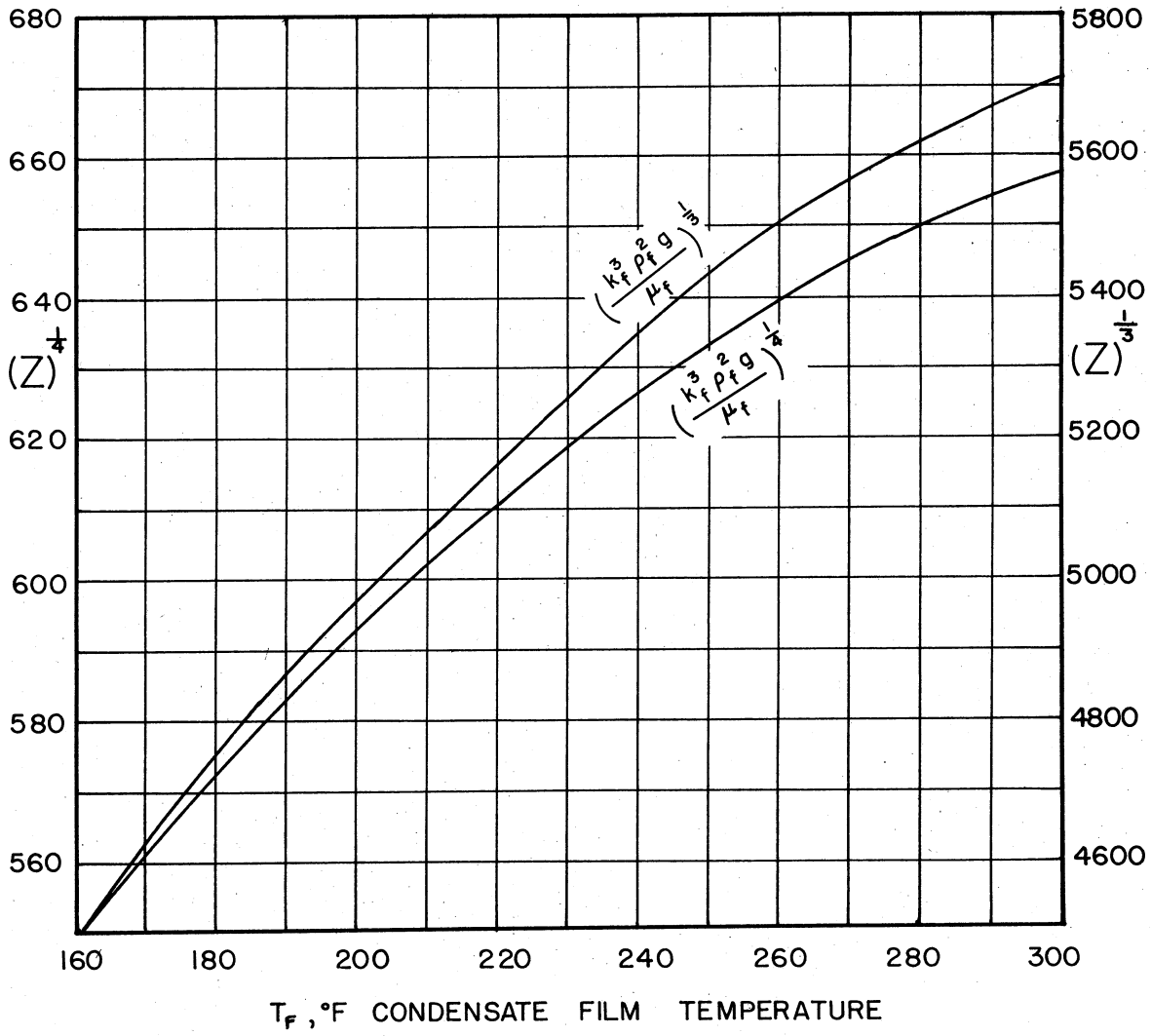

FIGURE 39 — NUSSELT PHYSICAL PROPERTY GROUP FOR WATER

NOMENCLATURE

a	intercept of Wilson-plot line
A	total outside area, sq ft
A_i	inside tube surface area, sq ft per ft
A_m	mean metal heat transfer area, sq ft per ft
A_o	outside tube surface area, sq ft per ft
b	slope of Wilson-plot line
B	equivalent to the group $\sqrt{\frac{g_c M}{2RT}}$
B_g	value of B at $T = T_g$
c	coefficient in equation for h_w
C_p	specific heat, Btu per (lb)(°F)
d_i	inside diameter of tube, inches
d_m	mean metal diameter, inches
d_o	outside diameter of tube, inches
D_o	outside tube diameter, ft
$\sum e^2$	least mean square deviation
$E(f)$	correlating group involving m_s, T_s, $P_s{}^*$, and P_g
f	condensation coefficient
f_i	inside fouling factor, (hr)(°F)(sq ft ins.) per Btu
g	gravitational constant, 4.17×10^8 ft per hr per hr
g_c	conversion factor, 4.17×10^8 (lb mass)(ft) per (lb force)(sq hr)
$G(f)$	correlating group involving m_s, T_s, T_g, $P_s{}^*$, and P_g
h	enthalpy of saturated liquid, Btu per lb
h_c	condensate film coefficient, Btu per (hr)(°F)(sq ft outside)
h_i	interfacial vapor film coefficient, Btu per (hr)(°F)(sq ft outside)

NOMENCLATURE (continued)

h_o	overall outside film coefficient, Btu per (hr)(°F)(sq ft outside)
h_v	convection coefficient for a gas or vapor, Btu per (hr)(°F)(sq ft)
h_w	water film coefficient, Btu per (hr)(°F)(sq ft ins.)
H	height of vertical surface, ft; enthalpy of vapor, Btu per lb
$(-\Delta H)$	total heat removed, latent heat for saturated vapor, Btu per lb
H(f)	correlating group involving h_i, T_s, T_g, P_s^*, P_g, and $(-\Delta H)$
k_f	thermal conductivity of condensate film, Btu per (hr)(°F)(ft)
k_m	thermal conductivity of metal, Btu per (hr)(°F)(ft)
m	condensing load, lb per (hr)(ft of surface width)
m_c	absolute rate of condensation, lb per (hr)(°F)(sq ft)
m_e	absolute rate of evaporation, lb per (hr)(sq ft)
m_s	condensing load, lb per (hr)(sq ft)
M	molecular weight lb mass per lb mole
n	number density of molecules; exponent of water velocity
d_n	number density of molecules with velocity C in velocity space dC
N	number of observations for least mean square deviation
P_g	pressure of gas phase lb (force) per sq ft absolute, lb (force) per sq in. absolute in equations 33 through 41.
P_s^*	equilibrium vapor pressure at T_s, lb (force) per sq ft absolute, lb (force) per sq in. absolute in equations 33 through 41.
Q	total heat transferred, Btu per hr
Q/A	heat flux, Btu per (hr)(sq ft outside)
r_c	condensate film resistance, (hr)(°F)(sq ft outside) per Btu
r_i	interfacial film resistance, (hr)(°F)(sq ft outside) per Btu
r_m	metal resistance, (hr)(°F)(sq ft outside) per Btu
r_o	overall outside film resistance, (hr)(°F)(sq ft outside) per Btu

NOMENCLATURE (continued)

R	gas constant, 1544 (ft)(lb force) per (lb mass)(°R)
s	velocity distribution function
Δt_c	temperature drop through condensate film, (T_s-t_o), °F
Δt_i	temperature drop through interfacial film, (T_g-T_s), °F
Δt_m	temperature drop through metal wall, (t_o-t_i), °F
Δt_o	overall outside film temperature difference, (T_g-t_o), °F
Δt_t	temperature rise of water, (T_2-T_1), °F
Δt_w	temperature drop through water film, (t_i-t_w), °F
t_i	inside tube surface temperature, °F
t_L	wall temperature at water outlet end, °F
t_m	mean tube wall temperature, °F
t_M	wall temperature at the middle of tube, °F
t_o	outside tube surface temperature, °F
t_R	wall temperature at water inlet end, °F
t_w	average water temperature, °F
T	average temperature between T_s and T_{sv}, °R
T_f	mean condensate film temperature, °F
T_g	superheated vapor temperature, °F
T_{LC}	condenser temperature at left end, °F
T_{MC}	condenser temperature at the middle, °F
T_s	condensate surface temperature, °F
T_{sv}	saturation temperature, °F
T_1	inlet water temperature, °F
T_2	outlet water temperature, °F
ΔT_{oa}	overall temperature difference, (T_g-t_w), °F
ΔT_s	degree of superheat, (T_g-T_{sv}), °F

NOMENCLATURE (concluded)

U_g	absolute mean molecular velocity representing rate of mass transfer
U_o	overall heat transfer coefficient, Btu per (hr)(°F)(sq ft outside)
V_t	water velocity, ft per sec
W_s	rate of condensation, lb per hr
W_t	water flow rate, lb per hr
x	abscissa of Wilson plot, $\frac{10^4}{W_t^n}$
y	ordinate of Wilson plot, $\frac{10^4}{U_o}$
Y_H	condensate film thickness at position H, ft
Y_m	tube wall thickness, ft
Z	physical property group, $\left(\frac{k_f^3 \rho_f^2 g}{\mu_f}\right)$

Other Symbols

f	subscript refers to (1) condensate properties at the mean film temperature and (2) gas or vapor properties at the mean gas or vapor temperature
β_f	coefficient of cubical expansion of vapor or gas, $°R^{-1}$
ρ	density, lb per cu ft
ρ_g	gas density, lb per cu ft
ρ_L	liquid density, lb per cu ft
ρ_s^*	saturated liquid density at T_s, lb per cu ft
μ	viscosity, lb per (ft)(hr)
Γ	correction factor, function of error integral $\Phi(B_gU_g)$
Γ'	condensing load, lb per (hr)(ft of tube length)
$\Phi(B_gU_g)$	error integral function
ϕ_g	equivalent to B_gU_g, variable defining Γ

BIBLIOGRAPHY

1. Alty, T., Proc. Roy. Soc. (London), A131, 554-64 (1931).

2. Alty, T., Phil. Mag., 15, 82-103 (1933).

3. Alty, T., Proc. Roy. Soc. (London), A161, 68-79 (1937).

4. Alty, T., and Mackay, C. A., Proc. Roy. Soc. (London), A149, 104-16 (1935).

5. Alty, T., and Nicoll, F. H., Can. J. Research, 4, 547-58 (1931).

6. Am. Soc. Ref. Eng., The Refrigerating Handbook, 6th Ed., New York, 1949.

7. Baker, E. M., and Mueller, A. C., Trans. AIChE, 33, 534-7, 542 (1937).

8. Baker, H. D., Ryder, E. A., and Baker N. H., Temperature Measurement in Engineering, John Wiley and Sons, New York, 1953.

9. Benning, A. F., and McHarness, R. C., Thermodynamic Properties of Freon-114, Kinetic Chemicals, Inc., Wilmington, 1944.

10. Bowman, R. A., U. S. Patent 2,279,552.

11. Bosnjakovic, F., Forsch. Gebiete Ing., 3, 135 (1932).

12. Bromley, L. A., Ind. Eng. Chem., 44, 2966-9 (1952).

13. Bromley, L. A., Brodkey, R. S., and Fishman, N., Ind. Eng. Chem., 44, 2962-6 (1952).

14. Brown, G. G., et al., Unit Operations, John Wiley and Sons, New York, 1950.

15. Claassen, H., Centr. Zukerind., 35, 129 (1927).

16. Claassen, H., Wärme, 61, 403 (1938).

17. Cornell, D., "Condensation of Superheated Vapors," Heat and Mass Transfer Seminar Report, Univ. of Michigan, 1952.

BIBLIOGRAPHY (continued)

18. Daniels, F., Outlines of Physical Chemistry, John Wiley and Sons, New York, 1948.

19. Dobkin, G. I., Teplosilovoe Khoz., 1, 21 (1941); see Chem. Abs., 37, 4278.

20. Fatica, N., and Katz, D. L., Chem. Eng. Progress, 45, 661-74 (1949).

21. Gibson, L. C., "Rate of Condensation of Water Vapor Under Vacuum," Ph.D. thesis in chemical engineering, Univ. of Wisconsin (1952).

22. Hampson, H., General Discussion on Heat Transfer (London), 58-61 (1951).

23. Jakob, M., Mech. Eng., 58, 729-39 (1936).

24. Jakob, M., Heat Transfer, Vol. I, John Wiley and Sons, New York, 1953.

25. Katz, D. L., Hanson, G. H., et al., Petroleum Refiner, 25, 419 (1946).

26. Katz, D. L., Hope, R. E., Datsko, S. C., and Robinson, D. B., JASRE, 53, 315 (1947).

27. Keenan, J. H., and Keyes, F. G., Thermodynamic Properties of Steam, John Wiley and Sons, New York, 1948.

28. Kirkbride, C. G., Trans. AIChE, 30, 170-86 (1933-34); Ind. Eng. Chem., 26, 425-8 (1934).

29. Lang, M., Forsch. Gebiete Ing., B5, 212 (1934).

30. Leeds and Northrup Co., Standard Conversion Tables, Philadelphia.

31. Lennard-Jones, J. E., and Devonshire, A. F., Proc. Roy. Soc. (London), A156, 6-44 (1936).

32. Markwood, W. H., and Benning, A. F., Thermal Conductances and Heat Transmission Coefficients of Freon Refrigerants, Kinetic Chemicals, Inc., Wilmington, 1942.

33. McAdams, W. H., Heat Transmission, 2nd Ed., McGraw-Hill Book Co., New York, 1942.

BIBLIOGRAPHY (concluded)

34. Merkel, F., Die Grundlagen der Wärmeübertragung, Leipzig, Steinkopff, 1927.

35. Monrad, C. C., and Badger, W. L., Trans. AIChE, 24, 84-119 (1930).

36. Nelson, M. A., U. S. Patent 2,306,895.

37. Nusselt, W., Z. Ver. deut. Ing., 60, 541-6 and 569-75 (1916).

38. Perry, J. H., Chemical Engineers' Handbook, 3rd Ed., McGraw-Hill Book Co., New York, 1950.

39. Prüger, W., Z. Physik, 115, 202-44 (1940).

40. Ramey, H. J., Henderson, J. B., and Smith, J. M., AIChE Heat Transfer Symposium Series No. 9, 50, 21-8 (1953).

41. Rizika, J. W., and Rohsenow, W. M., Ind. Eng. Chem., 44, 1168-71 (1952).

42. Robinson, D. B., "Effect of Vapor Agitation on Boiling Coefficients at Low Temperature Differences," Ph.D. thesis in chemical engineering, Univ. of Michigan, 1949.

43. Rohsenow, W. M., ASME Annual Meeting, Preprint No. 54-A-144, 1954.

44. Rohsenow, W. M., Webber, J. H., and Ling, A. T., ASME Annual Meeting, Preprint No. 54-A-145, 1954.

45. Schrage, R. W., Interphase Mass Transfer, Columbia Univ. Press, New York, 1953.

46. Silver, R. S., Engineering, 161, 505-6 (1946).

47. Stender, W., Z. Ver deut. Ing., 69, 905 (1925).

48. Timroth, J., and Vargaftik, N., J. Tech. Phys., 10, 1063-73 (1940).

49. Wilson, E. E., Trans. ASME, 37, 47 (1915).